Master Thesis

ASSESMENT OF HYDROGEN – ROCK INTERACTIONS DURING GEOLOGICAL STORAGE OF CH4 – H2 MIXTURES

Markus Pichler
2013

Department Mineral Resources & Petroleum Engineering
Chair of Reservoir Engineering

Advisor: Univ.-Prof. Dipl.-Geol. Dr. Stephan Matthäi

Abstract

To meet the demand of peak loads, renewable energy can be converted into hydrogen, which could be mixed into natural gas and stored in subsurface structures. Therefore an assessment of the influence of hydrogen methane mixtures on potential storage formations is needed. This thesis attempts to give an overview of what is already known about hydrogen-rock interaction and were more work needs to be done. Additionally, a fluid-gas-rock interaction model has been generated to make a first quantitative assessment of what influences, hydrogen methane mixtures, have on the geochemistry of potential subsurface storage structures.

The thermodynamic model was generated to get comparable results for a field test, which might be conducted after this thesis. The mineralogy and chemistry is taken from two representative core samples: one of them from the same formation as expected by the anticipated field test, and one with a similar mineral composition. A problem of generating the model was to get reliable thermodynamic data for clay minerals. Thermodynamic data for clay minerals is very difficult to generate, because of their numerous components and compositions which makes an assessment challenging. Therefore, not all clay minerals which are present in the rock samples could be included into the model. Fluid-gas-rock interaction models have been run for different gas compositions (0-100% hydrogen in the methane) and different pressure and temperature conditions.

The model shows that the titration of hydrogen changes the pH and Eh of the tested fluid. A pH is increase leads to dissolution of dolomite and precipitation of calcite. Additionally the generation of talc is observed. A potentially major issue is the stability of sulphides in the reservoir i. e. the generation of H_2S which would be harmful to health and environment. The models indicated however that the H2 does not destabilize the sulphides. The influence of temperature and pressure on the mineral assembly in the storage reservoirs has also been assessed. Within the range of plausible variations the influence of temperature is only minor and that as long as the phase is supercritical pressure does not influence the conditions at all.

Kurzfassung

Um erneuerbare Energien auch für Lastspitzen zu verwenden, können sie zum Beispiel in Wasserstoff umgewandelt werden. Dieser kann dann dem Erdgas beigemengt und auch in unterirdischen Strukturen gespeichert werden. Zu diesem Zweck beschäftigt sich diese Arbeit mit Daten, die schon aus der Literatur bekannt sind und stellt fest, wo noch mehr Forschung notwendig ist. Zusätzlich wurde ein thermodynamisches Model verwendet, um einen ersten quantitativen Überblick über den Einfluss von Wasserstoff-Methan Gemischen auf unterirdische Speicherstrukturen zu bekommen.

Um vergleichbare Werte für einen möglichen späteren Feldversuch zu bekommen, wurde ein thermodynamisches Modell erstellt. Die verwendeten mineralogischen und geochemischen Daten dieses Modells wurden zwei repräsentativen Bohrkernuntersuchungen entnommen. Ein Problem hierbei war die Beschaffung verlässlicher thermodynamischer Daten für Tonminerale. Diese sind Aufgrund ihrer vielen Komponenten und ihrer vielschichtigen Zusammensetzung sehr schwer zu beurteilen. Dies macht die Erstellung thermodynamischer Daten für Tonminerale schwierig. Aus diesem Grund konnten nicht alle Tonminerale die in den Bohrkernen vorhanden waren auch in das Model übernommen werden. Für die Modelle wurden verschiedene Gasmischungen verwendet (0-100% Wasserstoff im Methan) um auch den Einfluss höherer Wasserstoffkonzentrationen zu beobachten. Außerdem wurden auch verschiedene Druck- und Temperaturdaten verwendet um auch deren Einfluss auf die Speicherung zu beurteilen.

Das Ergebnis der Wasserstofftitration zeigt eine Änderung des pH- und des Eh – Wertes in der geochemischen Zusammensetzung. Der pH Wert wird erhöht, was zu einer Lösung von Dolomit und dem zusätzlichen Anlagern von Kalzit führte. Ein großes Anliegen der RAG war es die Stabilität schwefelhaltiger Minerale gegenüber Wasserstoff zu testen. Besonders aufgrund der möglichen Entstehung von Schwefelwasserstoff, welcher eine Gefährdung für Gesundheit und Umwelt darstellt. In den Modellen wurden jedoch keine größeren Mengen von Schwefelwasserstoff gefunden. Dies und die Stabilität der schwefelhaltigen Minerale konnte auch in der

Literatur nachgewiesen werden. Schlussendlich wurde auch noch der Einfluss von Temperatur und Druck auf die Wasserstoff-Methan Speicherung untersucht. Die Temperaturspanne, die für Speicherstrukturen normal ist, hat nur einen unwesentlichen kleinen Einfluss auf das Speichergeschehen. Schlussendlich konnte für Druckänderungen konnte überhaupt kein Einfluss festgestellt werden.

Affidavit

EIDESSTATTLICHE ERKLÄRUNG

Ich erkläre an Eides statt, dass ich diese Arbeit selbstständig verfasst, andere als die angegebenen Quellen und Hilfsmittel nicht benutzt und mich auch sonst keiner unerlaubten Hilfsmittel bedient habe.

AFFIDATIV

I declare in lieu of oath, that i wrote this thesis and performed the associated research myself, using only literature cited in this volume.

_____ _____

Datum Unterschrift

Acknowledgements

This thesis would not have been possible without the experience and financial support of RAG.
Here my special thanks to my advisor B. Griess for his professional input and great experience he shared with me. Additional thanks to A. Gubik and S. Bauer for the experience they added to this thesis, and to K. Halbmayer for all the professional discussions and the geological knowledge she supplied for this work.

I want to express my sincere gratitude to my university advisor Professor S.K.Matthäi (Montanuniversität Leoben) for his support and dedication to this work.
Furthermore I want to thank Dr. Wagner and Dr. Kulik from the Paul Scherrer institute who explained and helped me with GEMS.
Finally I want to thank my girlfriend, my family and my friends who supported me during my academic studies and beyond.

Table of Contents

List of Figures

Table of notations

GEM	Gibbs Free Energy Minimization
GEMS	Gibbs Free Energy Minimization Simulator (Program used for geochemical modeling)
P	partial pressure of dissolved gas above the liquid
KH	Henry's Law constant
c	concentration of the gas in the liquid
K(T,P)	equilibrium constant at defined temperature and pressure conditions
$a_{H_2(aq);(g)}$	fugacity of aqueous or gaseous hydrogen
j	diffusive flux under steady state conditions
De/Do	effective and opens space diffusion coefficient
z	distance from the source
t	time
Φ	porosity
δ	constrictivity: A function of pore diameter and the size of the diffusing particle
τ	tortuosity
ΔG	Gibbs Free Energy
vi	stochiometric coefficient
n(b)	bulk composition
A	matrix of the formula stoichiometry coefficient
vj	normalized chemical potential
gj0	standard Gibbs molar free energy
Cj	concentration of components
γj	chemical activity of different species
Θ	conversion ratio which is used to model gas, fluid and solids with the same equation

Introduction

Renewable energy failing as a replacement for fossil and nuclear ones has been discussed for several years. Recent events (Boss 2012) have given the topic an additional boost, thus leading to more research in the field of renewables and to the generation of new ideas. Several states have declared to finally stop their nuclear energy production (Knopf et al 2012) and to decrease their use of fossil fuels to a minimum. Renewable energies including wind, sun and wave-generated power are in most countries not able to swiftly replace the conventional ones. Especially when it comes to peak loads, renewable energy can't be used because of its lack of "spontaneity" (ORF Science 2012). One cannot just turn on and off your wind plant nor tell the sun to shine when needed. Thus, methods need to be found to effectively store and distribute the generated energy.

One promising idea is to generate hydrogen (Gtai 2012), mix it with natural gas and transport it via the existing pipeline network (Schmitz 2011). However introducing hydrogen into the natural gas network will also lead to its introduction into the existing subsurface storage facilities. As hydrogen is known to be a highly reactive element, this could change the geochemical conditions in these structures (Garrels et al 1990).

Pure hydrogen has been stored in the subsurface, for use in the chemical and aerospace industry for about 80 years (Foh et al. 1979). This was done in mined salt caverns in Amarillo (Texas), Teeside (GB), and Yakshunovskoe field (Russia) (Basniev et al. 2010),(Lord 2008). Probably due to the chemical inertness of the salt (Basniev et al. 2010), no geochemical reactions were observed here. However Foh et al (1979) and Evans (2008) mention the lack of volume and the sensibility to pressure changes of the salt caverns.

The storage of hydrogen as an addition to methane has been investigated in the Beynes (France) and the Lobodice (Czechoslovakia) fields (Buzek et al 1993), (Foh et al. 1979). Here manufactured gas, the so called town gas, was stored for use in communal heating systems. Town gas is a mixture of hydrogen (50-60%), carbon di- and monoxide (10-20%) and methane (10-20%) generated by coal gasification (Panfilov et al. 2006). Several observations have been made in these storage

facilities. During the storage cycle, gas composition changed reducing the share of hydrogen and carbon dioxide and increasing the share of methane (Panfilov et al. 2006). Additionally, traces of iron carbonyls and H_2S were found in the gas which made desulfurization necessary (Buzek et al. 1993), (Foh et al. 1979). Panfilov (2010) argues that these reaction products are due to bacterial activity in the reservoir, but Foh et al (1979) and Lord (2008) suggest, that H_2S could also be generated by geochemical reactions. The stability of minerals in subsurface structures, and the thermodynamic equilibrium within subsurface formations has been the topic of several scientific studies (Garrels et al. 1990), (Lassin et al. 2011).

Concerning pure hydrogen, much work has been done by the nuclear industry. Here subsurface shale layers, like the “Callov-Oxfordian” clay rock are used as a deposition for High-Level-Nuclear-Waste (HLW) (Oritz et al. 2001). Its decay generates heat, supporting the anaerobic corrosion of the metallic containers in which the HLW is stored (Lassin et al. 2011). Apart from damaging the storage containers, this corrosion generates significant amounts of hydrogen, which have to be prevented from migrating to the surface. Therefore the nuclear waste industry has done a lot of research on the topic of clay tightness to hydrogen migration.

Since that hydrogen has a lower density and viscosity as well as a smaller molecule size, its mobility is higher than that of methane (Basniev et al. 2010). The authors also state that the higher mobility might be a problem for the tightness of the formation and Paterson (1982) adds that this might lead to irregular gas compositions in the storage reservoir.

This is the reason why different gas compositions are assessed in the geochemical model, which will be shown later in this thesis. Finally, Galle et al (1998) also points out that the solubility and diffusivity of hydrogen in subsurface fluids should be assessed. Irrespectively of the loss of hydrogen, the solubility of hydrogen needed to be investigated because dissolution pH and Eh of the reservoir fluid.

Literature Review

For chemical processes and remote small scale energy supply it is enough to store hydrogen in tanks because the volume needed is not extensive. Hydrogen as an energy carrier for large scale use however would require tremendously larger volumes. About three volume units of hydrogen would be needed to replace one volume unit of methane (Götz et al 2010). These volumes need to be stored in huge subsurface formations, in order to be available when the customer needs them.

Since the early 1950's hydrogen gas is stored in the subsurface (Foh et al. 1979). This includes pure hydrogen for use in the chemical industry (Basniev et al. 2010), as well as hydrogen as an associated material in mixture with other gases (Buzek et al.1993).

Pure hydrogen was usually stored in salt caverns which have a completely different chemical setting compared to porous storages. Pray et al. (1950) did research on the solubility of hydrogen in salt saturated fluids. He found out, that the salt reduces the ability of the fluid to dissolve hydrogen and that the solubility of hydrogen is smaller than the solubility of methane in those fluids. This points is important as it gives an indication, that in case of subsurface hydrogen storage, diffusion would not be the limiting factor (Lassin et al. 2011). However Pray et al (1950) did not consider for chemical interaction between other dissolved species and the hydrogen which is the focus of this thesis.

Additional work on the storage of hydrogen was done by Buzek et al (1993). He did research on a porous aquifer town gas storage in the Czech Republic (Lobodice) to investigate the reason for hydrogen losses. Town gas as was explained in the introduction is a mixture containing hydrogen, methane and carbon di/monoxide which is generated by coal gasification. During storage a loss in hydrogen and carbon di/monoxide concentration could be monitored while at the same time the methane fraction increased. Buzek et al (1993) assumed a reaction between the hydrogen and the carbon di/monoxide, but could not explain how this reaction was possible at such low temperature conditions (35°C). It was found that methanogenic bacteria were present in the reservoir which converted the hydrogen and the carbon di/monoxide into methane. These findings have later been verified by Panfilov et al (2009) who investigated a direct connection between the bacterial growth in the porous media and the amount of injected town gas.

In the field of geochemical hydrogen rock interaction, Foh et al (1979) assumes that it is very unlikely that the hydrogen would react with any species present in the reservoir at low temperature conditions (<80 °C). To prove his statement he mentions the Gaz de France field Beynes where no problems with the reservoir rock have been measure after long periods of town gas storage.

Further work on the geochemical behaviour of hydrogen in the subsurface has been conducted by the nuclear waste industry. Primarily these studies focused on hydrogen migration in the subsurface (Galle et al. 1998), (Oritz et al. 2001) as the objective was to find viable solutions of preventing hydrogen to escape from nuclear waste storage sites. However Oritz et al (2001) did study the effects of hydrogen on clay minerals in the vicinity of the storage sites. They did evaluate the absorption of hydrogen into the clay minerals, to find out if there are any reactions with the clay. The idea was that hydrogen might decrease the water content of the clay layers, which would make the clay brittle and in turn would lead to a higher migration rate of hydrogen gas. However no such effects could be found for the investigated clay minerals (Callov- Oxfordian clays).

Lassin et al (2011) investigated the solubility of hydrogen into subsurface fluids. His findings were similar to Pray et al (1950) who predicted a low solubility. However Lassin et al (2011) also investigated the chemical effects of hydrogen on the reservoir fluids. They investigated that hydrogen dissolution decreases the pH of the fluid, which in turn changes the geochemical equilibrium of the system. Lassin et al (2011) did also investigate possible chemical effects of hydrogen on clay minerals. However due to insufficient thermodynamic data for clay minerals he could not make any predictions on this issue from simulations. From laboratory experiments, Lassin et al (2011) concluded that the influence of hydrogen on clay minerals is negligible, but suggests further research to confirm these results.

Mixing and de-mixing problems are the final issue in subsurface hydrogen storage. If left alone the mixture of hydrogen and methane would decompose because of the different densities. In a porous media this would need geological time scale. It is only possible that due to the higher mobility of hydrogen, a gas layer is formed during the injection, which contains a higher share of hydrogen than the rest of the gas. If mixing of the hydrogen with the cushion gas would be an issue, Foh et al (1976) states that

for homogenous reservoir no problems could be found. Even in heterogeneous reservoirs it is very unlikely that hydrogen would mix with any other gas because of its lower density which hampers its ability to displace gas of higher density. Gaz the France did convert the Beynes town gas storage to a natural gas storage facility leaving the town-gas as cushion gas in the formation. Numerous measurements have proven, that the gas withdrawn from the storage only contains up to 1% of the original town gas which indicates only minor mixing rates. There are no models for heterogeneous reservoirs, where the compartmentalization and the lower permeability might lead to more contact and mixing of dissimilar gases.

For all the research already done on the topic of underground hydrogen storage, nobody did yet consider a geochemical model for such purpose. Therefore this thesis will be an important milestone for the better understanding on the issue of storing hydrogen methane mixtures in the subsurface.

Claim

In this thesis, the influence of a hydrogen methane mixture on subsurface storage formations will be evaluated.
Geochemical modeling is the main focus of this thesis and will therefore be discussed in detail in the literature review. The knowledge gained will be applied to generate a geochemical model of a possible storage reservoir via a thermodynamic modeling program.
The research on this topic is important in order to make hydrogen an significant part of the energy supply chain and to support a higher fraction of renewable energies in the energy generation. Since renewable energies from wind or sun are fluctuating sources, it is necessary to develop efficient storage options in order to store overspills in production for later use. One such option is “Power to Gas” which converts electrical energy into hydrogen that can later be injected into the existing gas grid and could be possibly stored in the existing porous subsurface gas storages. As hydrogen is highly reactive, investigations need to be done to assess the influence of hydrogen on the storage formations. Therefore this thesis is an important milestone on the way to renewable energy supply.

Agenda

The first chapter of my thesis is an introduction to the topic of underground hydrogen storage. A literature review of this topic can also be found in the first chapter.

The focus of this work is on geochemical modelling and hydrogen rock interaction in the subsurface. However there are some basic concepts such as solubility, diffusivity and redox-potential of hydrogen which also influence the behaviour of hydrogen in the subsurface and I decided therefore to discuss them to get a basic understanding of this processes. This will be discussed in the second chapter of the thesis

The third chapter is dedicated to the geology of the formation where the rock samples used for the simulation have been taken. The chapter will shortly describe the environment of the formation and will then turn on more specific questions as the rock and water composition in the target reservoir.

The fourth chapter is the methodology section. It discusses what thermodynamic equilibrium means and how it can be evaluated via geochemical modelling. A look is taken on fluid-gas - rock interaction in the subsurface.
The methodology will explain the basic equations and assumptions behind GEMS (Gibbs Free Energy Minimization) which is the modelling tool used to perform the geochemical simulations. Here the focus is clearly to make the reader understand which equations define the models and what assumptions have been made to generated the model to make it possible for him to reconstruct the findings of this thesis. This section also includes a discussion on sulphides, to identify their stability against chemical alteration. The stability of sulphides is of special interest because, it rules out the possibility of larger quantities of H_2S to be generated.

In the results section which is the fifth chapter the findings from the GEMS model are presented and problems which occurred obtaining them are discussed.
Finally in the sixth chapter the discussion section compares the findings of the geochemical model with those already known from the literature.

Physical and chemical hydrogen behaviour

This thesis is dedicated to geochemical modelling and the gas fluid rock interaction of hydrogen during geological storage. These reactions can be best described via thermodynamic calculations. However there are other physical influences in the reservoir, which might also have an effect on the feasibility of subsurface hydrogen storage. These effects are discussed in a short manner in this section.

Hydrogen Properties

To understand the potential issues of hydrogen storage one has to understand the basics of the element hydrogen first. Hydrogen is the main element (about 75%) in the univers (Shimko 2008) and has the second lowest melting and boiling points with only Helium being below.

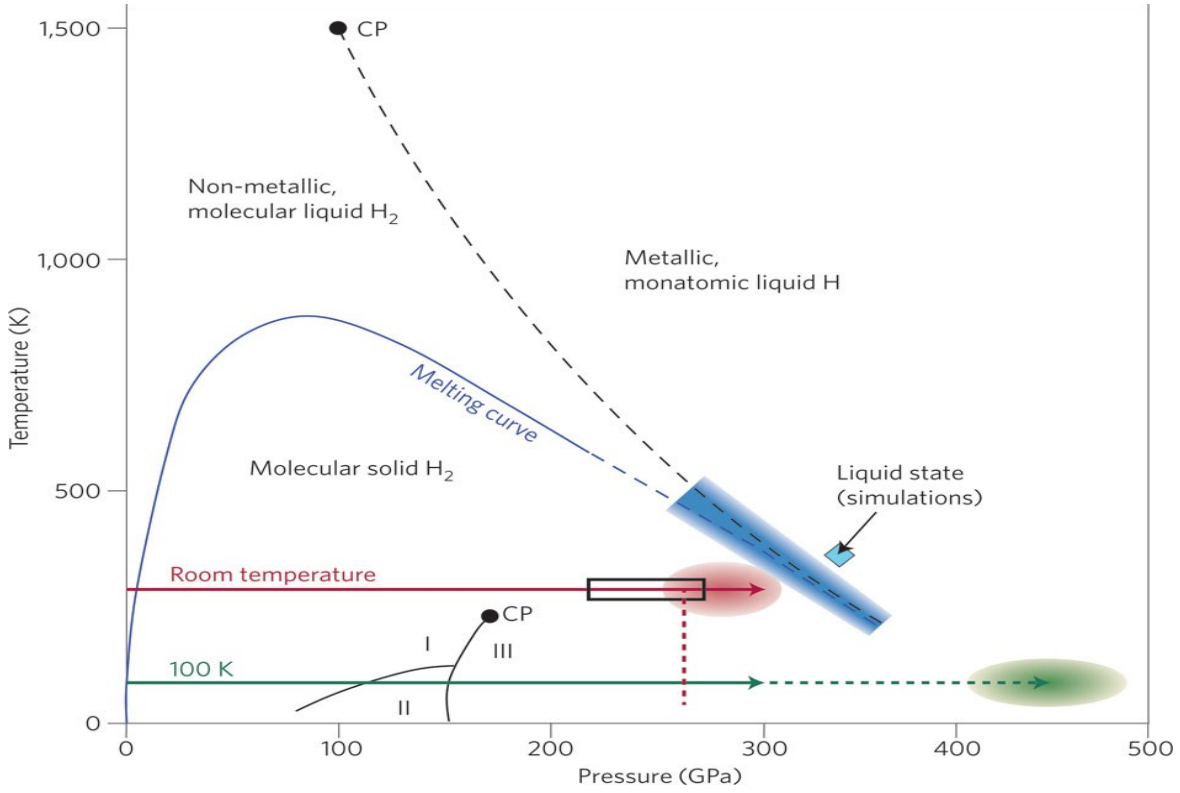

Figure 1: Hydrogen phase diagram

(Nature Materials 2011)

The melting point is at 14K and the boiling point follows closely at 20K. These points both are measured at atmospheric pressure. This is one of the reasons why hydrogen is no primary fuel because it is difficult to store under standard conditions (Shimko 2008). Other gases can be liquefied at standard temperature, but unfortunately the boiling point of hydrogen can only be increased to 33K peaking at a pressure of 13 bar (Figure 1). Thus as a vehicle fuel hydrogen can only be stored as high pressure gas, cryogenic liquid or in fuel cells. (Eere Energy 2012).

Pure hydrogen is a non toxic, odorless, color and tasteless gas. It can however contain some traces of sulfur if produced from fossil fuels which might lead to the typical fermented egg smell of H2S. Additionally, it may contain traces of nitrogen, carbon dioxide and carbon monoxide. Hydrogen is only dangerous if it is released in rooms where it can accumulate to explosive mixtures. In open areas, even big leaks do not pose a threat, because of the high buoyancy and diffusivity of hydrogen which make an accumulation impossible, but also increase the threat of leakage (Eere Energy 2012). Although hydrogen is highly reactive and can be ignited very easily, the risk of spontaneous ignition is low because of its auto ignition temperature is 585°C (NIST 2012).

Fuel	Energy Density (LHV)
Hydrogen	10050 kJ/m³; gas at 1 atm and 15 °C 1825000 kJ/m³; gas at 20 MPa and 15°C 4500000 kJ/m³; gas at 69 MPa and 15°C 8491000 kJ/m³; liquid
Methane	32560 kJ/m³; gas at 0,1 MPa and 15°C 6860300 kJ/m³; gas at 20 MPa and 15°C 20920400 kJ/m³; liquid
Propane	86670 kJ/m³; gas at 0,1 MPa and 15°C 23488800 kJ/m³; liquid
Gasoline	31150000 kJ/m³; liquid
Diesel	31435800 kJ/m³ minimum; liquid
Methanol	15800100 kJ/m³; liquid

Figure 2: Energy density of comparative fuels

(Eere Energy 2012)

The energy density of hydrogen is rather poor (Figure 2). While one cubic meter of methanol contains 100 kg of H_2 molecules, one cubic meter of liquid hydrogen only contains 71 kg.

Hydrogen Reactivity and Redox Potential

Hydrogen is highly reactive and does, if introduced into an aqueous system, changes its pH-Eh conditions. It forms compounds with strong electronegative halogens or oxygen taking on a partially positive charge. Under mostly alkaline conditions it tends to form metal hydrides where it takes on a partial negative charge (Foh et al. 1979). The largest group of compounds is the group of hydrocarbons also called organic compounds which make up the organic chemistry.
Hydrogen does also play an important part in acid base reactions, and does change the pH of every aqueous system in which it is introduced. If oxidized, hydrogen loses its electron giving it a positive charge H+ so that it resembles a proton. Thus hydrogen as such makes up the basic acid and added to an oxygen atom becomes the basic base OH- (Petrucci et al 2002).

In nature a common metamorphic reaction, the so called serpentinization creates greater amounts of hydrogen. This reaction was observed at oceanic rifts where due to the absence of oxygen elemental hydrogen is generated. The chemical reaction thereby is written as follows:

$$3\ Fe_2^{(+II)}SiO_4 + 2\ H_2O \rightarrow 2\ Fe_3^{(+II/+III)}O_4 + 3\ SiO_2 + 2\ H_2 \quad \text{.....(3)}$$

The oxidation reaction of fayalite and water generates magnetite and quartz release six hydrogen molecules. This reaction is quite similar to the Schikorr reaction (Reganozi 2010) which occurs under anoxic conditions. It has been agreed that such oxidation reactions with Fe^{2+} lead to the generation of naturally occurring H_2 that is present in some gas reservoirs (Berger 2007).

Hydrogen changes the redox potential of water (Eh). The redox potential is measured in volts, and it describes the tendency of a chemical system, to either accept (reduction) or donate electrons (oxidation). Thus, a positive value indicates a reducing

environment and a negative one an oxidizing environment (Garrels et al. 1990). For H_2 storage it is important to find out in which redox state the reservoir is originally and how the addition of H_2 influences it. Gaucher et al (2009) point out some important controls of the Eh and pH in a geological storage site. The first is the equilibrium between dolomite, calcite and siderite. If siderite is dissolved, this can change the redox potential because of freed Fe^{2+} ions. The second control that was also proposed by Truche et al (2009) and Lassin et al (2011) is the influence of sulfides (pyrite, marcasite, celestite) since they are easily oxidized and potentially dissolved at strong reducing conditions were elemental sulfur is stable.

Hydrogen Solubility

The dissolution of hydrogen water with variable salinity needs to be understood because it increases the pH and reduces the redox potential (Lassin et al. 2011). The solubility of gases in liquids is often approximated from Henry's Law (Eq. 2). It states that: "*At constant temperature, the amount of a given gas that dissolves in a given type and volume of liquid is directly proportional to the partial pressure of that gas in equilibrium with that liquid.".* Under constant conditions Henry's law can be written as follows (Atkins 2004):

$$P=k_H*c \quad \text{..... (1)}$$

The constant is species, temperature and pressure dependent and has to be measured. It should be noted that the law only holds true for infinitesimal dilute solutions. Lassin et al (2011) show an extended version of Henry's law that can be applied to real systems.

$$K(T,P)=\frac{a_{H_2(aq)}}{a_{H_2(g)}} \quad \text{.....(2)}$$

Equation 2 shows that for real systems Henry's law can be written as the relationship between the fugacity of aqueous H_2 ($a_{H_2(aq)}$) and the fugacity of gaseous H_2 ($a_{H_2(g)}$), at equilibrium. K(T,P) here is the equilibrium constant of the H_2 dissolution reaction at a given temperature and pressure.

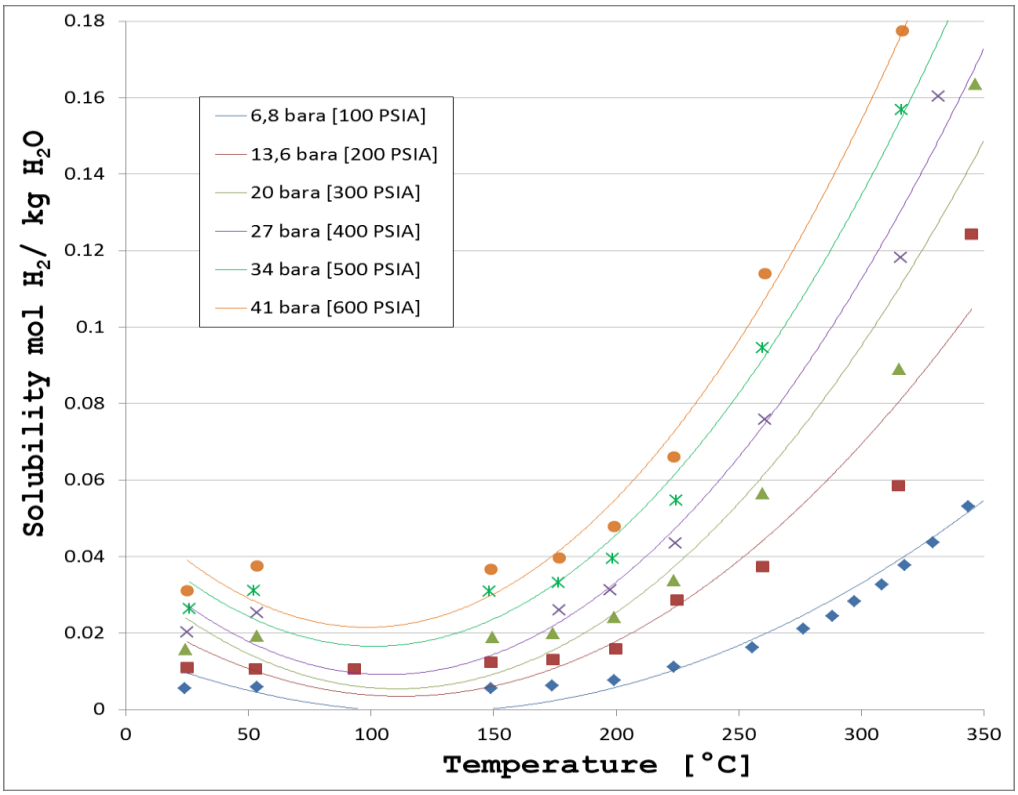

Figure 3: Solubility of hydrogen in water as function of temperatures

Pray et al (1950) Shows the solubility of hydrogen in pure water at isobaric conditions with increasing temperature. It should be noted that an increasing temperature decreases the solubility of gases in water up to a certain point, where it starts to increase again. This point for pure water is located at about 60°C (Lassin et at. 2011)

It is interesting to observe that the solubility of H2 in water increases with increasing temperatures (Figure 3). At temperatures about -6°C - 100°C solubility decreases with increasing temperature (Pray et al. 1950).

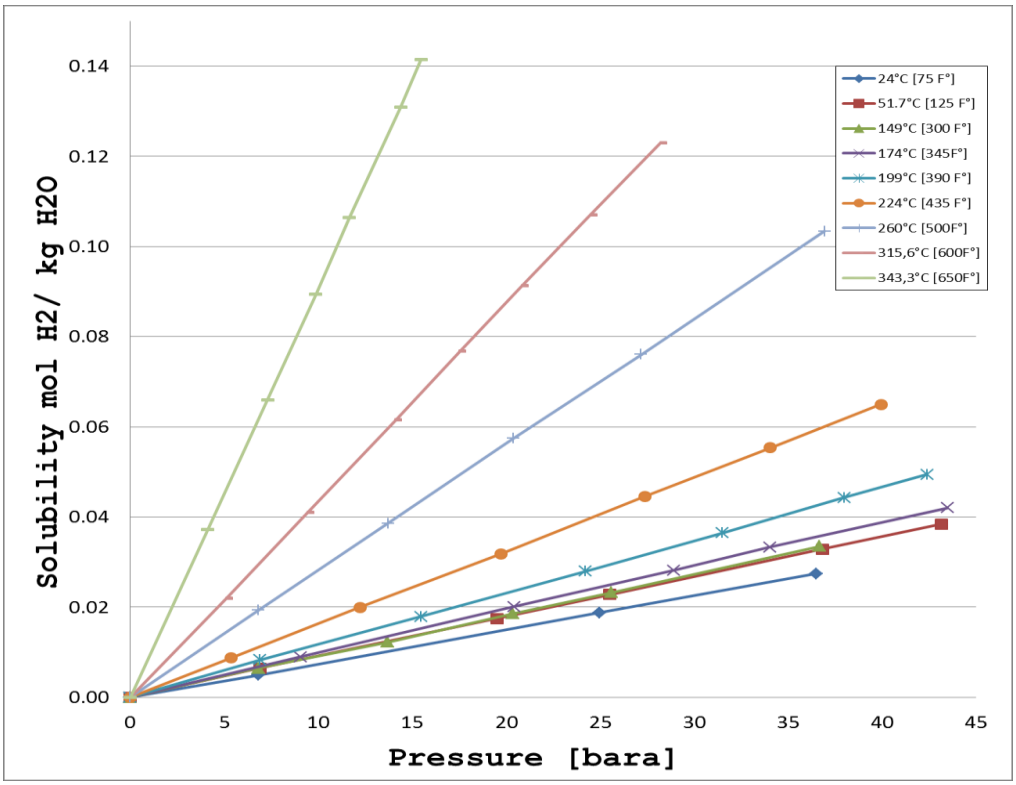

Figure 4: Solubility of hydrogen in water with varying pressures:

(Pray et al 1950) shows the isotherm behavior of the dissolution of hydrogen with increasing pressure. These curves are following Henry's law but are only valid in pure water.

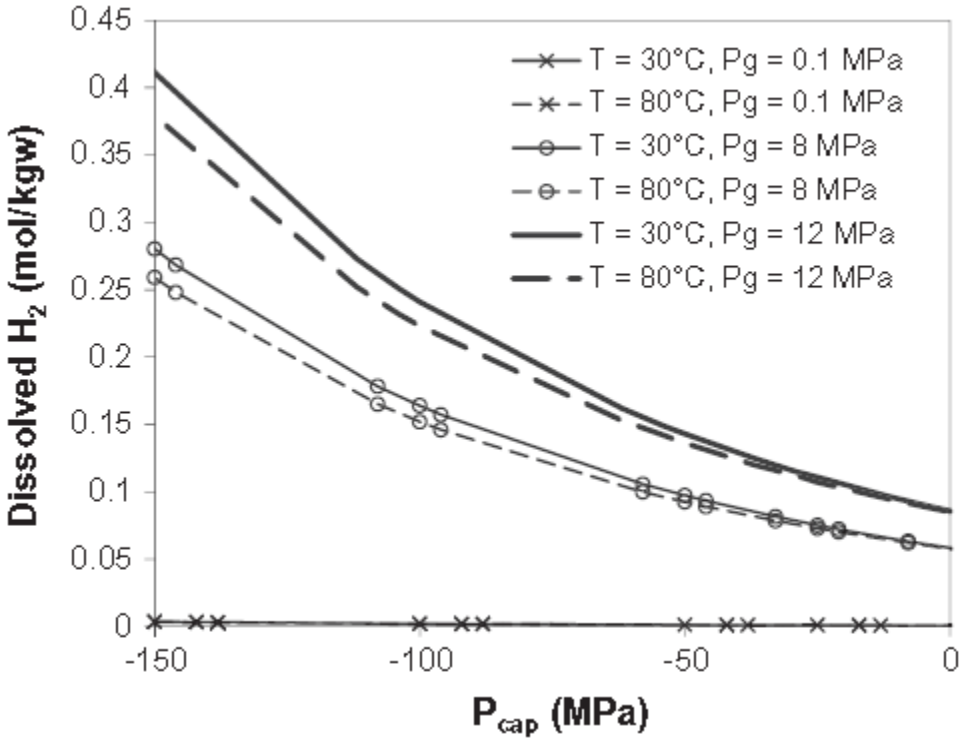

Figure 5: Solubility of hydrogen in pore water:

Measured for the pore water of an argillite clay formation (Lassin et al 2011)

For the pressure a straight line is received (Figure 4) which means a behavior as predicted by Henry's law. This also shows that the solubility of gases can be predicted over a rather wide range by Henry's law (Pray et al. 1950).

What Pray et al (1950) did not include was a correction factor for salinity. Any dissolved species reduces gas solubility in fluids (Lassin et al. 2011). This is also the reason why sea water is less oxygen rich than river water (PETE Lecture. 2012). As can be seen in (Figure 5) gas solubility mainly depends on partial pressure of the hydrogen phase and on the capillary pressure. The temperature has in this case only a minor influence on the solubility (Lassin et al. 2011). It has to be noted that salinity and temperature also influence the time in which the equilibrium between the aqueous and the gaseous phase is reached. Crozier et al (1974) states that equilibrium is reached more rapidly at higher temperature and in distilled water than at lower temperature and saline water.

For this thesis it is also important that there is a finite gas loss due to dissolution into the reservoir fluids, this is not only true for hydrogen but also for methane (Foh et al. 1979), which is even more soluble than hydrogen (Kaye et al. 1986).
Even if these losses are only minor, a regular exchange of reservoir fluids, such as by an active aquifer might lead to bigger losses because there will always be hydrogen under saturated water available that the gas can dissolve in.

Hydrogen diffusion in porous media

In gases diffusion progresses at a **rate** of about 5cm/ min (D=16 mm²/s), in liquids the rate is about 0,05 cm/min (D=0,0016 mm²/s) and in solids the rate is 0,00001 cm/min (D=1,66*10^{-9} mm²/s) (Cussler 2009). In general it varies less with temperature than do many other phenomena.
For this thesis it is important because it regulates the overall rate of the reactions if it is the slowest of the transport phenomena in the reservoir (Cussler 2009). For the overall topic of hydrogen storage and containment it is also important to predict diffusion rates through the cap rock (Oritz et al. 2001).

There are two laws defining the diffusion. One is the Fick's Law (Eq. 4) which is fundamental and uses the diffusion coefficient, and a second unnamed law which uses the mass balance. Fick's first law as mentioned below describes the diffusive flux j, under the assumption of steady state conditions

$$j = -D\frac{dc}{dz} \quad \text{.....(4)}$$

This is Fick's Law for the one dimensional case in a Cartesian coordinate system. In mathematical terms, the diffusion model is said to have distributed parameters, for the dependent variable (the concentration) is allowed to vary with all independent variables (like position and time). In contrast, the mass transfer model is said to have lumped parameters (like the average hydrogen concentration in the metal) (Cussler 2009).

For the semi-infinite case it is assumed that the diffusion process is at its beginning meaning that some parts of the medium is already saturated but at the fringes the medium is still under saturated. For this the assumption is made that the diffusion coefficient D is constant and that the concentration C_1 is time and space dependent. To predict how diffusion causes the concentration to change over time Fick proposed his second law.

$$\frac{\partial c_1}{\partial t} = D\frac{\partial^2 c_1}{\partial z^2} \quad \text{.....(5)}$$

This is the diffusion equation which gives $c_1=c_{inv}$ at time t=0 and $c_1=c_{10}$ at time t=inv. This is clearly understandable because in the beginning the boundary is totally unaffected giving it an infinitesimal small (meaning zero) concentration and at the end of the diffusion equilibrium is received (Cussler 2009). This equation is true for diluted solutions.

For diffusion in porous media the basic idea of diffusion in a capillary is taken, but expand it by a more detailed definition of the diffusion factor D. The characters necessary to describe the diffusion of gases through porous media are the same which can characterize the porous matrix and the fluid transmissibility itself, namely porosity (Φ), constrictivity (δ) and tortuosity (τ) (Chen et al. 1977). To take these constrictions into consideration, an effective diffusion coefficient (Equation 6) is estimated for the porous media (Grathwohl 1998).

$$D_e = \frac{D\phi_t\delta}{\tau} \quad \text{.....(6)}$$

The porosity in this assumption is the so called transport porosity, which is just an empiric reduction factor to account for plugged pores.

For dry rocks the ratio of the effective diffusion coefficient and the open space diffusion coefficient can be correlated on a log-log plot with the inverse of the resistivity factor. Several plots where generated to find the relationship between the reservoir parameters and the diffusion factor. The plot below (Figure 6) was generated from measured and literature data, and shows clearly a linear relationship between the diffusion factor and the permeability on a log-log plot.

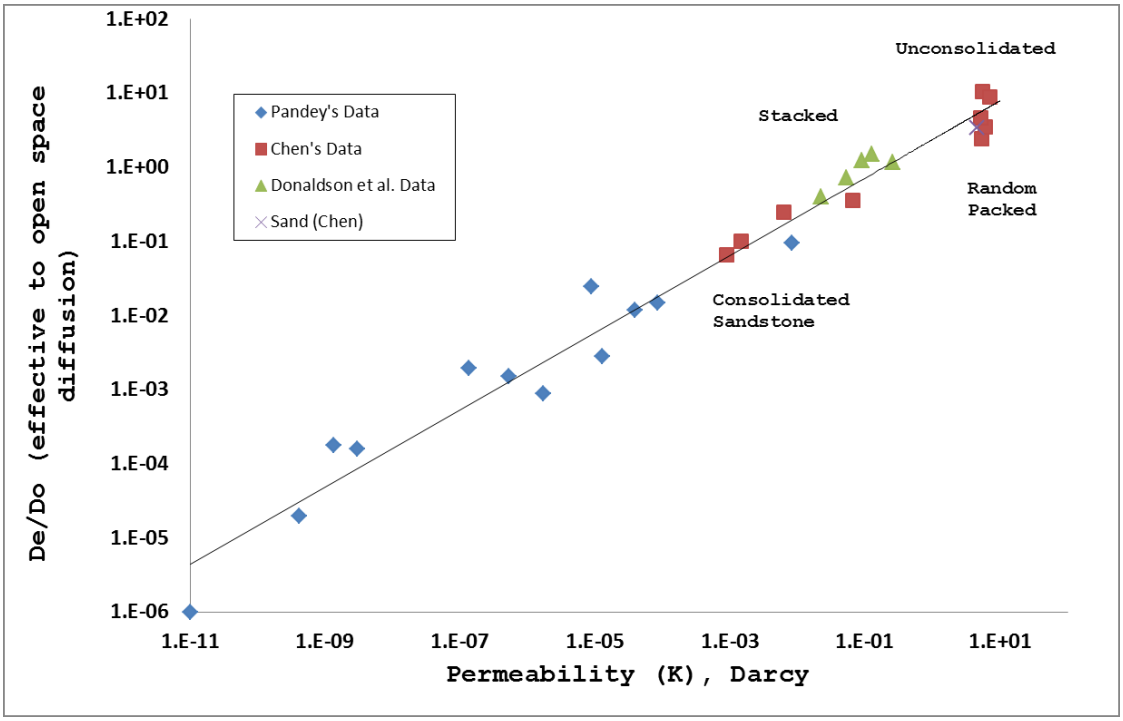

Figure 6: Diffusion factor vs. permeability for dry porous solids (Chen et al. 1977)

In the case of liquid saturation the diffusion rate is reduced by a factor of thousand. Chen et al (1977) states that apart from the obvious resistivity due to the liquid the swelling of native clays might lead to this drastic reduction. In their experiments Chen et al (1977) tried to establish steady stated diffusion through cores, measuring

diffusion coefficients. During the experiments the ambient pressure in the medium was not exceed so that the diffusion flux could take place across a totally liquid environment. Unfortunately Chen et al (1977) could not find a similar relationship for the saturated cores as for the dry ones. He suggests that this is because of uneven changes in the pore structure due to the flooding. However Chen et al (1977) state, that the conductivity of water saturated cores to diffusion is 10^3 times lower than of dry cores. This in combination with the results of Donaldson et al (1976) who did the same experiments with hydrogen states that there is no difference between hydrogen and methane storage concerning the cap rock.

A big part of the knowledge about the behavior of hydrogen in the subsurface comes from studies of nuclear waste management. If the bentonite is fractured or compromised in another way, fluids enter the system which would lead to migration of radionuclide's through the subsurface and eventually to the surface too. Thus a lot of research has been done to prove that clay layers are not compromised by the generation and contact of hydrogen.

The backfill cannot be directly compared to a naturally generated cap rock, but there are still some similarities which can help to understand issues of the storage of hydrogen methane mixtures. For migration it was found that clay formations such as the Boom Clay or the Callovo - Oxfordian clay rock provide a resistance against migration for at least 50000 to 100000 years (Lassin et al. 2011) (Galle et al. 1998). As in the storage of methane gas the diffusion of hydrogen is an issue, but will be of a comparable value (Oritz et al. 2001). Galle et al (1998) states that the diffusion of hydrogen for bentonite is about 10^{-11} [$m^2\ s^{-1;}$@25°C and 9,3 MPa].

Oritz et al (2001) states, that the difference between an engineered clay barrier and a cap rock is the fact that the barrier is homogenous whereas cap rock is not, thus opening the issue of preferential pathways. These are however an issue for both methane and hydrogen migration and Oritz et al (2001) suggests doing additional research on this topic to better estimate the rates migrating through this pathways. Oritz et al (2001) concludes that in his opinion migration of hydrogen is similar to that of methane and thus makes no difference for the cap rock.

A closer look in terms of hydrogen methane loss should be made on the wells (Hatscher 2010). It is not completely clear if the cement used to seal the formation is completely impenetrable to hydrogen. Further investigation is necessary. Foh et al (1979) state, that thus he could not prove the tightness of the packers nor the well itself. As the hydrogen molecule is very small it is able to enter the matrix of steel and thus migrate through it. The entering pressure of hydrogen into the steel matrix was found by Foh at 8.2 [MPa], hydrogen partial pressure. He states that this will lead to hydrogen migration and embrittlement of the steel. Based on experience from the chemical industry, only minor amounts of hydrogen tend to migrate by this process.

There is the option of storing the hydrogen not only in abandoned or depleted reservoirs, but also in aquifers, where water can be displaced by the gas, however this option brings with it additional problems to solve. The first is that it is not known whether the aquifer is tight enough to keep greater amounts of hydrogen from escaping or not. In a natural gas reservoir this is already proven due to the fact that it contains gas which was there for at least some period of time. Another issue is that the volume and the boundaries of the aquifer are not known. In a reservoir that has already been produced, it should be at least possible to re-inject the amount of gas that has been produced previously. In an aquifer this needs additional investigation from both seismics and down-hole measurement to find out about the volume and the boundaries of the chosen structure (Lord 2008).

Mobility and Viscous Fingering of Hydrogen

As a next step a short glimpse into the hydrogen properties concerning viscous fingering will be taken. The principle of viscous fingering is that a less viscous fluid will tend to finger into a more viscous fluid (Paterson 1982). The issues arising from viscous fingering for the storage of hydrogen mixtures in the subsurface can be summarized as followed.

Because of an increasing reactive surface, viscous fingers are a source of gas loss, because diffusion is surface dependent. So hydrogen might be lost due to dissolution. Another possible scenario is that during production parts of the gas are captured in

parts of the reservoir with lesser permeability where they are overhauled by the aquifer and thus will be unrecoverable.

Another thing which might be of particular interest if the share of hydrogen is increased in the gas is de-mixing. As Paterson (1982) and Perkins et al (1965) state, hydrogen is a little less viscous than natural gas ($9{,}5*10^{-3}$ [cp] for H_2 vs. $1{,}1*10^{-2}$ [cp] for natural gas) and has therefore a higher mobility (Lide et al. 2006). Thus it is possible that at the boundaries of the reservoir (Paterson 1982) gas with higher hydrogen content accumulates. This might lead to an increase in hydrogen concentration in the gas which can be an issue for the geochemical model and also for the gas quality at the end of the production cycle gas with higher hydrogen content is produced.

Geological Data

The geology explains from macro to micro scale the location where the core samples have been taken. This means a short introduction about the Molass basin, followed by a description of the "Hall Formation" and a detailed description of the core samples. Additionally the geological setting of the possible storage site which was proposed by RAG will be discussed. This will include a discussion on the minerals present in the formation as well as the fluid composition that was assumed for the target reservoir.

Geological Setting

Both core samples which will be used in the thermodynamic model have been taken from formations in the upper Austrian Molass Basin. The basin is located between the northern edge of the Alps and the southern edge of the crystalline Molass Basin. In the east it borders the Vienna basin and at the western edge it reaches the Bavarian shelf (Grunert et al. 2012) (see also Figure 7).

The development of the Molass basin started in the Mesozoic when the orogenic wedge of the forming Alps was pushed north and in this process started to narrow the Tethys Ocean (Labhart 2005). The weight of the orogenic pile bent the European plate down resulting in the development of a marine foredeep. During the Eocene (55 – 34 mio. years) the foredeep was bent deeper resulting in the formation of a small oceanic trench which started to fill up with flysch sediments (Malzer 1981). Sediments from the rising Alps where deposited into the trench by rivers from the south and started to fill it up making the basin shallower.

Figure 7: Location of the upper Austrian molasse basin
(Grunert et al 2012)

In the Oligocene and the Miocene the sedimentation continued and the basin was raised further due to tectonic uplift (Aberer 1957), finally resulting in the termination of sedimentation. The deformation due to alpine motion continued resulting in folding and partial overthrust. This caused the formation of the deformed subalpine molasse zone (Labhart 2005).

Hall Formation

The core samples taken for the thermodynamic model belong to the Hall Formation. The reason for choosing this formation is that this thesis might be followed by a field test which would be conducted in a reservoir in the Hall Formation. Thus results which can at a later point be compared to what happened in the reality shell be generated.

The Hall Formation was deposited during the early Burdigalian (16-20 million years) (Wagner 1998) in the deep marine PuchkirchenTrough (1500m-2500m) which belongs to the deep sea channel system of the late Aquitanian. The up to 800m thick formation consists of greenish – grey marls, but locally contains thick sandstone and

conglomerate intercalations. These are especially prominent in the lower part of the formation (Grunert et al. 2012) and are also the reason why the Hall Formation is divided into an upper and a lower part. The sediments are mainly deep sea sediments because at the time of their generation, a sea level rise reduced the deposition of sediments from the Alps (Rögl 1980). Glaukonite and mineral detritus show also that the sediments where originally deposited in shallower water and then re-deposited via turbidites.

Especially at the base of the lower Hall Formation the influence of submarine channels is apparent due to traces of strong reworking (meaning uneven sedimentation) (Wagner 1998). Yellow – grey sands and clayed marls make up the bulk from the upper part of the Hall Formation. The detritus which can be found in the whole formation was brought in by rivers from the south and originates in the Alps. These rock fragments mainly consist of mica schists, quartzite and gneiss. (See Appendix 3).

Core Sample Description

Two core samples have been used to generate the input for the thermodynamic model. This section sums up the findings of the core analysis done by OMV. Additional thin sections and thin section analysis of the core samples can be found in the Appendix 2+3.

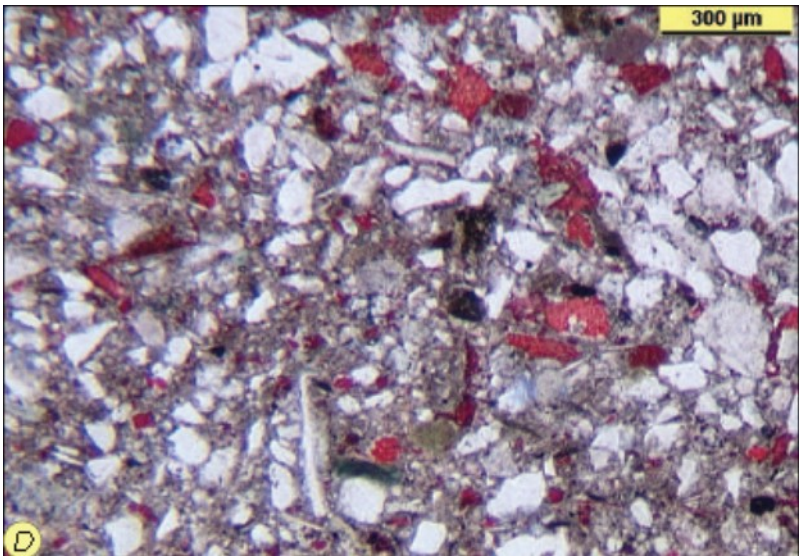

Figure 8: Thin section of core sample 2

Core sample two is from the Hall formation. Figure 8 is a thin section from this core sample which shows a fine grained lithic wacke-stone. From all core samples available from the Hall Formation this one was from the well closest to the anticipated test reservoir.

The core sample is described as a fine grained, matrix rich lithic wacke-stone in the petrographic report. This can also be confirmed by taking a look on the Dunham classification. The grains in the thin section are sorted moderate to bad and the roundness of the grains is sub angular to angular.

mono crystalline quartz	12%
poly crytalline quartz	2%
chert	1%
isolated feldspar grains	6%
crystalline rock fragments	3%
traces of bioclasts (seashells)	1%
dolomite grains	3%
isolated micas flakes	2%
glauconite	1%
calcite cement	4%
carbonate fragments	4%
fine grained carbonate matrix	60%
heavy minerals	1%

Figure 9: Petrographical composition of core sample 2

Additional traces of mudstone, Fe-carbonate cement and opaque substances could be identified. The crystalline rock fragments are composed of sericite, chloride-cement, quartz-mica and quartz feldspar aggregates as well as traces of phyllite and decayed vulcanite fragments.

Carbonate particles (Figure 9) are composed of sparite and bioclasts (formanifera, sea urchin needles, and residuals of shells). Sometimes it is difficult to tell the difference between single carbonate crystals and the carbonate cement. Isolated feldspar grains are usually serecitic and composed of plagioclase and alkali feldspars. The heavy metals are composed mainly of garnet (55%), but additionally brookit, zircon, rutile, titanite, chromspinell and tourmaline can be found.

The porosity is intra crystalline micro porosity because of the high clay share in the reservoir. Only traces of secondary porosity due to dissolved feldspar can be found.

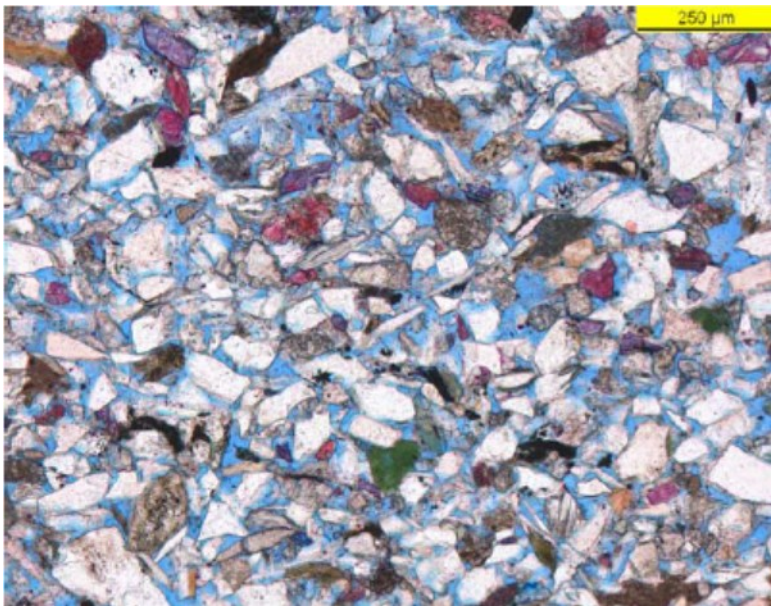

Figure 10: Thin section of core sample 1

Core sample (Figure 10) one does not belong to the Hall Formation. It was chosen because a core is not available from the anticipated test reservoir.
The thin section shows a fine grained, weak carbonatic, litharenitic sandstone which is cemented by a calcite- fe-dolomite matrix. It contains more than 25% of detrital rock (Figure 11) and a somewhat lesser fraction of feldspar grains (Pettijon et al. 1987).

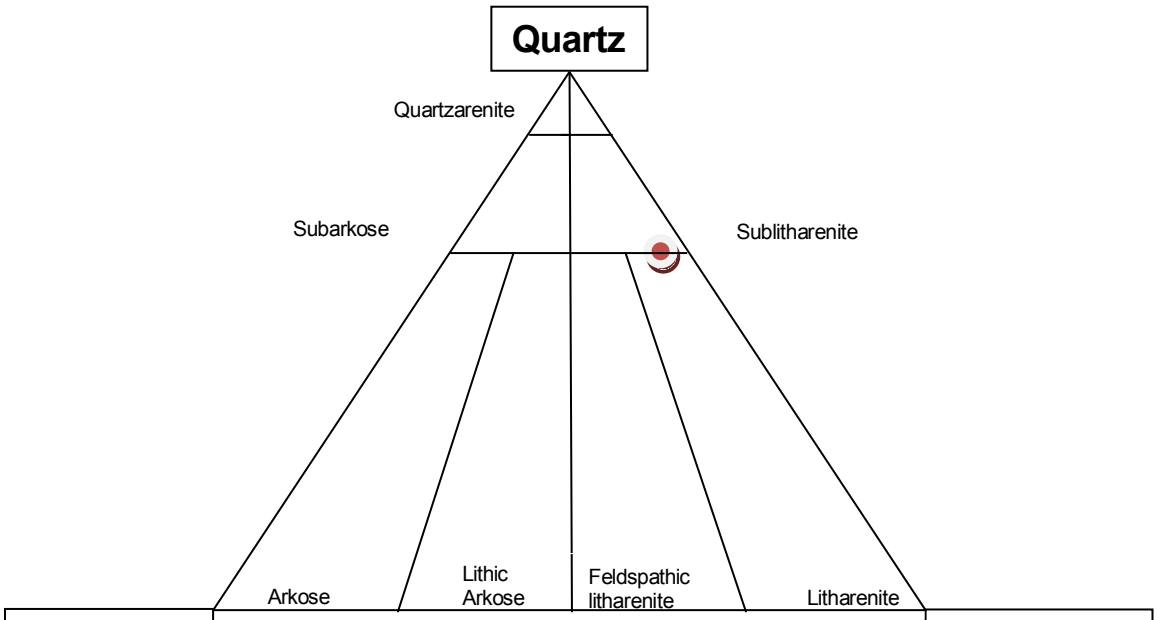

Figure 11: QFL diagram for litharenite core sample (Pettijon et al. 1987)

The high share of rock fragments (Figure 12) is indicator for domination of mechanized weathering and the short transport distance of this sediment. This can also be seen in the angularity of the grains. It should be noted that the structure of these sediments is grain supported, thus matrix (clays and other fine grained material) makes up only a fraction of the core minerals (>5%) (Pettijon et al. 1987).

The sample has a grain supported structure with long grain contacts and some subordinate point contacts. The roundness of the siliciclastic grains is sub round to very angular with moderate to good sorting.

mono crystalline quartz	39%
poly crytalline quartz	5%
isolated feldspar grains	2%
crystalline rock fragments	12%
traces of bioclasts (seashells)	14%
dolomite grains	13%
isolated micas flakes	1%
glauconite	1%
Fe- dolomite cement	1%
calcite cement	2%
carbonate fragments	3%
clay matrix	2%
heavy minerals	1%

Figure 12: Petrographic composition of core sample 1

The matrix contains traces of additional minerals namely mudstone, pelite clasts, plagioclase quartz cement and organic matter.

The reservoir properties have also been determined by OMV. The arithmetic mean of the effective porosity was determined via 34 samples and has a value of 24%.The porosity is defined as inter –particle porosity, which is only slightly reduced by cement. Additionally some porosity was generated by feldspar dissolution. The arithmetic mean of the permeability was determined with 94 md. The core sample has similar properties as are expected for the test reservoir, like porosity and clay content.

Water Composition

Water composition		Water Composition measured by RAG			
Additional expected species for reservoir fluid (calcualted)		Species		Input	Equilibrium
Species	Molality [mol/l]			Molality [mol/l]	
HCl	1.07E-11	Potassium [K^+]		3.03E-05	1.11E-05
NH3	2.95E-07	Calcium [Ca^{2+}]		2.05E-04	1.46E-06
H2S	1.13E-09	Chlorine[Cl^-]		6.33E-03	1.25E-03
HS-	6.54E-09	Carbon Dioxide [CO_2]		1.07E-06	4.36E-05
OH-	1.14E-07	Bicarbonate [HCO_3^-]		1.11E-04	9.34E-04
H+	1.53E-09	Magnesium [Mg^{2+}]		7.98E-05	1.02E-06
CO	5.41E-12	Sodium [Na^+]		5.95E-03	2.17E-03
N2	3.65E-09	Ammonium [NH_4^+]		1.08E-05	1.70E-06
H2	6.13E-08	Sulfate [SO_4^{2-}]		2.52E-05	1.36E-15
Fe+2	4.20E-09	I2		1.00E-05	6.60E-09
AlSiO4-	3.02E-11				
CaCl+	5.15E-07				
CaCl2	2.95E-08				
CaOH+	9.60E-11				
Ca(HSiO3)+	7.53E-11				
Fe(HCO3)+	2.34E-09				
Fe(CO3)	3.47E-10				
Fe+2	1.72E-08				
FeCl+	2.79E-09				
FeOH+	1.37E-10				
KCl	1.57E-08				
Mg(CO3)+	4.55E-09				
Mg(HCO3)+	1.59E-07				
MgCl+	3.63E-07				
MgOH-	6.38E-10				
Na(HCO3)	5.18E-06				
NaOH	6.15E-10				
Na(HSiO3)	5.95E-08				
HSiO3-	7.92E-09				
SiO2	2.12E-06				
CO3-2	5.41E-08				
I-	9.52E-10				

Figure 13: Water composition from the Hall Formation

RAG regularly takes water samples from some of their wells which are tested in the lab. The water samples are taken at the surface. For oil wells sampling is done in the separator and for gas wells the water sample is taken directly at the wellhead where a special installation makes it possible to extract fluids from the gas stream. Due to de-pressurization both methods must lead to a change in the composition of the water. Lassin et al (2011) states that even when extracted from the subsurface formation

water samples are prone to change in composition due to changing pressure and temperature conditions during the extraction (Figure 13). For the method applied by RAG it can be expected that fluid composition might further be influenced by oxygen from the air because sulfide and iron ions in the fluid will react with it (Lassin et al. 2011).

The measurement of the water samples investigates speciation, salinity and pH. This data is essential for the simulation. If properly sampled it describes the conditions in the reservoir and makes clear if they are oxidizing or reducing. Still the samples taken are of use, as they give a general direction on the fluid composition in the subsurface. The salinity is important because it reduces the ability of water to dissolve methane and hydrogen (PETE Lecture. 2012).
The dissolved species in the reservoir water can be divided into major (<5 mg/l), minor (<5 mg/L) and trace components (<0,1 mg/L). The salinity is measured on the basis of chloride and sodium concentration in the liquid. For the Hall Formation Abereri (1957) found a range from 9 g/L for the upper and 18 g/L for the lower Hall Formation. This reduces the ability of the water to dissolve gases by a factor of 0.55 at a pressure of 100 bar (PETE Lecture. 2012).

Preparation of Core Data

Petrological data of two cores was taken as base data for the GEMS Simulation. The first one is from a typical storage reservoir with excellent reservoir properties low shale content and mainly stable quartz sandstone as a matrix. Here the focus will be on the cement and how it changes with increasing hydrogen content.
The second one is taken from a well with higher shale content. This is necessary to investigate the influence of hydrogen on the clay minerals which will give us also an idea of how the cap rock behaves when it comes in contact with the hydrogen rich gas.
To standardize both experiments, both cores where based on the pore volume, meaning that a standardized pore volume of 0.001 m³ was assumed (see Appendix 1). This was done to have the same amount of hydrogen in both of the simulations available so that the amount of reactant available would be the same for both cases. The XRD analysis provided the percentage amount of the single rock

components which then could be recalculated to the actual weight for each of the minerals.

The clay minerals however proved a little problematic because only there shares of the groups (namely illite, smectite, chlorite) have been provided from the XRD-Analysis but not their actual minerals. Thus I made some assumptions with the help of RAG's geologist's team to choose the proper clay minerals which they usually encounter in their reservoirs (Figure 14). The assumptions where, that the clay minerals where substituted by their mineralogical endmebers.

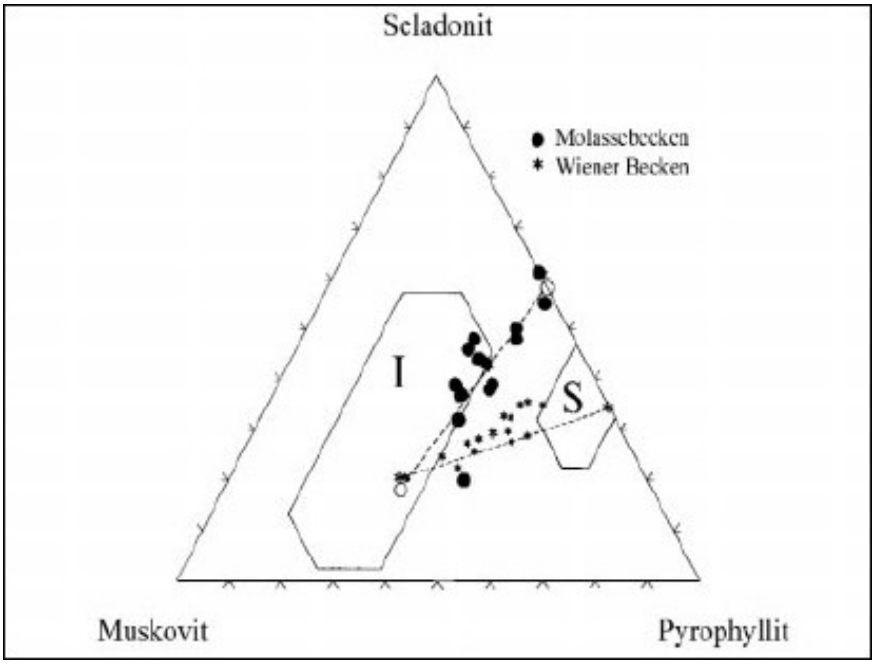

Figure 14: Comparison of clay distribution

Measurement in core samples from the molasse and the Vienna basin. Octahedral-, tetrahedral- and interlayer potentials of I/S are plotted in the muscovite-pyrophyllite-seladonite diagram. Gier 1998

Additionally data for clay minerals, concerning the formations of upper Austria was provided by Gier (1998). She states that in general the smectites and the illites of the investigated formations have the structural formula

Smectite: K0.14 X+0,44(Al1,10 Mg0,46 Fe0,36 Ti0,01) Si4,03 O10 (OH)2
Illite: K0.44 X+0,19(Al1,26 Mg0,42 Fe0,38 Ti0,01) (Si3,52 Al0,48) O10 (OH)2

With depth these formulas change due to illitization. The cores investigated by Gier (1998) are from a reservoir slightly (~150m) deeper than the ones targeted by the simulation.

Methodology

Following this the modelling section will describe the thermodynamic modelling program GEMS which was used to assess the processes hydrogen triggers in the reservoir. This will include the basic equations used as well as the assumptions made by the program itself. Finally the last section is dedicated to the assumptions made via the data gathering process. This section includes fluid data of the reservoirs, behaviour of the clay minerals and behaviour of the sulphates in respect to changes in the modelling result.

Gibbs Free Energy Minimization (GEM)

This section describes equations and laws which explain thermodynamic modeling. For this purpose it is necessary to understand the basic thermodynamic principles. Starting from the basic second law of thermodynamics this section will explain how it is used to arrive at thermodynamic equilibrium.

The Gibbs free energy of a system is defined as the maximum amount of non-expansive work that can be extracted from it (Perrot 1998). If the initial and final state of a reversible process is well known then the Gibbs free energy ΔG (Equation 7) in a closed system is the work exchanged by the system with its surroundings (ΔE) plus the work used for increasing the pressure minus the changes in entropy (Atkins 2004).

$$\Delta G(p,T) = \Delta E + V\Delta P - S\Delta T \quad \text{.....(7)}$$

The last term is of special interest because it defines (depending on the temperature) the spontaneity of the reaction. If ΔG is negative the reaction is favored (spontaneous) and if it is positive additional energy is needed to make it work (non-spontaneous) (Atkins 2004).

If temperature and pressure of the system are held constant, it will at some point reach a chemical and thermodynamic equilibrium, meaning that no further reactions will occur unless energy or other components are introduced (Garrels et al. 1990). Under constant temperature and pressure conditions the total free energy of the system is at its minimum. Chemical equilibrium is defined as the point where reactants and products have a concentration which has no further tendency to change with time

(Atkins 2004). This is an important point, because it makes the GEM time-independent which is different to geochemical modeling systems which use kinetic energies. The big advantage of GEM compared to the other systems is that is less complex and does not include ineffective (empirically derived) iterative processes (Krulik et al. 2009).

Normalizing Equation 8 to one mole and taking into account that G is an extensive property the free energy for a single species can be written as

$$\Delta G^\circ_f = \Delta H^\circ_f - T\Delta S^\circ_f \quad \text{.....(8)}$$

To get the Gibbs free energy of the whole system (Equation 9), ΔG°_f is summed up over all species. This is done by introducing the stochiometric coefficient ν_i which is negative for reactants and positive for products.

$$\Delta G_r = \sum_{i=0}^{reactants\&products} \nu_i \Delta G^\circ_{f,i} \quad \text{.....(9)}$$

At equilibrium ΔG_r is zero because the free energies of the products and that of the reactants cancel each other out.
Another way of explaining the equilibrium of a system is via the equilibrium constant. It is defined as the ratio of the activities of the products of a reaction to the reactants of that reaction (Equation10). The exponent is the stoichiometric number of moles from the used reaction.

$$K = \frac{[C]^\delta [D]^\varepsilon}{[A]^\alpha [B]^\beta} \quad \text{.....(10)}$$

The relationship of ΔG_r too K can be seen in Equation 11.
Most of the equilibrium constants can be taken from thermodynamic databases where tables are available (Garrels et al. 1990).

$$\Delta G_r = -RT \ln K \quad \text{.....(11)}$$

For the following model most of the species where already available in the database provided by GEMS. GEMS offers the possibilities to implement new minerals into its database. If the necessary thermodynamic data of the mineral is known, then it can simply be entered into the database and GEMS itself calculates the missing data.

GEMS needs at least the entropy, the heat capacity and the Debey-Hückel activity coefficients as well as the temperature range at which this data is valid to generate a chemical species in the GEMS database. The activity coefficients are originally derived empirically and describe the deviations of chemical mixtures from ideal behavior. This means that they compensate for the interaction effects between chemical species by modifying its concentration. Gases are also adjusted for non-ideality by scaling partial pressure by a fugacity coefficient (Garrels et al. 1990). The extended Debey-Hückel equation offers the opportunity to approximate some of these coefficients. The entropy to calculate the free energies of the clay minerals was taken from the database of Wilson et al (2004).

I tried to implement montmorillonite into the database, which is one of the most prominent clay minerals in the examined formations. However, the assumptions Wilson et al (2004) did for the activity coefficients (temperatures above 250°C) did not work for the proposed model. Therefore I chose to stick to the given species and substituted montmorillonite by a phylosillicate end-member already given in the database.

Equilibrium calculation

Just as an introduction I want to state again that the results of the GEMS simulation are by no means time related. A simulation run shows what would happen if the mixture or in our case the model, is given infinite time to reach geochemical equilibrium. Thus it will be necessary to compare the results with and without the titration of hydrogen, to find out which of the changes in the model are the results of hydrogen injection. A good example are the detritus components of the reservoir like the feldspar. It is not generated in the reservoir and needs certain conditions to be stable. Thus it can be predicted that in the end no feldspar will be present in the

results of the simulation even without hydrogen injection. The reason why this program was chosen instead of other geochemical modeling tools is, that it can be easily adjusted to different reservoir conditions by simply adding new species or canceling others out.

To understand the working principle of the GEMS modeling system it is simply necessary to imagine a piece of calcite which gets partially dissolved in a glass full of acid. At some point the pH of the whole system will arrive at a point where calcite is stable and no longer prone to being dissolved. Thus a thermodynamic equilibrium is reached (Krulik et al. 2009). If just two or three substances are added to our "brew" this can still be solved by hand. However in this case where it is necessary to describe and model a whole subsurface system many more chemical species in different phases are added, thus making it necessary to use a system of non-linear equations. To find the minimum of this equation system computer tool (MatLab or similar software) are needed.

GEMS minimizes the total Gibbs energy G of the whole chemical system. The Gibbs minimum is a fundamental criterion of equilibrium in an isobaric-isothermal system. The program takes all chemical species and dependent components into consideration and allows all related gaseous, aqueous and solid components related to the base ingredients during the whole calculation. Therefore not only the ingredients will be shown in the solution, but also the products of their reactions. Also the program differentiates between the different aggregates of the chemical species. For example hydrogen can either be gaseous or dissolved in water and GEMS considers both forms in the input as well as in the output.

The system solves the non-linear complex equation system for equilibrium and can thus simulate very complex, heterogeneous multi-phase systems with many non-ideal solutions in a single numerical run. (Krulik et al. 2009)
The goal of the GEMs forward calculation is to find the phase assemblage at equilibrium for a defined system. For this system T, p, b, g_0 and parameters of mixing in solution phases have to be provided. With T being the temperature of the system, p being the pressure, b being the bulk composition and g_0 being the standard Gibbs energy of each component.

To now find the equilibrium, it is necessary to find those dependent components and their amounts so that G(n(x)) (total Gibbs energy function)has a minimum. For this the equation system is given as

$$A * n^{(x)} = n^{(b)} \quad \text{.....(11)}$$

where n(b) is the input vector of the bulk composition b and A={a_{ij}, i ϵ N, j ϵ L} is the matrix of formula stoichiometry coefficients of species (Karpov et al. 1997). G(n(x)) is defined as

$$G(n^{(x)}) = \sum_j n_j^{(x)} v_j \quad \text{.....(12)}$$

where v j l the normalized chemical potential of j-th dependent component which is defined as $v_j = \frac{g_j^0}{RT} + \ln C_j + \ln \gamma_j + \Theta$ .....(13)

Here g_j^0 is the standard Gibbs molar free energy function at the defined temperature T (no pressure dependents. The second term C_j is the concentration of components and is defined as the mole fraction x_j for gas condensed mixtures and water solvents. For multi component phases and aqueous electrolytes it is defined by the molality m_j. The third term defines the chemical activity of the different species and is a function of the respective phase composition. It has to be calculated during each iteration step because of the non-ideal mixing in each phase.

The final term Θ is defined by Krulik et al (2004) as conversion into the rational scale and depends on the chosen standard state. This means that it is substituted for gas phase components with ln p, for aqueous species with 1-x_w (x_w being the mole fraction of water in the aqueous phase), $2 - x_w - \frac{1}{x_w}$ for water solvents and finally 0 for solid mixture end members and pure phases.

The method used by GEMs to find the solution from the above problem is the so called Interior Points Method. This algorithm uses the Karpov – Kuhn – Tucker conditions to simultaneously find the primal $\hat{n}^{(x)}$ (amounts of dependent components)

and the dual u solution (chemical potential of independent components). The three conditions that have to be met are defined in the following equations.

$v - A^T u \geq 0$ Stability (dual thermodynamics)……...(14)

$A\hat{n}^{(x)} = n^{(b)};\ \hat{n}^{(x)} \geq 0;$ Mole balance, non-negativity……... (15)

$\hat{n}^{(x)}(v - A^T u) = 0$ Orthogonality (Dependent Components selection)…(16)

These criteria help to define which components are unstable and have to be eliminated, giving GEMs the possibility of finding a stable phase assemblage even for highly non-ideal phases.
The first condition defines, that for each species with the concentration C_j in its phase, the primal chemical potential v_j numerically equals the dual chemical potential (Karpov 2001).
For the second criterion Karpov (2001) states that:" From the duality theorem, it follows that the GEM dual solution u_j values (Lagrange multipliers) are chemical potentials of independent components at the equilibrium state of interest. u_j has the same value in all co-existing phases".
The third condition is the condition of linear independence from the molar amount of unstable species and phases. It defines the basis of Karpov's phase stability criteria.

With the basic knowledge now obtained a closer look can be taken at the code. To compute concentrations and activity coefficients of species in different phase's generic dual thermodynamic equations (GDTE) are used. The dual thermodynamics (DualTh) approach is used because the thermodynamic data of solid solutions is still sparse as they are very difficult to obtain experimentally (Kulik 2005). GEMS derives from the GDTE the equations to calculate the activities of the different species, the activity functions such as pH, pe and Eh, as well as the saturation indices of single component condensed phases. The GDTE is derived by expanding the first Karpov-Kuhn-Tucker condition (Equation. 5) which was mentioned previously. For this the first condition (Equation 14) is taken and re-write it with indexes obtaining

$$\frac{g_j^0}{RT} + \ln C_j + \ln \gamma_j + \Theta - \sum_j a_{ij} u_i \geq 0 \quad \text{.....(17)}$$

implying that $v_j \geq \eta_j$ where η_j is the dual chemical potential given as

$$\eta_j = \sum_j a_{ij} u_i \quad \text{.....(18)}$$

For the GDTE $\eta_j = v_j$ and Equation 18 can be re-written obtaining

$$\sum_i a_{ij} u_i = \frac{g_{j,T}^0}{RT} + \ln C_j + \ln \gamma_j + \Theta \quad \text{.....(19)}$$

This equation can solve activities down to 10^{-20} because C_j and γ_j are both functions of the primal solution vector. All species below these values are zeroed for convergence reasons. For those species GEMS uses the DualTh activity equations which are described in detail in Kulik (2009).

Calculated Properties

Now the activity functions (pH, Pe, Eh) can be derived from the DualTh equation. Normally these functions would be determined from the aqueous electron species $\ln a_e = -1 * u_{charge}$. With the DualTh approach of GEMS this is not necessary and the functions can even be determined without explicitly including H+. The benefit is that the calculations are more accurate because an estimation of the ion-size and the interaction parameters is not necessary and therefore the global error is reduced. Now pe can be redefined as $-\log 10 * a$ to get from this expression the equation for pe being:

$$pe = -\frac{1}{\log_{10}}(-u_{Charge}) \quad \text{.....(20)}$$

From this an equation for the redox potential can also be directly derived since pe*RT*Log10=F*Eh

$$Eh = \frac{RT}{F} * u_{Charge} \quad \text{.....(21)}$$

With F being the Faraday's constant. Finally the activity of H+ has to be added to the redox potential to yield the equation for pH.

$$pH = -\frac{1}{\log_{10}}(u_H + u_{Charge}) \quad \text{.....(22)}$$

These are now the same equations derived from DualTh which are used in the GEMS-Selektor code.

Assumptions

As a first assumption this model is assumed to be closed. This means that diffusion, gravity induced migration and water influx are not present for the system and that neither energy nor chemical species are introduced from outside.
The geochemical model is simply an expression of the reactions in the brine, mineral gas system. Once validated by comparison with physical experiments, it can be used to understand the pH buffering of the system by mineral solubility and exchange-reaction controls for other similar systems. To get the data for the simulation running, RAG provided core and fluid data of several reservoirs. Two of which have been chosen because core sample one is also from the Hall Formation and thus represents the best comparable fluid data and core sample two because its overall properties (permeability, porosity, water saturation) are the best match for the intended storage reservoir. Unfortunately there is no core or fluid data available from the intended storage reservoir. However this data could not be directly applied to the GEMS simulation and therefore some preparations and assumptions are necessary.

Thermodynamic Rock Data

The GEMS database and the slop07 database provide thermodynamic data for a wide variety of minerals and other species. For the non – clay minerals, this data can be used in the simulation. Solid solutions where not accounted for, but as was explained in the methodology the DualTh accounts for this.
Not so for the clay minerals. Due to the compositional complexity of these minerals it is very difficult to obtain representative data. Thus a compromise between the species which actually occur in the reservoir and those for which reliable data is available had to be found. In the end the assumption was made that each clay mineral group could be represented by one species in the simulation (see Appendix 1). I further decided to use the slop07 database because Lassin et al (2011) already conducted similar experiments with pure hydrogen in a clay formation. They tested different thermodynamic databases based on the solubility of hydrogen in pure water and found out that slop07 data matches best the solubility of hydrogen (see Figure 15). Note that Lassin et al (2011) used the database slop98 which is only the older version of slop07.

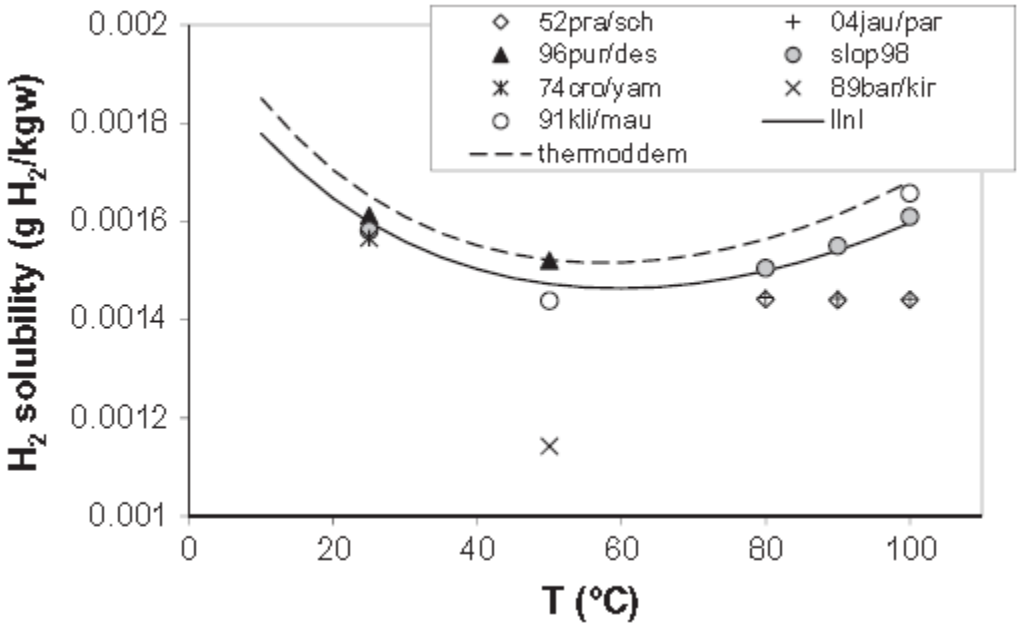

Figure 15: Hydrogen solubility in pure water (P_g= 1 atm)

Comparison between measured data points from the literature versus ones modeled with different thermodynamic databases (thermoddem, llnl, slop98). The program used to obtain this graph was (PhreeqC Lassin et al. 2011)

The issue of reliable thermodynamic data for clay minerals is discussed also by Wilson et al (2005). He states that at the uncertainties which are associated with the thermodynamic modeling of clay minerals are especially severe regarding the stability and robustness of the data. For clay minerals in water saturated systems he found that the field where the data is stable data is even smaller. In a saturated reservoir, the stability for the thermodynamic data has to be determined for each different P, T point and can hardly be used over wider ranges. He suggests that it would be possible to find better approximations with additional research. Wilson et al (2005) also mentioned that clay minerals like saponite and montmorillonite tend to be more stable in formations with a higher salinity. Gaucher et al (2009) observed a similar increasing stability of clay minerals with increasing salinity. He also states that the stability is also increased when carbonates are present in the reservoir. He however suspects that both conditions are only related to the Oxforian Calcov clay and suggests verification from other sources. The clay which Gaucher et al (2009) used for his experiments was a mixture of Na- and Mg rich montmorillonites. This would explain their stability in the high salinity brines and the pH buffering due to high carbonate content. However Wilson et al (2005) findings also apply to Fe-rich clay minerals, which in turn means, that the $Fe^{2+/3+}$ ratios of the mineral phases could be ignored.

Sulfides

Hydrogen is a potential electron donor and thus supports numerous reduction processes with different metal oxides. In case of sulfides, elemental sulfur could be released eventually leading to the generation of H2S (Truche et al. 2010). Due to this threat, a special effort was undertaken to estimate the stability of pyrite under potential reservoir conditions. Pyrite is the only potential source in the target reservoir for substantial amounts. The factors influencing the reaction of pyrite with other species are the pH value, the temperature, the microbiological activity, the hydraulic conductivity and the oxygen concentration in the dissolving fluid. At the surface pyrite immediately reacts with the oxygen in the air and therefore gets oxidized, or dissolved into water very quickly. Thus it can be concluded that pyrite under oxidizing conditions is not stable and will be dissolved as Fe2+/3+ or forms the insoluble $Fe(OH)_3$ (Nagy 2008). Unfortunately these iron ions could work as catalyst for the reaction of elemental sulfur and hydrogen to generate H2S (Garrels et al. 1990). However these

are oxidizing conditions which cannot be reached in the reservoir as long as oxygen is not injected, but never the less they describe the stability of pyrite. In the reservoir reducing conditions are present. As we can see from the Eh-pH diagram (Figure 16) pyrite is stable for those conditions where no oxygen is present.

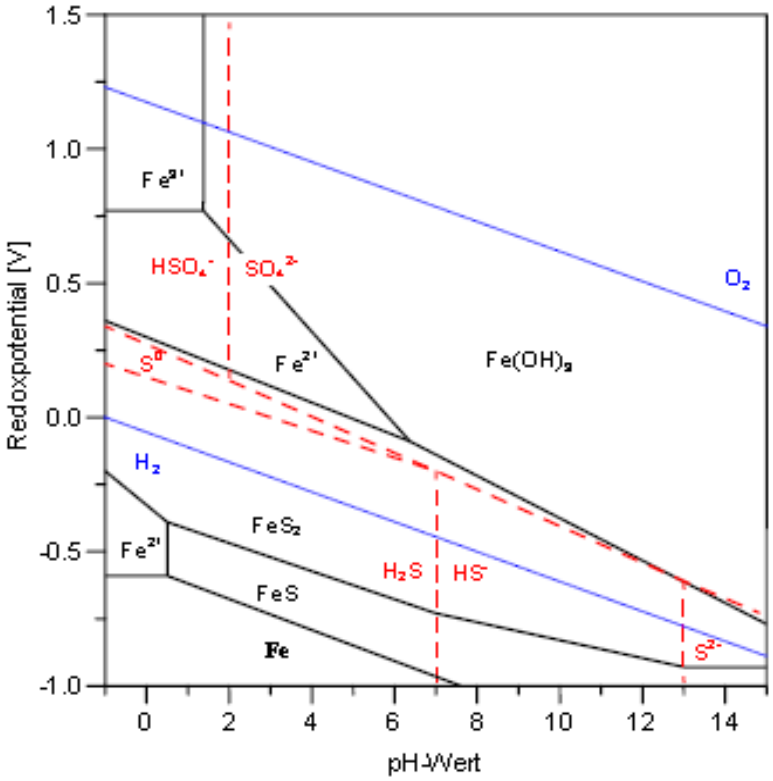

Figure 16: Eh-pH-Diagram for the Fe-S-H_2O system at 25°C
Nagy (2008)

A possible risk would be the injection of oxygen into the reservoir. As bio-gas could contain up to 2% of oxygen (Smitz 2011) this could be an issue, but Nagy (2008) states that oxidation reactions would be slow.
Nagy (2008) identified a possible reaction (Equation 23) that could produce hydrogen sulfide. However Truche et al (2009) states that it would need higher temperatures and probably a lower pH for the reaction to be quick enough to generate significant amounts.

$$FeS_2 + H_2SO_4 + H_2 \rightarrow FeSO_4 + 2H_2S \quad \text{.....(23)}$$

Even for temperatures above 90°C, Truche et al. (2009) found out, that redox reactions of hydrogen and sulfur on a larger scale would need a geological time scale.

For aqueous sulfate, which is also present in minor quantities in the reservoir, he predicts a half-life of 210'000 to 800'000 years at a pH of 2.5.

Truche et al. (2010) also conducted an experiment to find out which influences hydrogen has on pyrite under different physical and chemical conditions. For this purpose, fine grained pyrite was mixed with calcite (as a pH-buffer) and hydrogen in a NaCl solution, and put under different pressures and temperatures, to see the changes in pyrite stability. Additionally different initial pH's produced by addition of hydrochloric acid and caustic soda. The ranges of the different parameters where 90-180°C for temperature, 80-180 Bar for pressure and pH's of 6,8-10.
They found out that under alkaline conditions pyrite (FeS_2) reduces to pyrrhotite ($Fe_{1-x}S$) while releasing H_2S to the water and the gaseous phase. I was able to confirm these results with GEMS where the same setting as was used by Truche et al (2010) produced similar results.

However there are several reasons which speak against the fact that the same reactions could happen in one of the storage reservoirs. Notably Truche et al (2010) used fine grained pyrite to increase the reaction surface and stirred it in the liquid mixture to increase the reaction rate. Most of the experiments have been conducted under temperatures above 120°C which is 40°C above the temperature of RAG's storage reservoir. This is an important parameter because Truche et al (2010) stated that the temperature is one of the main driving mechanisms in the reaction of hydrogen and pyrite. The only experiments which could possibly be compared to RAG's reservoirs are those conducted at 90°C. Unfortunately those results were not discussed in that much detail as those from the higher temperatures, however the observed volumes of reduced pyrite and generated H_2S where mere traces. Additionally it was observed by Gaucher et al (2009) that the addition of siderite, dolomite and calcite to the pyrite – hydrogen mixture buffered pH and prevented the reduction pyrite.

Preparations and Experimental Setup

As mentioned previously, the first step to set up the model is to identify the mineral, aqueous and gaseous species which are present in the target reservoir (see Appendix 1). Additionally the pressure and temperature conditions of the target reservoir are identified and established in the model.

The existing reservoir is not in equilibrium as it still contains minerals which would normally not exist in this milieu (e.g. feldspars). Therefor the first step after entering all the known and assumed species into the model was to equilibrate the model. An additional assumption here was a water saturation of 100%, to get undisturbed initial conditions. GEMS has a built in function that automatically generates equilibrium conditions for the entered geochemical system. It should be noted that this is done every time when a new composition is entered. In GEMS each model generated is independent of the previously generated and has its unique composition.

Even though GEMS does generate equilibrium, it tends to generated minerals which would usually be not present in the reservoir. As GEMS takes into account all possible minerals in its database, some of them needed to be enabled (Graphite, Magnetite) in order to achieve suitable results.

The next step was to uniformly decrease the water saturation form 100% to 20% as is custom in the target reservoir. This was done via the built in titration function which I used to gradually reduce the amount of water while increasing the amount of the hydrogen methane mixture in the model. The titration function makes it possible to change the amount of a species in the system stepwise which makes it possible to observe the influence this species has on the system. In this first step, the pressure and the temperature where kept constant to observe only the effects of the gas on the system. It should be noted, that I calculated the amount of gas entered into the model via the ideal gas law to take the reservoir conditions into consideration.

This was the base case simulation where I added gas mixture of 85% of methane and 15% of hydrogen to the model. In a next step I changed the concentration of hydrogen in the gas. This was also done via the titration function where I gradually reduced the

methane fraction and increased the hydrogen fraction. All this was still done under constant pressure and temperature conditions.
To account for temperature and pressure changes, I used the so called batch function. This is used to change temperature and pressure conditions. The pressure difference used is the range measured in one of RAG's storage formations during a storage cycle. The temperature range is only minor and represents the difference in gas temperature injected during low temperature periods up to reservoir temperature. I did this to find out whether the temperature and the pressure do also have an influence on the hydrogen behavior in the target reservoir.

Based on the calculations done by Dilip et al (1998) the author did an assumption on the probable loss due to diffusion for the target reservoir. It was assumed that the reservoir is a perfect cylinder, which is covered by a clay seal of 5m thickness. The diffusion coefficient used was taken from the paper of Galle et al (1998). As it is a mixture of methane and hydrogen that is stored, the author assumed a similar diffusion coefficient for methane and hydrogen. Additionally the reservoir was assumed to be static (no flow) and the concentration of hydrogen in the gas was set constant. For all these assumptions the authors' model assumed a loss of 210 Nm^3 of gas per year. This was verified by using pure natural gas for the model. It is generally assumed for storage facilities, that over a period of 40 years the loss in working gas is about 2% of the volume. The model predicted a loss of 2,3% which seems to be reasonable. The author therefore assumes that diffusion has only minor influence on hydrogen migration in the subsurface.

Results

To find out the influence of hydrogen injection on the storage reservoir, different simulations have been generated. This includes the modeling of different water rock ratios because water saturation has an influence on the behavior of hydrogen, as well as different concentrations of hydrogen in the gas phase. Additionally the changing reservoir conditions pressure and temperature have been represented in the model, and are also changed during the simulation to identify their influence on the behavior of the methane hydrogen mixture. This chapter sums up the findings.

Influence of Hydrogen

Minerals Core Sample 1			Minerals Core Sample 2		
	Input	Equilibrium		Input	Equilibrium
Dolomite [$(Ca,Mg)(CO_3)_2$]	3.44	3.5	Dolomite [$(Ca,Mg)(CO_3)_2$]	3.16	3.17
Calcite [$CaCO_3$]	3.97	4	Calcite [$CaCO_3$]	6.6	6.59
Muscovite [$KAl_2(AlSi_3)O_{10}(OH)_2$	0.03	1	Muscovite [$KAl_2(AlSi_3)O_{10}(OH)_2$	0.14	1.33
Pyrite [FeS_2]	1.05	1.1	Pyrite [FeS_2]	0.89	0.89
Quartz [SiO_2]	33.88	36	Quartz [SiO_2]	17.86	20.22
Rutil [TiO_2]	0.13	0.13	Rutil [TiO_2]	0.15	0.15
Siderite [$FeCO_3$]	0.9	0.9	Siderite [$FeCO_3$]	1.39	1.39
Plagioklas [$NaAlSi_3O_8$]	1.46	1.2	Plagioklas [$NaAlSi_3O_8$]	0.84	0.83
Talc [$Mg_3Si_4O_{10}(OH)_2$]	0	0.2	Talc [$Mg_3Si_4O_{10}(OH)_2$]	0	0.77
Paragonite [$NaAl_2[(OH)_2\|AlSi_3O_{10}]$]	0	0.3	Celadonite [$K(MgAl)Si_4O_{10}(OH)_2$]	1.32	0
Celadonite [$K(MgAl)Si_4O_{10}(OH)_2$]	0.29	0	Pyrophyllite [$Al_2Si_4O_{10}(OH)_2$]	0.88	0
Pyrophyllite [$Al_2Si_4O_{10}(OH)_2$]	0.19	0	Greenalite [$Fe_3Si_2O_5(OH)_4$]	1.2	0
Greenalite [$Fe_3Si_2O_5(OH)_4$]	0.67	0	Kalifeldspat[$K(AlSi_3O_8)$]	0.4	0
Kalifeldspat[$K(AlSi_3O_8)$]	0.5	0	Kaolinite [$Al_2Si_2O_5(OH)_4$]	1.2	0
Kaolinite [$Al_2Si_2O_5(OH)_4$]	0.99	0	Annite [$KAl_2(AlSi_3)O_{10}(OH)_2$]	2.98	0
Annite [$KAl_2(AlSi_3)O_{10}(OH)_2$]	1.16	0	Phlogopite [$KMg_3(AlSi_3O_{10})(OH)_2$]	0.28	0
Phlogopite [$KMg_3(AlSi_3O_{10})(OH)_2$]	0.11	0	Garnet [$Ca_3Fe_2(SiO_4)_3$]	0.1	0.1

Figure 17: Core data for GEMS modeling

The data instability of the clay minerals is clearly visible in this chart as all of them are no longer present under equilibrium conditions.

As mentioned before two core samples of two different subsurface formations where compared. Figure 17 shows the results of the GEMS simulation without the injection of hydrogen. It should be noted that for the initial situation 100% water saturation was

assumed for both rock samples. Due to different porosities this means a water rock ratio of 0,48 for core sample 1 and 0,55 for core sample 2.
Here we can clearly see that the stable minerals such as rutile are unharmed when calculating the equilibrium even though GEMS allows other Ti species. This is also a good indicator that our previous modeling assumptions are correct and that the model works properly and does not produce some fantasy volumes or species. As was mentioned before the data for the clay minerals is not reliable, but I expected some of them to vanish as parts of the clay are also detrital. The clay is partially converted into micas which are shown in the increasing volume of muscovite. As was mentioned by Gier (1998) the boundary between illite and smectite are not so clear and thus one could under the right conditions be converted into the other one. Unfortunately that could not be observed in these models as data for illite or smectite is not yet available.

The output minerals from above represent the equilibrium state for both core samples as predicted by GEMS. It should again be mentioned that the results are time independent and only valid in closed reservoirs. This means that diffusion, gravity induced migration and water influx are not present for such a reservoir.

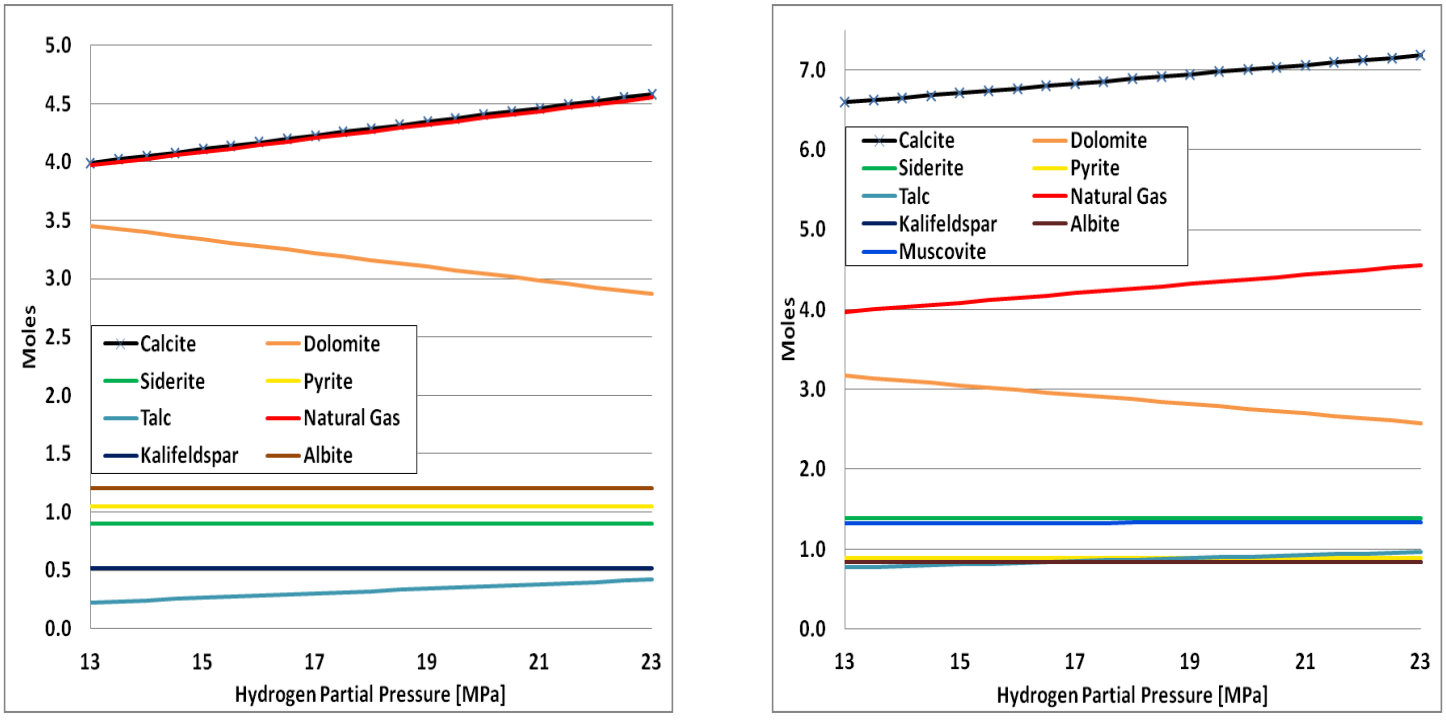

Figure 18: Hydrogen titration (Core 1 left, Core 2 right)

For constant pressure and temperature conditions

The next step after establishing equilibrium with 0 bar hydrogen partial pressure is doing the same simulation again, but now with hydrogen in the input parameters. It should again be noted that we do not inject hydrogen to the solutions from Figure 17, but instead we do a completely new simulation. Figure 18 shows the injection of hydrogen from 13 to 23 MPa hydrogen partial pressure of the pore volume for core sample 1 and core sample 2.

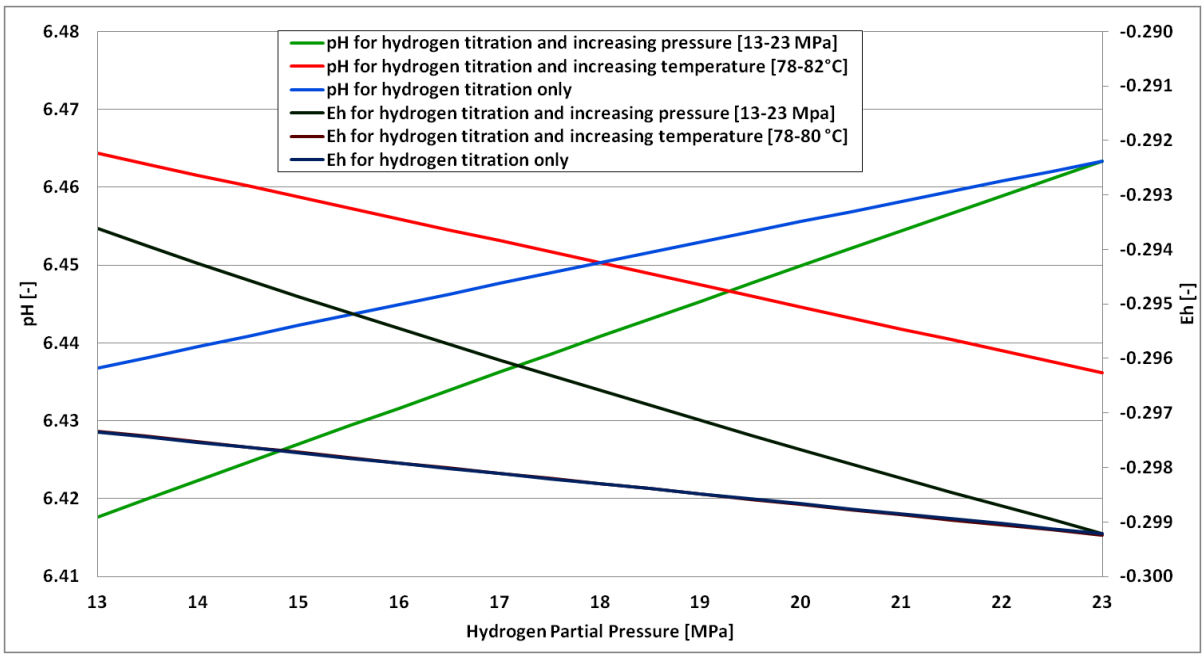

Figure 19: pH-Eh change during hydrogen titration

(Core sample 1)

For the minerals plotted, the same behavior on hydrogen injection can be observed. Due to the fact that the hydrogen addition slightly increases pH (Figure 19) some of the dolomite is dissolved while calcite and talc are precipitated. The overall converted carbonate volume is 14% for 100% of hydrogen injection. However at 10-20% as it is planned for RAG's storages the amount of converted rate is only 3%.

Equation 24 shows a possible reaction which would explain the de-dolomitization. As Machel et al (1986) describe it the process of dolomitization is the replacement of one calcium ion by a magnesium ion. This process depends on the Ca: Mg ratio in the solution and is therefore deemed plausible for this case.

$$5H_2 + MgCa(CO_3)_2 \;<=>\; CH_4 + Mg^{2+} + 3H_2O + CaCO_3 \quad \text{.....(24)}$$

This reaction would explain the increase of calcite and methane in the model. The Mg^{2+} which is represented as free ion here is also bound in talc which also slightly increases with increasing hydrogen concentration.

The pyrite also stays stable, which means that from this source rock no H_2S generation is expected.

From the minor minerals, only talc changes and starts to increase the volume. The pH-Eh diagram for core sample 1 show's that it increases for pure hydrogen injection, but does in fact slightly decrease with increasing temperature

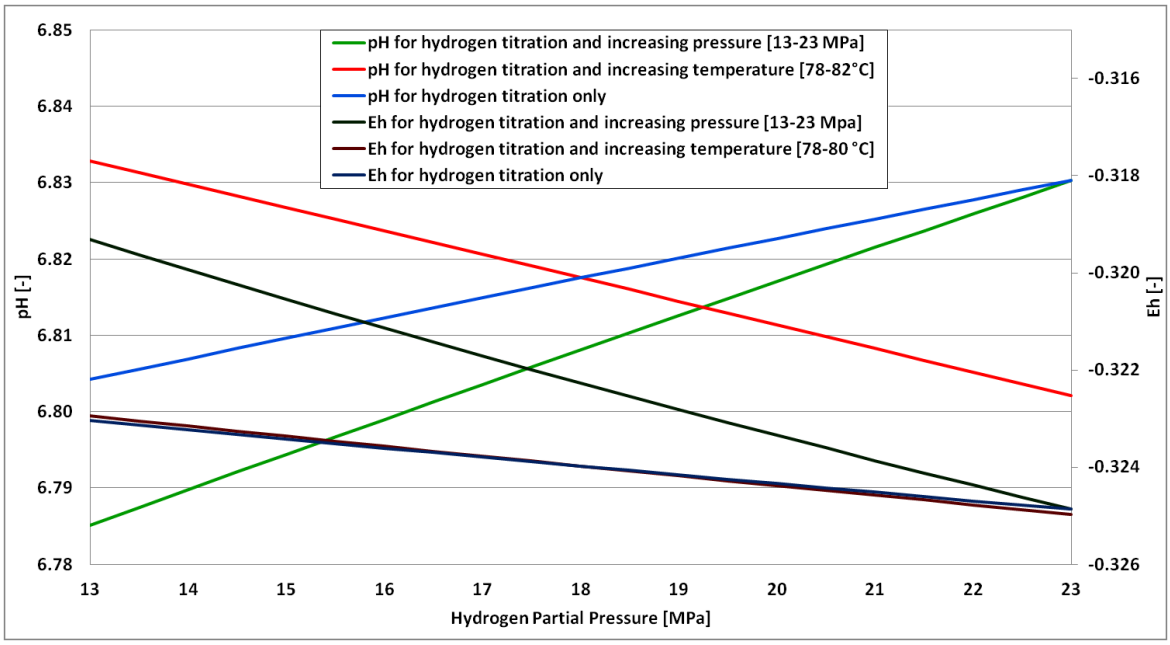

Figure 20: pH-Eh change during hydrogen titration

(Core sample 2)

A decrease in pH due to hydrogen injection can also be observed in core sample 2 (Figure 20). In this graph however the difference between the Eh lines can be seen. Here the pH is slightly higher than in core sample one which can be explained by the fact that the share of carbonates in the core sample is higher than in core sample one. Apart from this the behavior is similar, with increasing pH during hydrogen injection. The decrease in pH due to temperature changes is also true for core sample. It can be seen from the scale the changes are only in the range of 0,05 pH units.

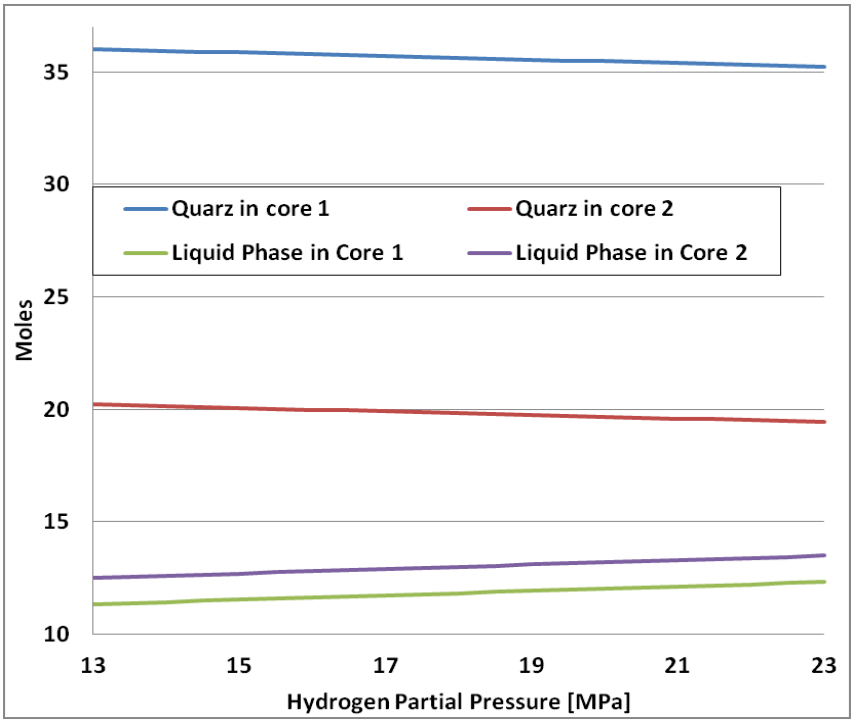

Figure 21: Quartz behavior

H_2 titration for core sample 1 & 2 [80°C; 23 MPa] major species

The decrease of quartz is influenced by the generation of H_2O during hydrogen injection which leads to a dis-equilibrium between solid and dissolved SiO_2 which needs to be compensated for.

It was observed previously (Figure 17) that quartz does increase its fraction when the model equilibrates. This is expected because most of the silica bearing minerals are not stable under such low temperature conditions (Garrels et al. 1990) and thus tend to be converted into quartz and during the titration with hydrogen the amount of quartz in the core sample slightly decreases. This can be related to the increase of the fluid phase. There is equilibrium between solid and dissolved SiO_2 which is changed when more water is added to the model, or as in this case water is generated due to hydrogen injection. Thus some fraction of the quartz dissolves. This can also be seen in Figure 21 for core sample one and two where a slight increase in dissolved SiO_2 can be observed.

Other changes in the composition of the core fluid can also be explained. The increase of HCO_3^- is an intermediate step of the de-dolomitization reaction presented above, were the CO_3 from the dolomite is first dissolved into the fluid and later precipitated as calcite. This would also explain the decrease in Ca^{2+} ions.

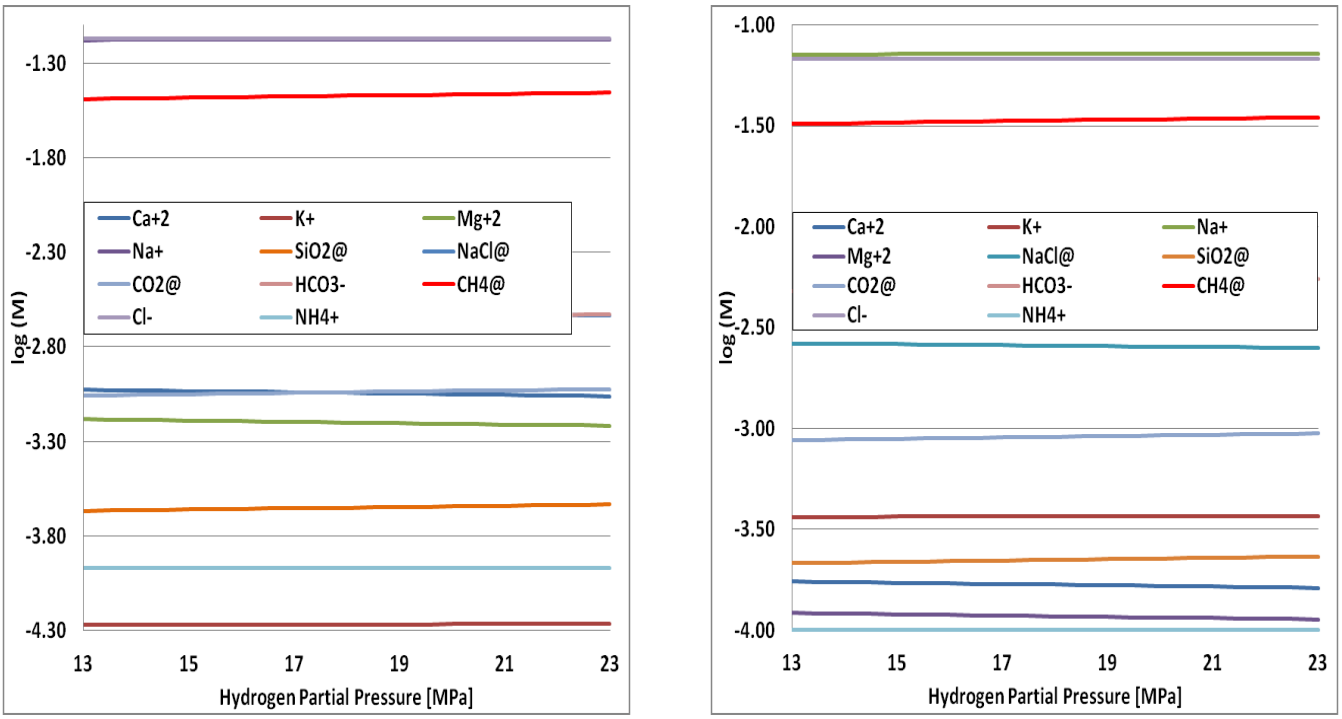

Figure 22: Dissolved species

H2 titration for core sample 1 (left) & 2 (right) [80°C; 23 MPa] aqueous species

The speciation of in the fluid can be used to determine the redox conditions of the reservoir as well as explain the dissolution and precipitation of some of the solid phases as for example quartz which was shown at the previous page.

The amount of aqueous Mg^{2+} decreases hand in hand with the increase of talc in Figure 18. Also the NaCl decreases because the equilibrium between the salt and its ions Na^+ and Cl^- is disturbed due to the additional amount of water (Figure 22.) generated during hydrogen titration (about 1 mol).

One thing that is unexpected is that the feldspars stay stable under the given conditions. Gaucher et al (2009) and Lassin et al (2011) state that these minerals are not stable and should be converted into clay minerals. It would have been expected that the kalifeldspar was converted into kaolinite which is stable under this low temperature conditions, but the calcite seams to prevent this converion.

$$2KAlSi_3O_8 + 9H_2O + H^+ \quad \Leftrightarrow \quad Al_2Si_2O_5 + 2K^+ + 4H_4SiO_4$$

As can be seen in Figure 23, there should be an increase in K^+ and H_4SiO_4 ions observed, but this could not be found in the model. The model also allowed gibbsite

and pyrophyllite to be generated, but GEMS did never consider them as stable phases. Instead GEMS always keeps equilibrium between muscovite and k-felspar. This equilibrium is never changed during the hydrogen injection (Figure 18).

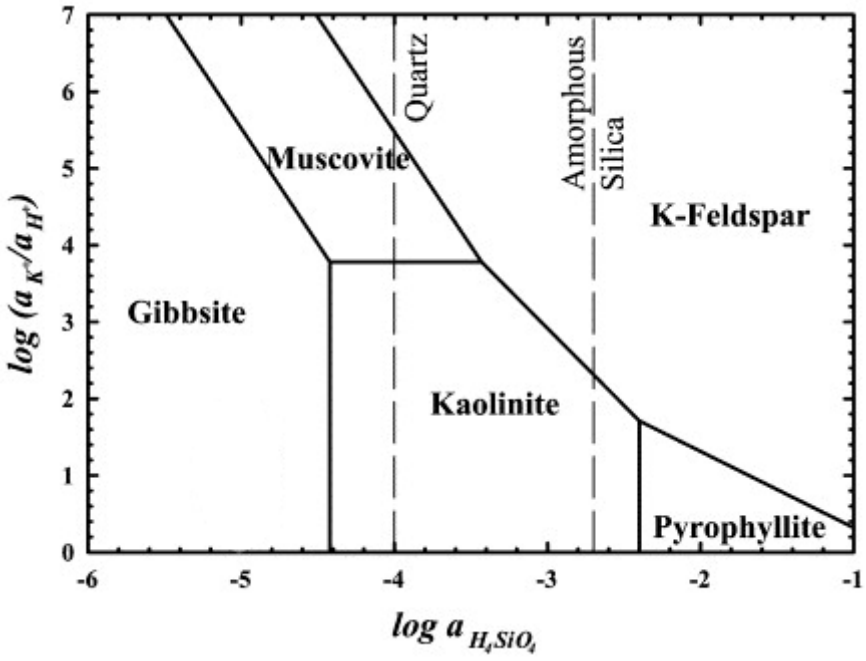

Figure 23: Feldspar stability field

Feldspar stability depending on K^+/H^+ concentration in the fluid (Le Roux et al 2006)

Temperature and Pressure Influence

Many chemical reactions are temperature sensitive because they provide additional energy for the reactions. The pressure has also an important rule for the balance between free and dissolved gases. Thus additional modeling was done to investigate the behavior of the reservoir under changing conditions. For that purpose, the temperature and the pressure were increased during hydrogen titration to resemble a typical storage cycle. It should be noted, that during injection the reservoir temperature normally slightly decreases but, after some time, again reaches initial conditions. Thus it is realistic to use this discrepancy between injection and reservoir temperature as a simulation variable.

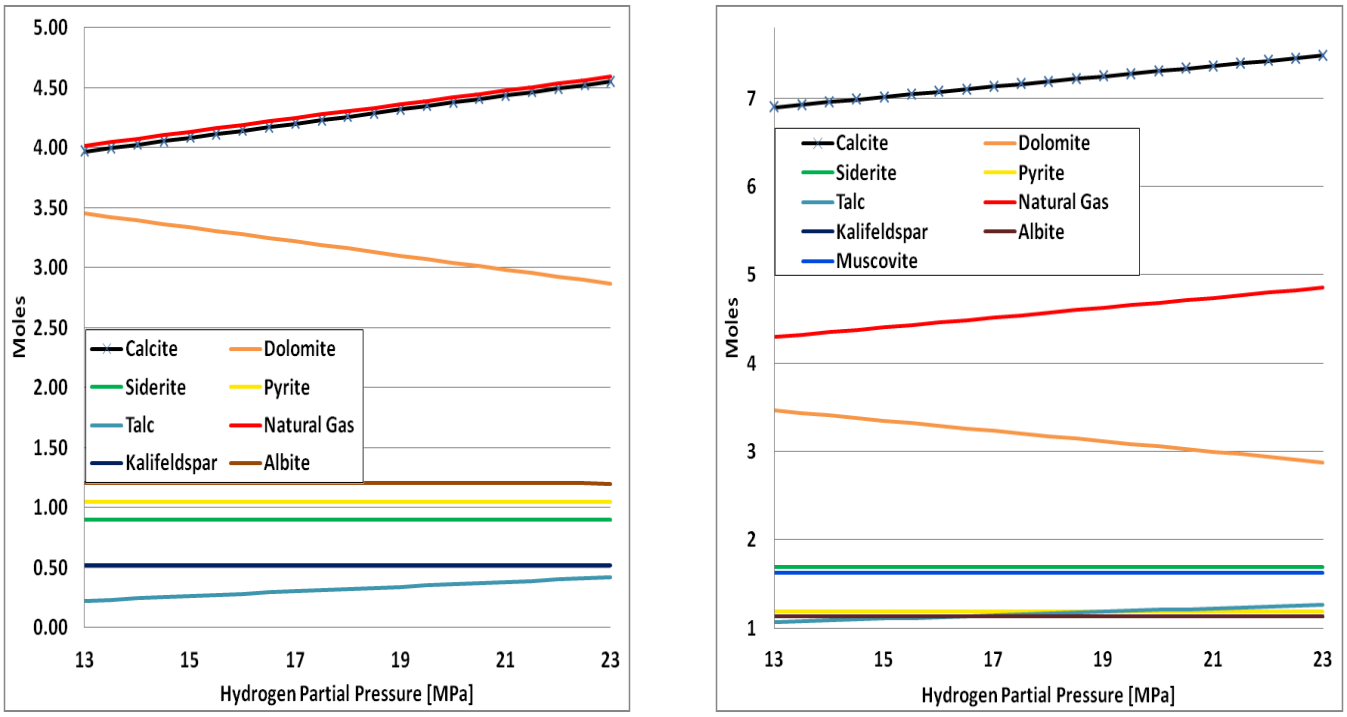

Figure 24: Non isobaric hydrogen titration (Core 1 left, Core 2 right)

H_2 titration and increasing pressure [80°C; 13-23 MPa]

Figure 24 basically looks the same as the plots in the previous chapter. However, when studied more closely it can be seen that the amount of free methane is slightly less than before. The reason is simply that the solubility of gases in liquids is pressure dependent. This can also be proven by the fact that the amount dissolved methane is

higher than in the previous chapter. Apart from this the pressure seems to have no influence on fluid speciation and mineral stability.

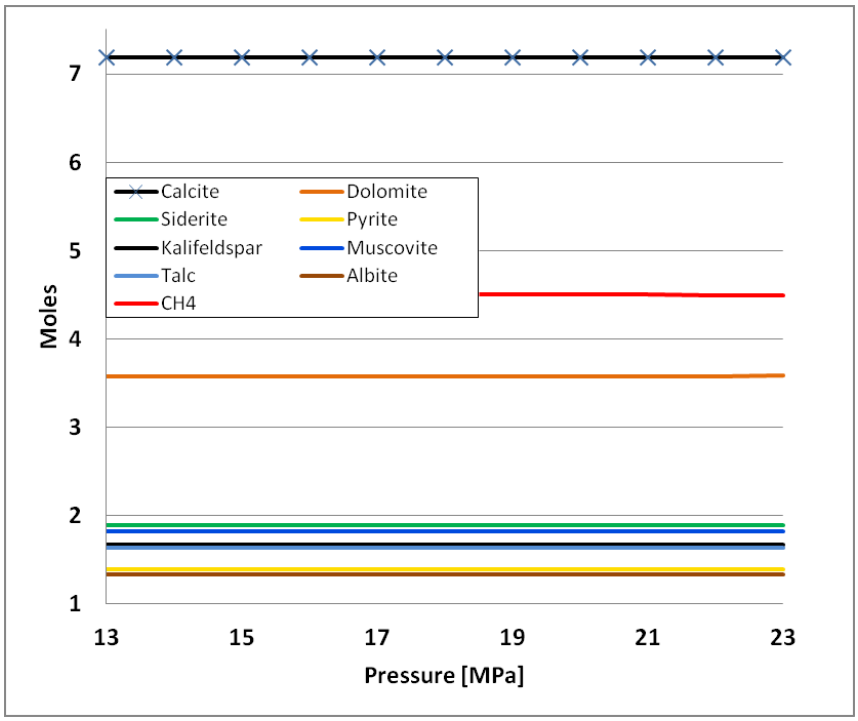

Figure 25: Increasing fluid pressure in core sample 2

Changing pressure from 13-23 MPa for core sample 2 [80°C]

Additional evidence that the pressure in this range has no influence on the setting is given in Figure 25. Here it can also be seen that only the amount of free methane slightly decreases at 20 [MPa] of hydrogen partial pressure. No other changes are observed.

A different matter is the change of temperature. As it was shown in the pH graphs (Figure 19. + 20), the temperature has an influence not only on pH but also on the carbonate stability. This influence is only minor because the temperature range applied ($\Delta T = 4°C$) is too small for significant changes. It however gives an indication that a greater change in temperature will change the equilibrium conditions.

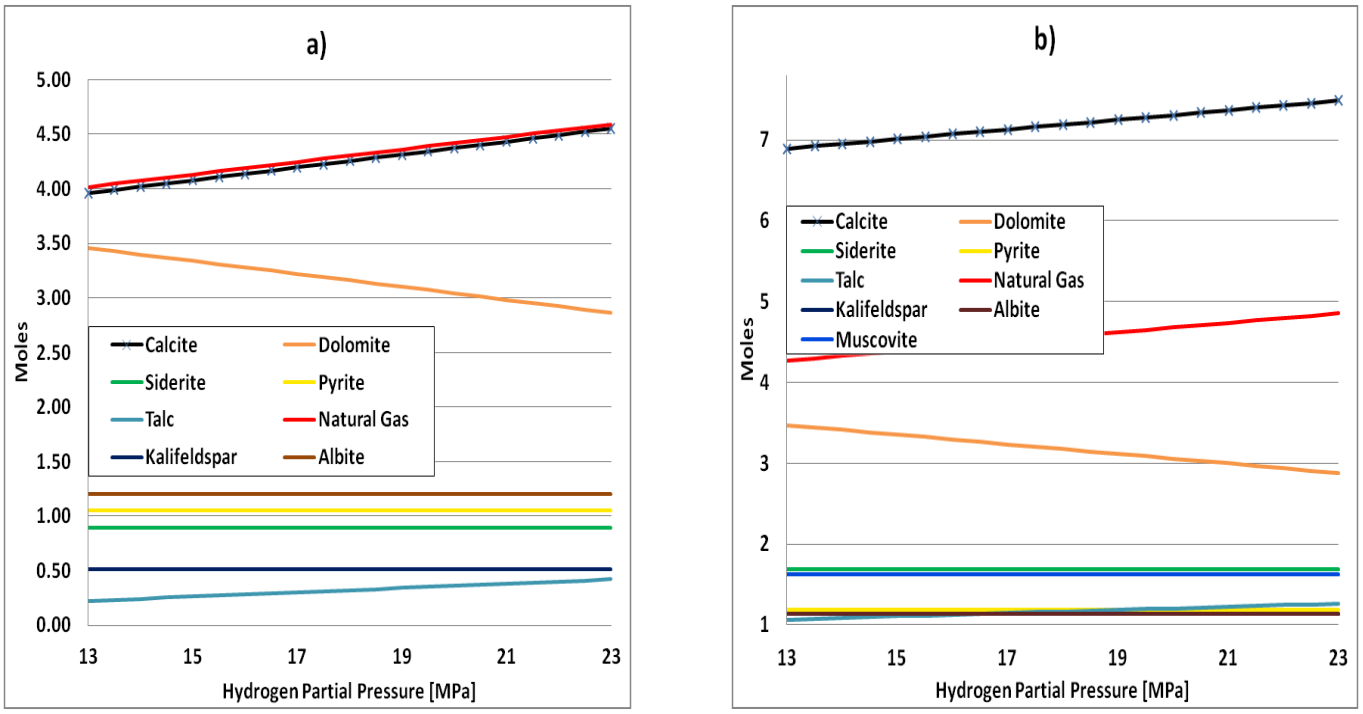

Figure 26: Non –isothermal hydrogen titration

Titrating hydrogen into core sample 1 (a)) and 2 (b)) there are changes in amount of dolomite and methane. In contrary core sample 2 (c)) was monitored while only changing the temperature. This is done to prove, that only the titrated hydrogen changes the composition of the core samples and not the change in temperature

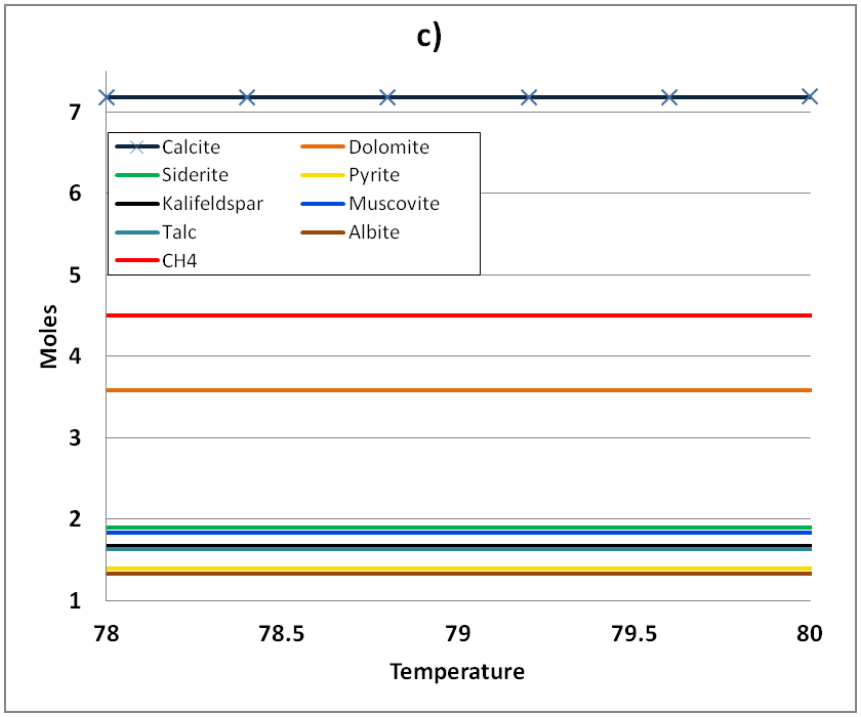

No evidence on changing conditions can be found in Figure 26. The reason is that the changes are that minor, (three points after the digit) that they are not visible in the plot. Increasing temperature over a wider range leads to significant changes in the reservoir that need to be discussed. It is not expected that the storage reservoirs will be heated up at any point, but there are still different temperatures in different reservoirs. Thus the temperature is viewed at a broader range to see its influence on the stability of minerals. For oil, gas and storage reservoirs, temperatures between 40 to 140°C can be expected. On this range no severe changes were observed in reservoir fluids. To prove that there are indeed variations the model temperature in the core samples was raised up to 200°C.

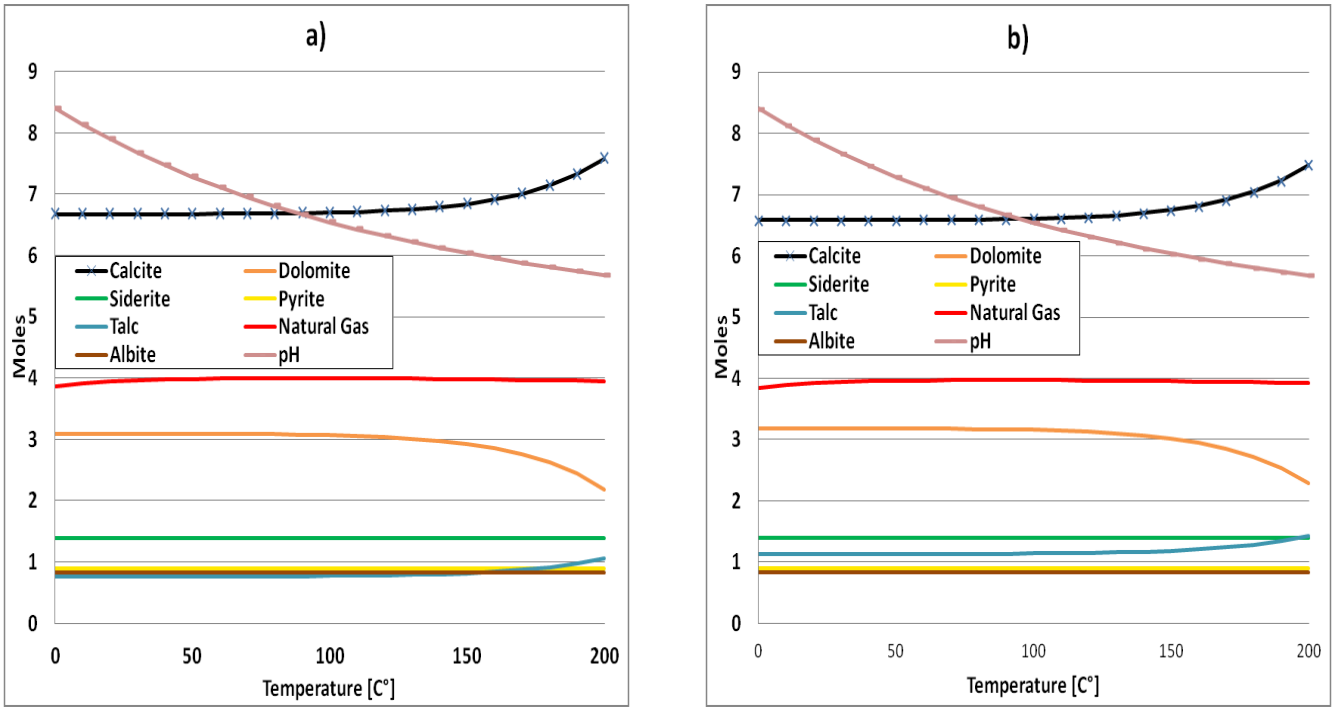

Figure 27: Temperature increase up to 200°C [23 MPa] (core sample 2)

On the left (a)), the temperature is increased in a core saturated to 100% by water at the right (b)) the water saturation is decreased to 40% and the rest of the pore volume is saturated with a methane-hydrogen gas mixture.

Figure 27 shows the influence of temperature on the chemical conditions in the reservoir. To see which influence the hydrogen has in this case, Figure 27 b contains a mixture of 15% hydrogen and 85% methane. Here changes from the hydrogen, namely the higher amount of talc generated can be observed. This hands additional

support to the hypothesis that titration with hydrogen fosters the conversion of dolomite to calcite.

For the minerals the simulation shows a reduction in the amount of dolomite coupled with an increase in the amount of calcite and decrease of pH (Figure 27). The explanation for this is an increase in H_2S generation (Figure 28). Above a temperature of 120°C, H_2S is produced in health threatening volumes. Still it is interesting to notice that hydrogen sulfide is generated in the reservoir even if it are only smaller amounts.

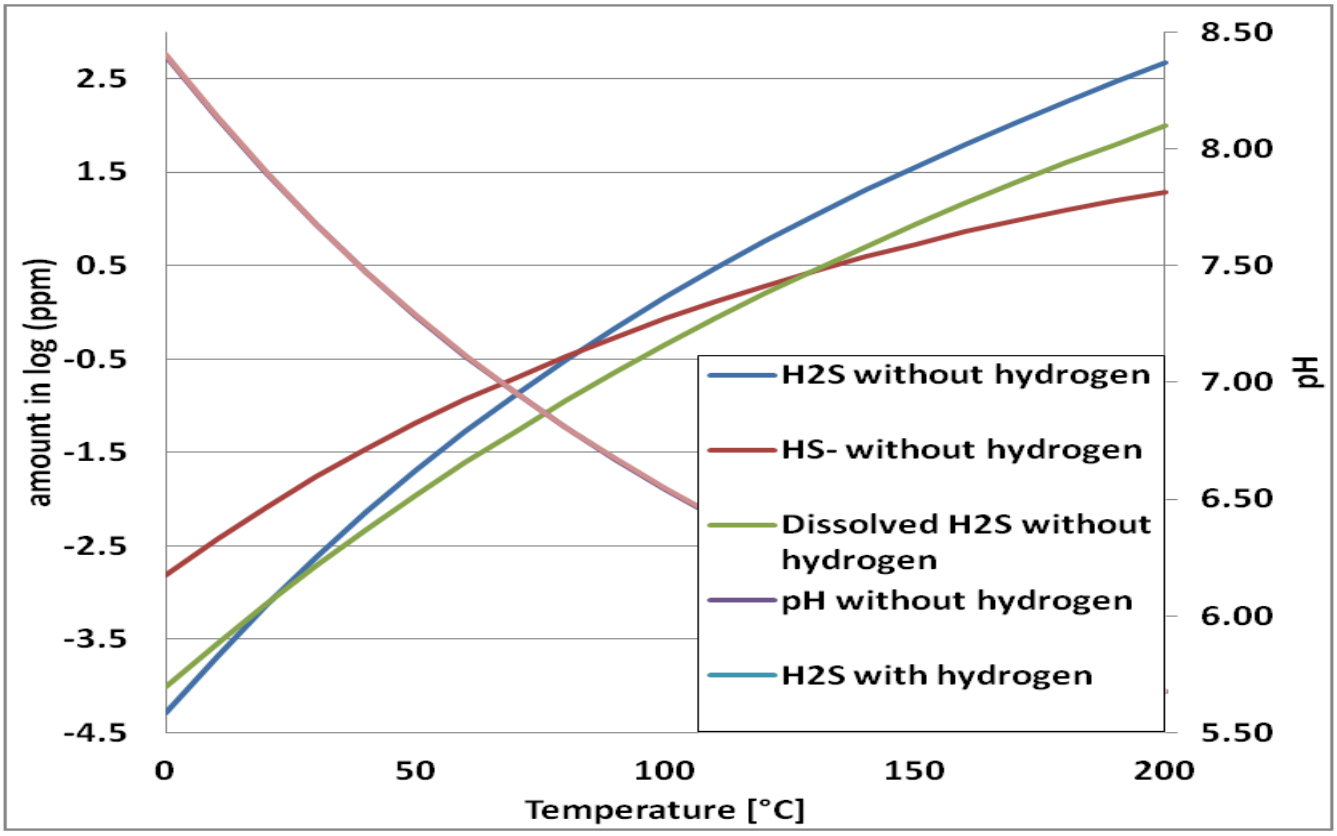

Figure 28: H_2S generation with increasing reservoir temperature (core sample 2)

Increasing temperature for core sample 2 [0-200°C; 23 MPa; 0 and 15% hydrogen]

The results are nearly the same (discrepancies in the third decimal point), therefore only one curve can be seen were actually two are plotted.

There is a small difference between the plotted curves, but none that is obviously noticed. Observing the values clearly shows that hydrogen does slightly buffer the pH.

Titration with supercritical hydrogen

A question arose during the thesis which could not be easily answered with GEM's. The question was:" What would happen if we inject hydrogen for so long that all possible reactions that could happen with hydrogen would have happened. This would be the point when free supercritical hydrogen would exists in the mixture. Additionally this answers the question what happens to the hydrogen. How much is dissolved, how much reacts with other species and how the pH is influenced. The point where free hydrogen gas exists in the reservoir was found via a "what if" calculation. It is the point when 119mol of hydrogen are added to the system. This matches approximately 20 times filling the core sample with pure hydrogen under static conditions and for infinitely long time. It should be noted that the point was defined as the point when the first mole of free hydrogen gas exists.

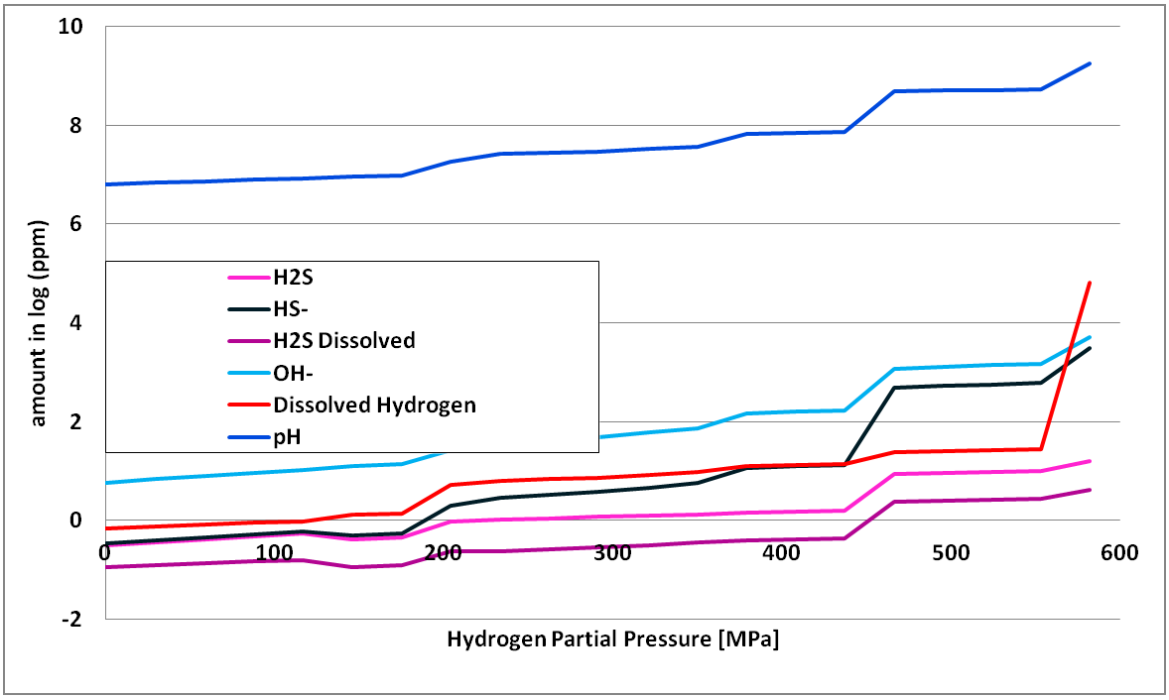

Figure 29: Hydrogen injection up to 120 g

H_2 titration for core sample 2 up to 600 MPa H_2 partial pressure [80°C]; trace species

Figure 29 shows the behavior of the gas phase during the titration of hydrogen into the core sample. The injection of 120g of hydrogen can be compared to a hydrogen partial pressure of up to 580 MPa. Thus some things that happened during the titration can be ruled out as relevant immediately such as the generation of mineral

like diopside, which is a pyroxene only stable under very high pressure. Still this titration explains some of the reactions happening in a reservoir, and can help making predictions on long time storage. Starting with Figure 29 we can see that OH^- and with it related the pH increases during hydrogen injection. The log plot also shows a steep increase in HS^- generation which further increases the pH. Hydrogen sulfide is not that prominent, but is generated in greater volumes after most of the hydrogen is already titrated.

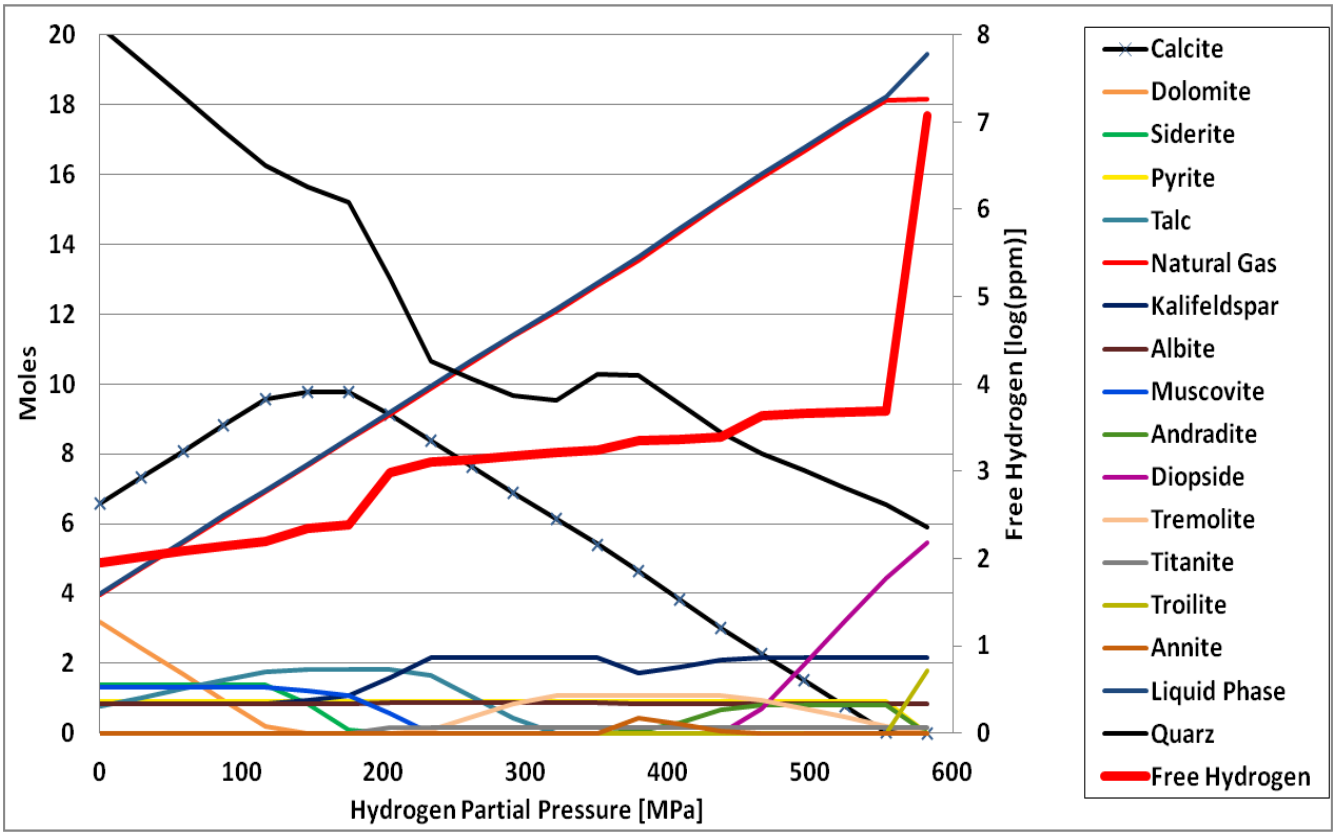

Figure 30: Mineral dissolution and generation during hydrogen titration

H_2 titration for core sample 2 up to 600 MPa H_2 partial pressure [80°C].

Figure 30 should be regarded with care. As it was stated before, minerals such as diopside, tremolite, and titanite are only stable in this system because of the high pressure. Still there are some interesting trends to observe. All carbonates are dissolved during titration, but due to the increasing pH, calcite is the most stable and only starts to dissolve after all other carbonates vanished (Figure 31).

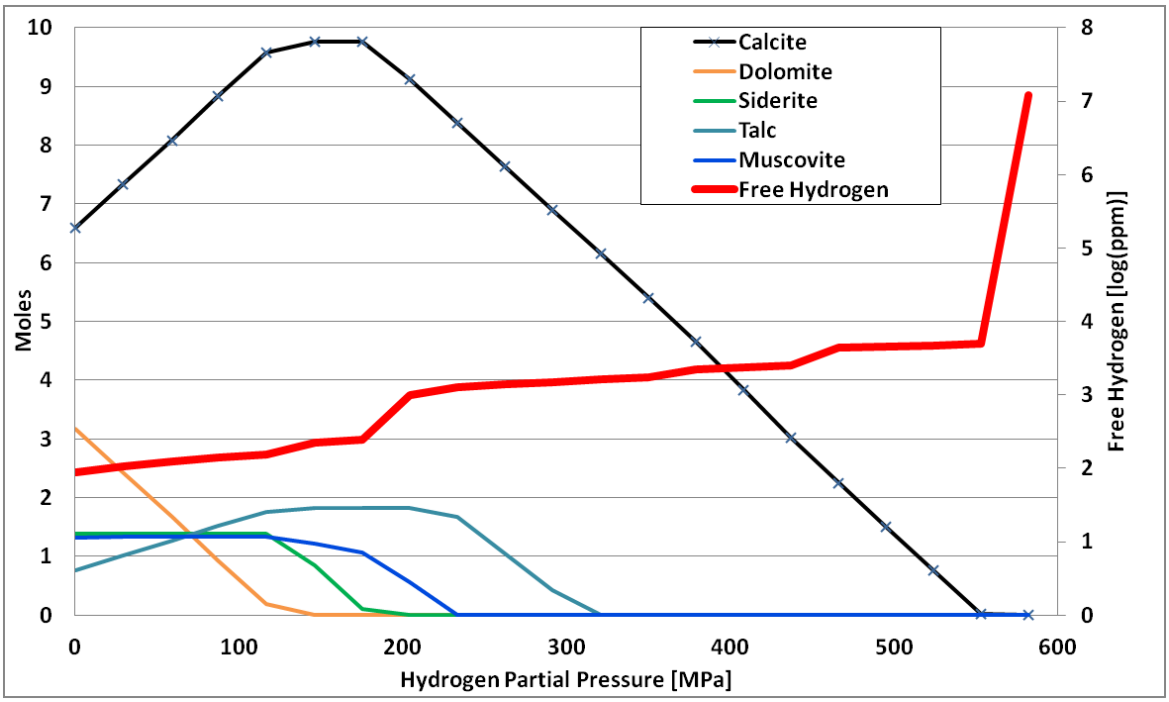

Figure 31: Carbonate stability during hydrogen titration

H_2 titration for core sample 2 up to 600 MPa H_2 partial pressure [80°C]; Major Mineral Relations

The silicates start to develop many different species using parts of the ions dissolved from the carbonates. The steeply increasing pressure also increases the solubility which explains why the liquid phase gets all more prominent the more hydrogen is injected. Additionally more water is generated, thus dissolving even more solid minerals. It is interesting to observe that there is a small window where annite is present, which might be an indicator that at this point clay minerals could be modeled. However I did some modeling in this range and found no evidence that clay minerals can be stabilized there.

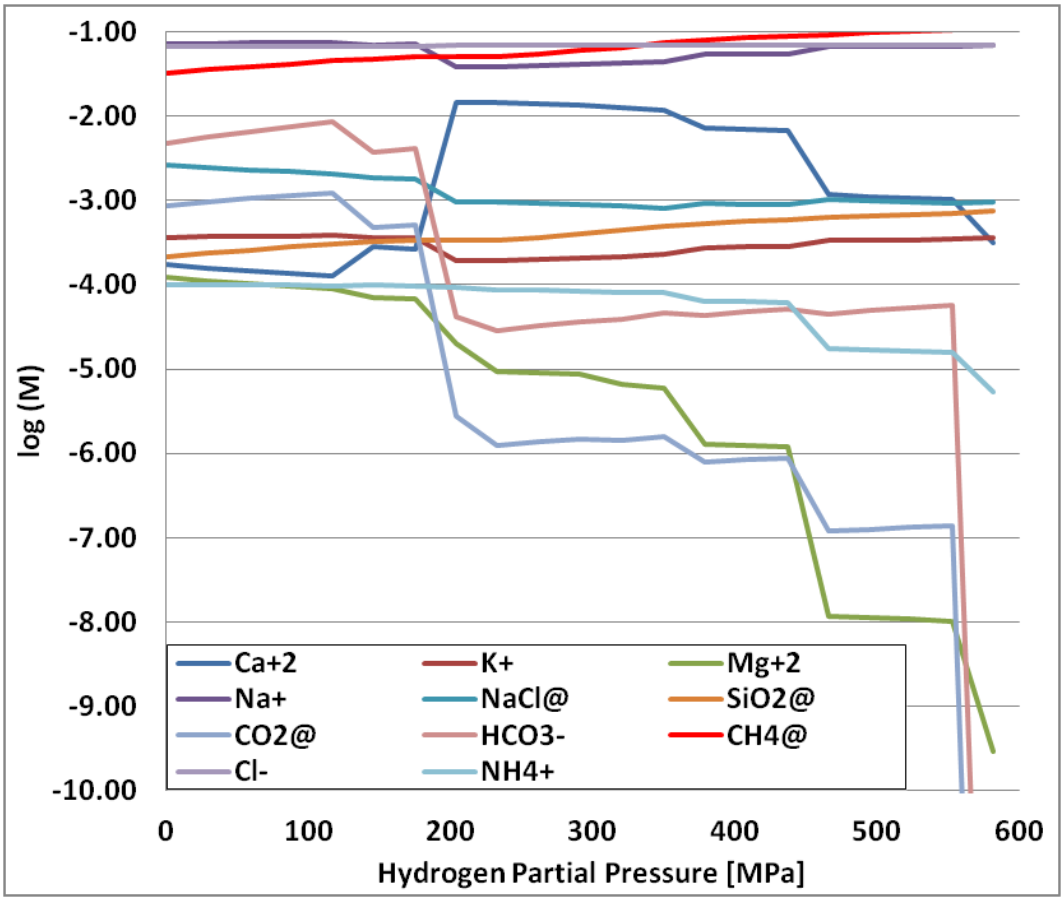

Figure 32: Dissolved species

H_2 titration up to 120 mol for core sample 2 [80°C; 23 MPa] aqueous species

I expected the dissolution of the minerals and with it the concentration of its aqueous species (Figure 32) to be linear due to the linear increase of water. Instead their concentrations in the fluid lower with increased pressure. This in relation with the increase in water (Figure 30), suggest that the solid species reach a point of equilibrium with their aqueous species. The reason why we do not observe greater amounts of dissolved species is, that as was said before the model is not time dependent. Changing the system by titrating hydrogen will surely see some of the minerals dissolved into the fluid. Later these dissolved species are re-precipitated as a different mineral which is then plotted by GEMS. Thus we cannot see this intermediate step, but only the result. An indicator for the correctness of the mass balance conditions by the model is the steadily decreasing NaCl concentration. This is because the more water is generated the more NaCl is dissolute due to its equilibrium with Na^+ an Cl^-.

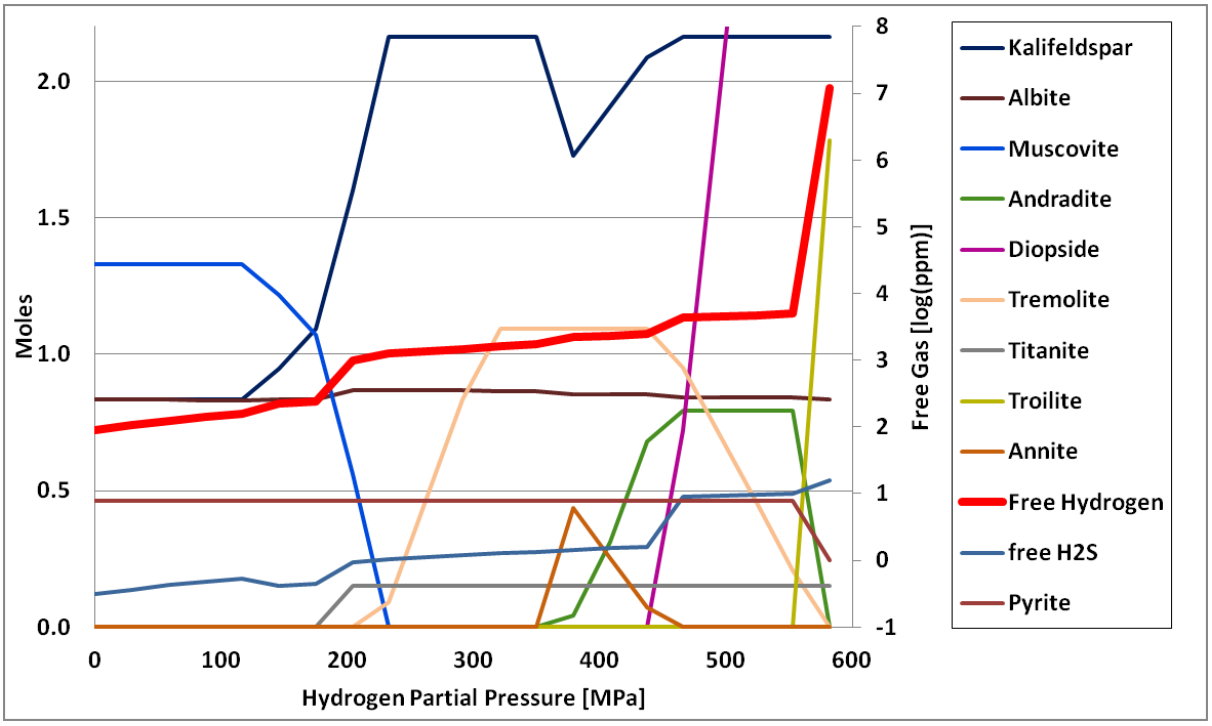

Figure 33: Iron bearing minerals

H_2 titration for core sample 2 up to 600 MPa H_2 partial pressure [80°C]; minor mineral relations

Here the effect of hydrogen on the generation of hydrogen sulfide and the iron bearing minerals is plotted. The iron bearing minerals have a great influence on the system because they provide Fe^{2+} and Fe^{3+} which determines the oxidation state of the model.

The final plot (Figure 33) shows the generation of hydrogen sulfide during the hydrogen injection. The huge amount of hydrogen available produces the right conditions for tremolite and andradite to be generated. These minerals need the iron which is bound in the siderite and the pyrite for their generation. This release on the one hand C and O atoms from the siderite, which GEMS converts into water and methane, and on the other hand elemental sulfur from the pyrite, which is converted into H_2S. It should be noted that this reaction is totally unrealistic and only happens because GEMS doesn't include kinetics.

Discussion

This section compares the results of the geochemical simulation and attempts to evaluate if these results can be used in a real reservoir. It will sum up the findings from the literature and compare them with similarities in this thesis.

Clay Minerals

The result section did not show any new solutions to the problem of clay mineral stability. Still it can tell us some evidence about general mineral stability. As it was observed the stability of minerals is directly related to the equilibrium with the dissolved species. For this model this can best be seen for quartz which is in equilibrium with dissolved SiO_2 and accordingly if one of the two changes the other does follow. The same was found by Wilson et al (2005) when he observed the stability of clay minerals and observed that they also correspond to dissolved species in the reservoir brine. The titration of hydrogen changes the composition of this brine and will thus lead to dissolution and precipitation of minerals in the subsurface storage facilities.

As it was mentioned, the data for simulating clay minerals is not yet very reliable and thus can be used in geochemical models only to a small extend. In the models generated in this thesis, none of the clay minerals stayed stable as they have been all converted or dissolved. Still there are some findings from the literature concerning the given problem of storing a hydrogen mixture in the subsurface.
It was already discussed that Lassin et al (2011) found, that the influence of hydrogen on clay formations should be only minor which was also found by Wilson et al (2005). Taking a closer look on their findings, it can be seen that they did their experiments in Fe- and Na- rich clays. These clays showed some resistance to changes induced by hydrogen generation or injection. Comparing this to the clay minerals found in the molass basin where also Mg-rich clays Gier (1998) are quite prominent, these findings from the literature can only be compared partially. In the model several attempts have been made to find stable conditions for clay minerals both with data from GEMS and with thermodynamic data generated by Wilson et al (2006). Unfortunately no attempt did yield proper results, with most of the models ignoring the clay minerals totally and

some presenting unrealistic results. This showed the weakness of gibbs free energy minimization not only for GEMS but also for PREEQUEC, which does consider kinetics and thus generates species in the reservoir which would never be generated. For clay minerals at least the kaolinite should have stayed stable, but was instead converted into microcline which should not be stable under given reservoir conditions. Summing up, this means that the GEMS model can only be used to simulate the behaviour of clay minerals during hydrogen injection if proper thermodynamic data is generated by lab's. Still the behaviour of the reservoir fluid and its dissolved species is modelled accurately and can at least be a guideline for laboratory and field tests.

Sulphides

The only sulphur bearing mineral found in the core samples was pyrite and minor amounts of aqueous SO_4 in the reservoir brine. The models showed that only this minor amount of SO_4 is converted into other sulphur bearing species and that the pyrite stays stable. Truche et al (2009) predicts that pyrite should react under the influence of hydrogen generating H_2S and HS^-. These results have been found for pure grinded pyrite which was treated with pure hydrogen at temperatures of 90 to 120°C (slightly higher than RAG reservoirs) and surface pressure. The experiments of Truche et al (2009) have been remodelled by the author to check if GEMS yields the same results. Finding that GEMS could remodel the results of Truche et al (2009), it was necessary to find out why pyrite stayed stable in the core sample model and why not in the pure model. Two reasons have been found. (1) The first and minor reason was that Truche et al (2009) in his laboratory experiments used fine grained pyrite which offered a greater surface for reactions with hydrogen taking place. (2) The second and more important reason was found by introducing other minerals to the experiment. After adding calcite and dolomite, the reaction ceased to happen, which suggests that carbonates work as a buffer which keeps the pyrite stable. This could also be proven during critical hydrogen titration where hydrogen was injected up to a partial pressure of 580 MPa. After all the carbonates had been dissolved or converted, the pyrite immediately started to dissolve. Thus the stability at the reservoir conditions mentioned in the results section can be taken as given. For temperatures above 100°C this changes, but this is of no concern for this thesis.

It should be noted that the introduction of other sulphur bearing minerals as for example marcasites, does change the stability conditions again (Wilson et al 2005). Thus if other storage reservoirs would be chosen for the storage of hydrogen methane mixtures, the new mineral composition would need to be tested again to rule out other influences. The same holds true for iron bearing minerals which change the concentration of Fe^{2+} and Fe^{3+} in the reservoir fluid (Foh et al 1979). These ions change the redox state of the reservoir fluid and are responsible for the stability of iron bearing minerals especially clay as was mentioned before.
Summing up it could be proved that the results of the model concerning sulphur are reliable and can thus be used to describe trends and make predictions for further laboratory or field tests.

Other minerals and reservoir fluid

All silicate minerals tend to be converted into quartz under low temperature conditions as are present in the given model. This is accurately predicted by GEMS with the volume of quartz increasing compared to the input data. Also other relationships in the reservoir could be solved by observing the behaviour of quartz during modelling and hydrogen titration.
It was mentioned before that the simulations and models of GEMS are not time dependent and thus describe the final state. Sometimes however this final state is unlikely and thus calibrations are necessary to get proper results. Quartz helps in calibrating the model as its behaviour can be predicted quite easily (Garrels et al. 1990). The reservoir fluid, which is as mentioned before very important to establish the equilibrium, does also dissolve parts of the quartz depending on the amount of fluid and the pressure which both control the solubility (Gaucher et al. 2009). Some of the titrated hydrogen is converted into water and some into methane with C and O coming from the dissolution of carbonates.
The generation of water changes the equilibrium conditions in the reservoir as does the methane which decreases the pressure by binding one C and four hydrogen atoms. Unfortunately this is another error of GEMS which is induced because it does not use kinetics. Under the given conditions it is very unlikely that methane would be generated unless some hydrogen devouring bacteria where present (Buzek et al 1993). GEMS does only model rock-fluid-gas interaction and no bacterial activity, thus

this prediction must be seen as wrong. However the dissolution of parts of the quartz due to increasing amount of fluid proves that the relationship between reservoir rock and reservoir fluid is modelled correctly. Thus it can be used to predict the behaviour of silica minerals. It is interesting to notice that even the quartz volume immediately changes after hydrogen is titrated into the core sample. This suggests that the quartz is dissolved in the water which is generated due to hydrogen injection.

The prediction of feldspar however needs further investigation. Especially k-feldspar is not stable under the given conditions (Figure 23), but is still predicted as such by GEMS.

Finally the change in carbonate composition predicted by GEMS seems reasonable. It corresponds to the equilibrium conditions bound to the reservoir fluid as well as to the changes due to changing pH. The precipitation of calcite could be an issue. From Garrels et al (1990) it is stated that these reactions should happen very slow under low temperature reservoir conditions. Additionally none of the other companies which stored hydrogen did report any precipitation problems (Lord 2008).

The dissolution or better conversion of dolomite into calcite as it is described in the reaction in the results section cannot be taken as granted because some intermediate steps are missing however it is one possible explanation of what happens to the dolomite. The changes in the solid solution of dolomite, siderite and calcite have also been observed by Lassin et al (2011) which further prove that the model works properly.

Bacterial Influence

Another issue concerning the storage of hydrogen in the subsurface is the influence of bacteria in the reservoir. Oil and gas reservoirs are home to numerous kinds of methanogenic bacteria (Panfilov et al. 2006). Under these circumstances, I thought it necessary to add this short chapter to this thesis. Some bacteria are able to convert hydrogen to methane (Panfilov et al. 2010), which changes the overall composition of the stored gas and leads to volume loss. The prominent equation here for is

$$4\ H_2 + CO_2 \quad \rightarrow \quad CH_4 + 2H_2O$$

The reason for this reaction, which would not be possible under reservoir conditions, is that the bacteria bypass the activation energy which would normally be needed to

activate this reaction. According to the chemical and geological data which was presented in the previous section, this seams not reasonable because we do not have big amounts of Carbon – Dioxide or Sulfate in the reservoir. But it might be that the introduction of hydrogen produces Carbone – Dioxide due to Carbonate dissolution. Another possibility of these species to occur in the reservoir is the previously discussed bio-gas which also contains these components. Additionally Panfilov et al (2006) predicts that in the near future gasified coal will again become an energy source of major importance. This gas is the famous town gas which contains only up to 20% (Foh et al. 1979) of hydrogen with Methane and Carbon Dioxide making up the rest.

The bacteria are active at reservoir temperatures up to 90°C, with ideal growth conditions between 35-40°C at a neutral pH (Panfilov et al. 2006). Apart from H_2S generation there is a second issue concerning these bacteria. Under ideal conditions they can grow at such a high rate, that they can block the pores. Panfilov et al (2006) built a mathematical model based on the reaction diffusion equation which predicts growth rate and spreading of the bacteria in the reservoir. The growth rate is mostly dependent on the nutrient supply and therefore has its maximum around the injection wells.

However methanogenic bacteria have not been reported in all of the mentioned reservoirs. The town gas storage in Lobodice (Czech Republic) had problems with bacteria and provided the data for Panfilov et al (2006) study, while studies in the town gas storages of Beynes (France) or Teeside (England) did not mention the bacteria issue. It will be necessary to analyze the water of the reservoir for which the storage is planned.

Conclusions

Summing up this thesis shows that there are several issues that could have a negative influence on concerning hydrogen in subsurface structures. In conclusion 3 points of interest where found that might prove challenging for the storage of hydrogen. Each of them was discussed in this thesis an is summed up here with recommendations for further work.

1.) Reactivity and influence on the different reservoir materials

For the reservoir the simulation shows that some of the minerals, especially the carbonate minerals, are influenced by the injection of hydrogen. As it was expected, hydrogen changes the pH but not in the acidic but into the alkaline direction which is also found in the literature. This leads to dissolution of dolomite, and a precipitation of calcite. In total the fraction of material which is converted is 1.3%. This however only occurs when pure hydrogen is injected into the reservoir. For hydrogen shares of up to 20% the loss found is only 0.6%. As it was mentioned the major share of the material converted are the carbonate minerals. When pure hydrogen is injected up to 14% of the dolomite is converted. However for the intended 20% of hydrogen in the methane this fraction decreases to 3%. Nevertheless the literature states that these reactions will probably be very slow under the given pressure and temperature conditions. To prove all this results I strongly suggest running some laboratory tests in real applications.

For the validity of thermodynamic modeling of clay mineral fluid interactions the literature did identify mainly three reasons why difficulties occur; (1) clay minerals do not comply with the phase rule and therefore should not be included in thermodynamic models; (2) clay minerals exist in a state of disequilibrium and; (3) thermodynamic models including clay minerals such as illite and smectite may not represent true equilibrium conditions and it has been argued that clay minerals are metastable with respect to phyllosilicates of greater

homogeneity, such as those belonging to the talc-pyrophyllite and mica groups. For Gibbs free energy minimization where no kinetics are included, it was found in the literature that the influences of clay minerals is still not that big (e.g. up to +/- 0.2 points of pH value), but will increase if kinetics are included.

For the models generated in this thesis no reactions of clay minerals with the hydrogen could be found which leads to the conclusion that the cap rock will also stay undisturbed by the hydrogen. In the literature clay formations have been tested on their resistivity against changes from hydrogen. So far no issues could be found therefore it can be predicted that the clay minerals won't be affected. However I still strongly suggest doing some laboratory tests on cores to confirm the findings of this thesis.

2.) Hydrogen Conversion

A simulation was generated which calculated the injection of hydrogen up to 600 MPa partial pressure. This was done to simulate the injection of hydrogen over a long time period, where always new hydrogen is injected and thus is available for reactions. At some point (120g of H2 for the data from the test reservoir) the system is saturated with hydrogen and no further losses due to mixing, dissolution or reactions occur. However this is only true for a static reservoir. If there is any aquifer or some inflow from somewhere else the whole calculation will change again.

The simulation shows that the major part of the hydrogen is converted into water and methane, and only minor amounts dissolve into the reservoir fluids.

3.) Hydrogen Sulfide Generation

For the occurrence of H_2S it was found that it is not possible to simulate the generation of major volumes of H_2S within the temperature boundaries of the given reservoirs. I simulated different cases with different mineral compositions and under different p,T conditions. For all

the cases which used possible values, the maximum H_2S generation which I observed was 0.5 ppm which is way below any safety boundary. Additionally I found out that the limiting factor for the H_2S generation is not only the amount of H_2 in the reservoir, but the temperature as well. At temperatures above 130°C, the generation of H_2S drastically increases, but these conditions are never ever reached in the storage reservoirs.

References

Aberer F.,"Die Molassezone im westlichen Oberösterreich und in Salzburg", Vienna, Austria, 1957

Atkins P.W.," Physikalische Chemie" Fifth Edition, Oxford University Press, 2004

Basniev K.S., Omelchenko F.A., Adzynova F.A., "Underground hydrogen storage problems in Russia", Essen, proceeding WHEC (May 2010)

Berger W. H., "The Future of Methane", University of California, San Diego, Nov. 2007

Boos S., "Fukushima lässt grüßen. Die Folgen eines Super-GAUs", Rotpunktverlag, Zürich 2012, ISBN 978-3-85869-474-4

Buzek F., Onderka., Vancurat P., Wolf i., "Carbon isotope study of methane production in a town gas storage reservoir" Charles University Prague, Czech Geological Survey, March 1993

Carden P. O., Paterson L., "Physical, Chemical and Energy Aspects of Underground Hydrogen Storage", AiChE Journal (Vol. 23, No. 3) Department of Engineering Physics, Research School of Physical Sciences, The Australian National Univerisity, Canberra, A.C.T., Australia, (July 1979)

Chen L.L., Katz D.L., Tek M.R.," Binary Gas Diffusion of Methane-Nitrogen through Porous Solids" Department Chemical Engineering, University of Michigan, US, May 1977

Crozier T. E., Yamamoto S.," Solubility of Hydrogen in Water, Seawater and NaCl Solutions", Journal of Chemical and Engineering Data, Chemical Oceanographic Branch, Naval Undersea Center, San Diego, California, 1974

Cussler E.L.," Diffusion: Mass Transfer in Fluid Systems", Third Edition, University of Minesota, ISBN-13 978-0-511-47892-5 eBook (EBL), Cambridge University Press, (2009)

Dickson A. G.,"pH scales and proton-transfer reactions in saline media such as sea water". Geochim. Cosmochim. Acta 48 (11):2299-2308

Dilip K., Das P.E., Rajaram K., Prabhudesai P.E.: "EIT Chemical Review", Professional Publications Inc., 2nd edition, ISBN-10: 1576450236, Nov. 1998

Donaldson, E. *C.,* R. F. Kendall, and F. S. Manning, "Dispersion and Tortuosity in Sandstones," SPE 6190, Paper presented in New Orleans, La. (Oct., 1976)

Ebel D.S., Ghiorso M.S., Sack R.O., Rossman L.G.," Gibbs Energy Minimization in Gas + Liquid + Solid Systems", University of Chicago, Department of Geophysical Science, October 1999

Foh s., Novil M., Rockar E., Randolph P.," Underground Hydrogen Storage", Institute of Gas Technology, Brookhaven National Laboratory, New York, December 1979

Galle C., Tanai K.," Evaluation of Gas Transport Properties of Backfill Materials for Waste Disposal: H_2 Migration Experiments in Compacted Fo-Ca Clay" Clays and Clay Minerals, Vol46, No. 5, 498-508, 1998

Garrels M.R., Christ C.L.," Solutions, Minerals & Equilibria" ISBN-13: 978-0867201482, Jones and Bartlett Publisher, United States, February 1990

Gaucher E. C., Tournassat C., Pearson F.J., Blanc P., Crouzet C., Lerouge C., Altmann S.,"A robust model for pore-water chemistry of clayrock", Geochimica et Cosmochimica Acta, French Geological Survey, France, July 2009

Gier S., ”Diagenese Pelitischer Sedimente in der Molassezone Oberösterreichs”, Vortrag vor der Österreichischen Mineralogischen Gesellschaft, Petrological Department, Universität Wien, Nov. 1998

Grathwohl P., “Diffusion in natural porous media: Contaminant transport, sorption / desorption and dissolution kinetics”, Kluwer Academic. ISBN 0-7923-8102-5 (1998)

Jäger W., Rannacher R., Warnatz j.,“ Reactive Flows, Diffusion and Transport: From Experiments via Mathematical Modeling to Numerical Simulation and Optimization” ISBN-13**:** 978-3540283799, Springer Berlin Heidelberg, Oct. 2006

Kaye G.W.C., Laby T.H.: ”Tables of Physical and Chemical Constants” 15th edition Longman, NY, p.219, 1986

Knopf B., Pahle M., Kondziella H., Joas F., Edenhofer O., Bruckner T., “Germany’s nuclear phase-out: Impacts on electricity prices, CO_2 emissions and on Europe”, Potsdam Institute for Climate Impact Research, Institute for Infrastructure and Resource Management (University Leipzig), Germany, March 2012

Kulik D.A., ”Dual-thermodynamic estimation of stoichiometry and stability of solid solution end members in aqueous – solid solution systems”, Paul Scherrer Institut, Laboratory for Wastemanagement, August 2005

Kulik D.A.,” Gibbs Energy Minimization: Solving Equilibria with Solid Solutions” Laboratory for Waste Management, Nuclear Energy and Safety Department, Paul Scherrer Institut, University of Frankfurt February 2009

Labhart T.,”Geologie der Schweiz”, Ott Verlag, ISBN 3-7225-0007-9, 2005

Lassin A., Dymitrowska M., Azaroual M.," Hydrogen solubility in pore water of partially saturated argillites: Application to Callovo-Oxfordian clayrock in the context of a nuclear waste geological disposal", doi:10.1016/j.pce.2011.07.092, Elesvier Ltd .(2011)

Lichtner P.C., Steefel C.I., Oelkers E.H.," Reactive Transport in Porous Media" Mineralogical Society of America, ISBN 0-939950-42-1, Volume 34, Sept 1996

Lord A.S.," Overview of Geological Storage of Natural Gas with Emphasis on Assessing the Feasibility of Storing Hydrogen", Sandia Report, California, July 2008

Huemer H.," Petrologische, mineralogische und chemische Untersuchungen an Turbiditen und Hemipelagiten aus der Molassezone Oberösterreichs", Jahrbuch der Geologischen Bundesanstalt, August 1989

Malzer O.," Geologische Charakteristik der wichtigsten Erdöl – und Erdgasträger der oberösterreichischen Molasse", Erdöl-Erdgas-Zeitschrift 97. Jg., January 1981

Machel H.G., Mountjoy E.W., "Chemistry and Environments of Dolomitization – A Reappraisal", Earth Science Reviews 23 (3): 175-222, doi:10.1016/0012-8252(86)90017-6, May 1986

Nagy A.A., "Edelmetall Recycling beim Rückbau sulfidhaltiger Erzabgänge"Technical University of Clausthal, Department Energy –and Economy, May 2008

Oritz L., Volckaert G., Mallants D.," Gas generation and migration in Bloom Clay, a potential host rock formation for nuclear waste storage", Elsevier, Nuclear Research Center, Belgium, July 2001

Panfilov M., Gravier G., and Fillacier S.," Underground Storage of H2 and H2-CO2-CH4 mixtures", Netherlands, 10th European Conference on the Mathematics of Oil Recovery, September 4-6, 2006

Panfilov M.," Underground Storage of Hydrogen: In Situ Self-Organization and Methane Generation", Transport in Porous Media, Springer Link, May 2010

Paterson L." The Implication of Fingering in Underground Hydrogen Storage", Australian National University, Canberra, Australia, June 1982

Perkins T. K., Johnston O.J., Hoffman R. N.," Mechanics of viscous fingering in miscible systems". Soc.Petrol. Engng J. 5,301 (1965).

Perrot P.,"A to Z of Thermodynamics", Oxford University Press, ISBN 0-19-856552-6, 1998

Pettijohn F.J., Potter P.E., Siever R., "Sand and Sandstone", Springer-Verlag GmbH; Auflage: 2, ISBN 978-3540963509, Dec 1987

Petrucci R.H., Harwood W.S., Herring F.G., "General Chemistry", 8th edition, Prentice Hall, 2002

Prausnitz, J. M., F. H. Shair, "A thermodynamic correlation of gas solubility's," *AIChE J.* **7**, 682-687 (1961).

Pray H.A., Schweickert C.E., Minnich B.H.," Solubility of Hydrogen, Oxygen, Nitrogen, and Helium in Water: At elevated temperatures." Battelle Memorial Institute, Ohio, July 1950

Regazzoni, A. E.; G. A. Urrutia, M. A. Blesa, A. J. G. Maroto," Some observations on the composition and morphology of synthetic magnetites obtained by different routes", *Journal of Inorganic and Nuclear Chemistry* **43** (7): 1489–1493.doi:10:1016/0022-1902(81)80322-3. ISSN 0022-1902 (August 2010)

Robie A. R., Waldbaum.," Thermodynamic Properties of Minerals and Related Substances at 298.15°K (25.0°C) and One Atmosphere (1.013 Bars) Pressure and at Higher Temperatures" Geological Survey Bulletin 1259, Ohio State University, 1968

RÖGL, F. Die Grenzziehung zwischen Haller Serie und Oberer Puchkirchen Serie in den oberösterreichischen Molasseborhungen. RAG Wien, E-Report, 1980

Le Roux G., Shotky W., "Weathering of inorganic matter in bogs", Development in earth surface processes (Vol. 9); Elsevier, http://dx.doi.org/10.1016/S0928-25(06)09009-2, 2006

Schmitz S.," Einfluss von Wasserstoff als Gasbegleitstoff auf Untertagespeicherung" DBI-Fachforum, Energiekonzepte und Wasserstoff, Berlin Sept. 2011

Shimko M.A., Parkster M., Gruber.,"V.E.1 Combined Reverse-Brayton Joule Thompson Hydrogen Liquification Cycle", DOE Technology Development, Gas Equipment Engineering Corp., USA Milford 2005

Srinivasan B.S.," The Impact of Reservoir Properties on mixing of Inert Cushion and Natural Gas in Storage Reservoirs" Master Thesis, Morgantown University, West Virginia (2006)

Truche L., Berger G., Destrigneville C., Pages A., Guillaume D., Giffaut E., Jacquot E.," Experimental reduction of aqueous sulfate by hydrogen under hydrothermal conditions: Implication for the nuclear waste storage", University Toulouse, France, May 2009

Truche L., Berger G., Destrigneville C., Guillaume D., Giffaut E.," Kinetics of pyrite to pyrrhotite reduction by hydrogen in calcite buffered solutions between 90 and 180°C: Implications for nuclear waste disposal", University Toulouse, France, March 2010

Wagner, L.R., "Tectono-stratigraphy and hydrocarbons in the Molasse Foredeep of Salzburg, Upper and Lower Austria". In: Mascle, A., Puigdefábregas, C., Luterbacher, H.P., Fernández, M. (Eds.), Cenozoic Foreland Basins of Western Europe. Geological Society Special Publications, vol. 134. Geological Society, London, 1998

Will S.” Gibbs Free Energy Minimization: A Numerical Approach” Massachusetts Institut of Technology October 2011

Wilson J., Savage D., Cuadros J., Shibata M., Ragnarsdottir V.K.,” The effect of iron on montmorillonite stability (I) Background and thermodynamic considerations”, Geochimica et Cosmochimica Acta 70 (2006) 306-322, Elesvier, Sept. 2005

Yen, C. L., J. J. McKetta, “A thermodynamic correlation of nonpolar gas solubilities in polar, nonassociated liquids,” *AIChE J.* **8**, 501-507 (1962)

WEB Sources

Evans D., Highley D., Gale I., Cowley J.,” Underground Storage”, British Geological Survey (BGS) 2008
https://www.google.com/search?q=Underground+Storage+British+Geological+Survey&ie=utf-8&oe=utf-8&aq=t&rls=org.mozilla:de:official&client=firefox-a
(accessed Decbemder 2012)

Eere Energy,” Hydrogen Properties”
http://www1.eere.energy.gov/hydrogenandfuelcells/tech_validation/pdfs/fcm01r0.pdf
(accessed June 2012)

Engineering Toolbox, “Solubility of Gases in Water,”
http://www.engineeringtoolbox.com/gases-solubility-water-d_1148.html
(accessed June 2012)

Euturbines,” Mixing Hydrogen into Natural Gas”,
http://www.euturbines.eu/fileadmin/user_upload/Event_Files/Mixing_hydrogen_into_natural_gas_P_Nitschke-Kowsky_E.ON_Ruhrgas.pdf
(accessed May 2012)

Götz M., Buchholz D., Bajohr S., "Speicherung elektrischer Energie aus regenerativen Quellen im Erdgasnetz", DVGW-Forschungsstelle, http://www.fachzeitschriften-wvgw.de/ewp_0511/files/ewp_0511_internet_gesamt-pdf.pdf (accessed May 2012)

Gtai, "Power to Gas", http://www.gtai.de/GTAI/Navigation/EN/Invest/Industries/Smarter-business/Smart-energy/Germanys-energy-concept/power-to-gas.html (accessed December 2012)

Hatscher S. T., "Hydrogen in Underground Gas Storages for natural Gas: Open Questions", Wintershall Holding, http://gerg.dgc.eu/activities/workshops/UGS_workshop_Hatscher.pdf (accessed April 2012)

Lide D.R., "CRC Handbook of Chemistry and Physics, Internet Version 2006, Accessed via: http://www.hbcpnetbase.com, Taylor and Francis, Boca Raton (accessed December 2012)

Nature Materials," Phase Diagram of Hydrogen", http://www.nature.com/nmat/journal/v10/n12/fig_tab/nmat3189_F2.html (accessed May 2012)

NIST Chemistry Handbook," Hydrogen Properties", http://www.boulder.nist.gov/div838/Hydrogen/Properties/Properties.htm (accessed August 2012)

PETE Lecture (Petroleum Techniques) Texas A&M WEB Resources," Gas Solubility" http://www.google.com/url?sa=t&rct=j&q=&esrc=s&source=web&cd=3&ved=0CDEQFjAC&url=http%3A%2F%2Fwww.pe.tamu.edu%2Fschubert%2Fpublic_html%2FPETE%2520625%2F4.%2520Gas%2520Solubility.ppt&ei=lO5MUPLEMIntsgaLnIGgAg&usg=AFQjCNGIZDGPWblq4tUsUqWwZf_jQ66LWg (accessed June 2012)

GEOPIG Numerical Tools, “Slope07: Database for thermodynamic Rockproperties”,
http://geopig.asu.edu/sites/default/files/slop07.dat
(accessed August 2012)

Renewable Energies, “Replacing conventional energy”,
http://www.renewable.at/
(accessed January 2013)

Other sources which have been provided by RAG

RAG., “Analysis of the dissolved species in the reservoir water for different wells”. (Excel Sheet)

OMV, “Mineralogical and Petrological Analysis of the Core from Well Reichering 1” Laboratory for Exploration and Production, OMV

OMV, “Mineralogical and Petrological Analysis of the Core from Well Bierbaum 1” Laboratory for Exploration and Production, OMV

Meeting., ”Meeting for the hydrogen storage project at the 24th April 2012”, Office Kärntner- Ring, Vienna

Appendix 1 Input Data for GEMS Simulation

Core Sample 1 is from the same formation as the intended reservoir for the field test. (Provided by RAG).

Core Preperation				**Water Analysis**		
Porosity	27.35%			K	0.013	
Water Sat	40.00%			Ca	0.091	
Water Vol	200	[cm³]		Cl	2.492	
Pore Vol	500	[cm³]		CO2	0.001	
Core Vol	1828	[cm³]		HCO3	0.075	
Gas Volume	300	[cm³]		J	0.000	
Pressure	23000000	Pascal		Mg	0.022	
Temperature	353	K		Na	1.519	
Rspec,meth	518.232	J/KgK		NH4	0.002	
Rspec,hyd	4124.00794	J/KgK		SO4	0.027	
Density,meth	0.1257271	[g/cm³]		Sum	4.242	[g]
Density,hyd	0.01579915	[g/cm³]		H2O	200	[g]
Non Clay Minerals			Volumes	Mole weights		
	[g]	Moles	[cm³]	[g/mol]		
Quarz	2035	33.9	768	60		
Dolomit	636	3.4	219	185		
Plagioklas	382	1.5	146	262		
Kalifeldspat	144	0.5	55	278		
Kalzit	397	4.0	146	100		
Siderit	104	0.9	27	116		
Pyrit	126	1.0	25	120		
Garnet	0	0.0	0	508		
Brookit/Anatas	10	0.1	3	80		
Zirkon	0	0.0	0	183		
Clay Minerals and Mica	V[cm³]=	439	Volumes	Mole weights		
	[g]	Moles	[cm³]	[g/mol]		
Illite (Annite)	551	1.2	174	476		
Illite (Phlogopite)	55	0.1	19	512		
Kaolinite	255	1.0	97	258		
Chlorite (Greenalite)	250	0.7	83	372		
Smectite (Celadonite)	112	0.3	37	387		
Smectite (Pyrophyllite)	70	0.2	25	360		
Muskovit	12	0.0	4	398		

The second sheet is also from well one and does show the calculation and preparation of the gas amounts. The exact description can be found in the Methodology chapter.

Free Gas						
Gas Weight	38	[g] Methane				
Gas Weight	0.041	[g] CO2				
Gas Weight	0	[g] Nitrogen				
Gas Weight	27	[g] Methane dissolved				
Gas Weight	4.74	[g] 100% Hydrogen				
Gas Weight	1	[g] 2% Oxygen				
Methan	Hydrogen	Hydrogen [%]				
38	0.000	0.0%				
38	0.118	2.5%				
37	0.237	5.0%				
37	0.355	7.5%				
37	0.474	10.0%				
37	0.592	12.5%				
37	0.711	15.0%				
37	0.829	17.5%				
37	0.948	20.0%				
37	1.066	22.5%				
37	1.185	25.0%				
36	1.303	27.5%				
36	1.422	30.0%				
36	1.540	32.5%				
36	1.659	35.0%				
36	1.777	37.5%				
36	1.896	40.0%				
36	2.014	42.5%				
36	2.133	45.0%				
35	2.251	47.5%				
35	2.370	50.0%				

Core Sample 2 is from a very homogenous reservoir. It has only 24% of Mica and Clay Minerals in its bulk, and a very good porosity.

Core Preperation				**Water Analysis**		
Porosity	23.65	[%]		K	0.013	
Water Sat	40.00%			Ca	0.091	
Water Vol	200	[cm³]		Cl	2.492	
Pore Vol	500	[cm³]		CO2	0.001	
Core Vol	2114	[cm³]		HCO3	0.075	
Gas Volume	300	[cm³]		J	0.000	
Pressure	23000000	Pascal		Mg	0.022	
Temperature	353	K		Na	1.519	
R spec,methane	518.232	J/KgK		NH4	0.002	
R spec,hydrogen	4124.007937	J/KgK		SO4	0.027	
Density,methane	0.125727102	[g/cm³]		Sum	4.242	[g]
Density,hydrogen	0.015799147	[g/cm³]		H2O	200	[g]
None Clay Minerals			Volumes	Mole weights		
	[g]	Moles	[cm³]	[g/mol]		
Quarz	1073	17.9	405	60		
Dolomit	584	3.2	201	185		
Plagioklas	221	0.8	85	262		
Kalifeldspat	111	0.4	42	278		
Kalzit	660	6.6	243	100		
Siderit	161	1.4	42	116		
Pyrit	107	0.9	21	120		
Andradit	49	0.1	12	508		
Brookit/Anatas	12	0.2	3	80		
Zirkon	7	0.0	1	183		
Clay Minerals and Mica	Volume[cm³]	994	Volumes	Mole weights		
	[g]	Moles	[cm³]	[g/mol]		
Illite (Annite)	1417	3.0	447	476		
Illite (Phlogopite)	142	0.3	50	512		
Kaolinite	79	0.3	30	258		
Chlorite (Greenalite)	447	1.2	149	372		
Smectite (Celadonite)	509	1.3	167	387		
Smectite (Pyrophyllite)	316	0.9	111	360		
Muskovit	56	0.1	20	398		

Here is again the data from the Free Gas calculation now for the bigger porosity.

Free Gas						
Gas Weight	38	[g] Methane				
Gas Weight	0.041	[g] CO2				
Gas Weight	0	[g] Nitrogen				
Gas Weight	27	[g] Methane dissolved				
Gas Weight	4.74	[g] Hydrogen 100%				
Gas Weight	1	[g] Oxygen 2%				
Methane	Hydrogen	Hydrogen [%]				
38	0.000	0.0%				
38	0.118	2.5%				
37	0.237	5.0%				
37	0.355	7.5%				
37	0.474	10.0%				
37	0.592	12.5%				
37	0.711	15.0%				
37	0.829	17.5%				
37	0.948	20.0%				
37	1.066	22.5%				
37	1.185	25.0%				
36	1.303	27.5%				
36	1.422	30.0%				
36	1.540	32.5%				
36	1.659	35.0%				
36	1.777	37.5%				
36	1.896	40.0%				
36	2.014	42.5%				
36	2.133	45.0%				
35	2.251	47.5%				
35	2.370	50.0%				

Appendix 3 Thin sections of core sample 1

	1162.96 m	1165.80 m	1169.13 m	1174.73 m
Lithotyp	2B	2B	2B	2B
MONOKRISTALLINER QUARZ	33.3	45.0	42.6	35.0
POLYKRISTALLINER QUARZ	7.7	5.3	4.5	4.3
HORNSTEIN	0.0	0.7	0.3	0.0
K-FELDSPAT	4.7	2.3	1.3	1.0
PLAGIOKLAS	0.0	0.3	0.3	0.7
FELDSPÄTE	0.0	0.0	0.0	0.0
GESTEINSBRUCHSTÜCKE	4.0	15.3	13.5	16.3
BIOKLASTEN	1.0	0.0	0.0	0.3
GLAUKONIT	1.3	1.0	1.0	0.0
GLIMMER	18.0	5.3	7.4	19.7
TONIGE GRUNDMASSE	7.7	0.3	0.6	1.0
QUARZZEMENT	0.0	0.3	1.9	0.3
SIDERITZEMENT	0.0	0.0	0.0	0.0
EISENDOLOMITZEMENT	0.3	2.7	2.3	0.7
KALZITZEMENT	2.3	2.7	2.3	2.3
OPAKE/ORGANISCHE SUBSTANZ	3.3	1.0	0.3	0.7
KALKSTEIN FRAGMENTE	4.0	2.0	5.2	2.0
SCHWERMINERALE	1.7	1.3	1.3	1.0
DOLOMIT	10.3	14.0	15.5	14.7
POROSITÄT	15.7	15.0	12.4	8.8
MAXIMALE KORNGRÖßE [mm], 50 Körner	0.34	0.48	0.29	0.32
MITTLERE KORNGRÖßE [mm], 50 Körner	0.13	0.18	0.14	0.14

Figure 34: Results of the thin section analysis core sample 2
Provided by RAG

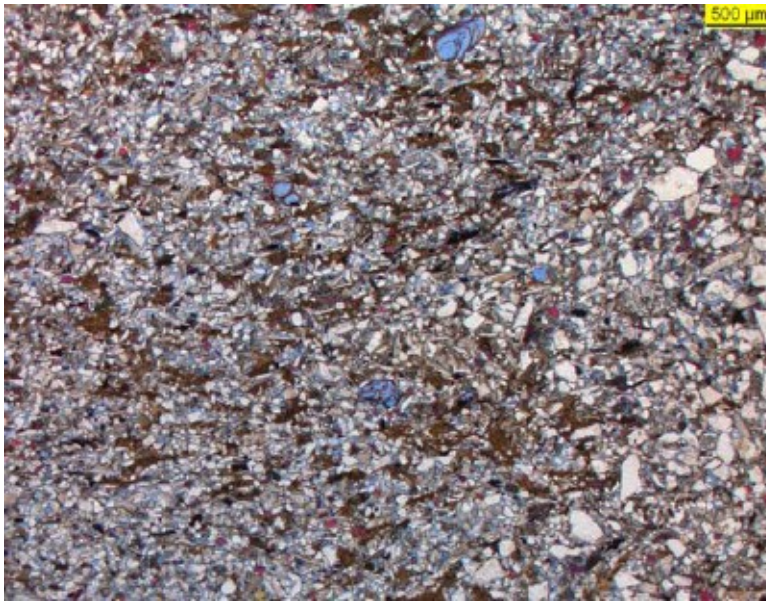

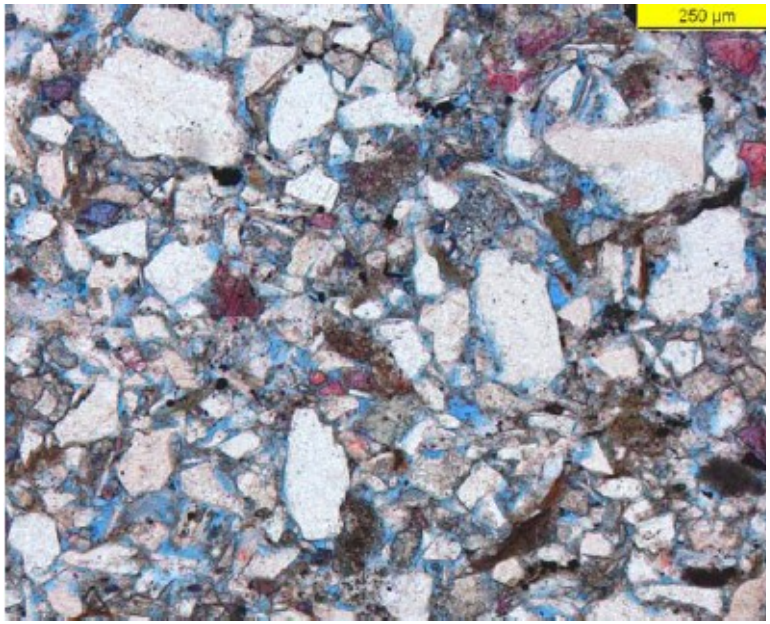

Upper Left: thin section overview; porous fine grained, moderately sorted Litharenite

Lower Left: Detail picture; the scaffold is composed of quartz, glaukonite and rock fragments such as dolomite, calcite, feldspar, peltklasts and muscovite.

Upper Right: As lower left

Lower Right: The scaffold is composed of quartz, glaukonite and rock fragments such as dolomite, calcite, feldspar and muscovite.

Sample 1 (1196,96 m)
Provided by RAG

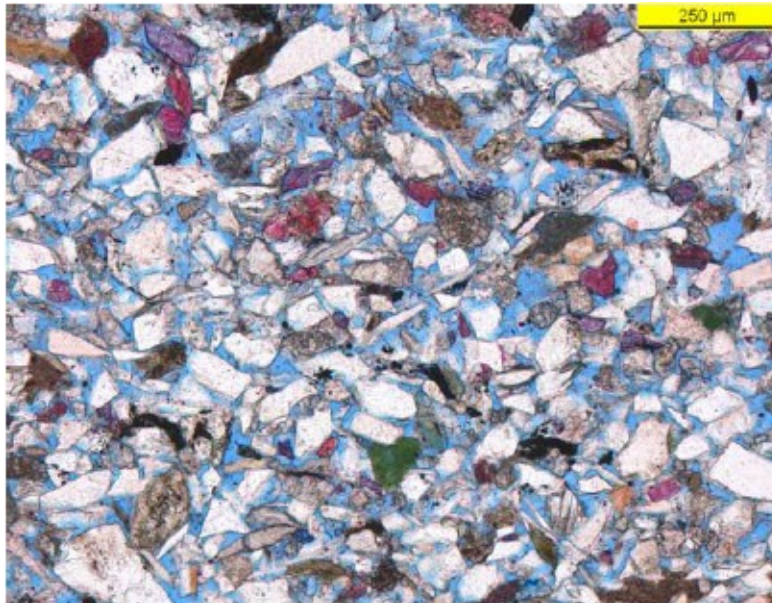

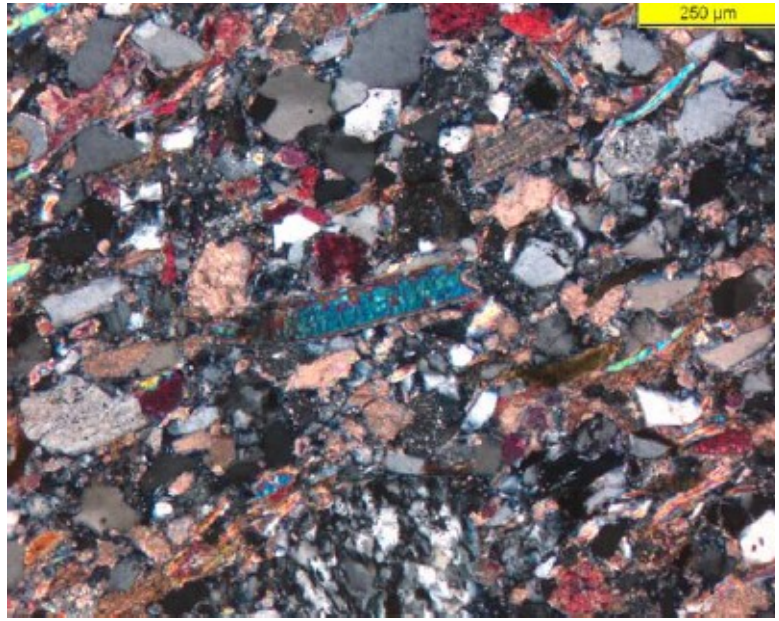

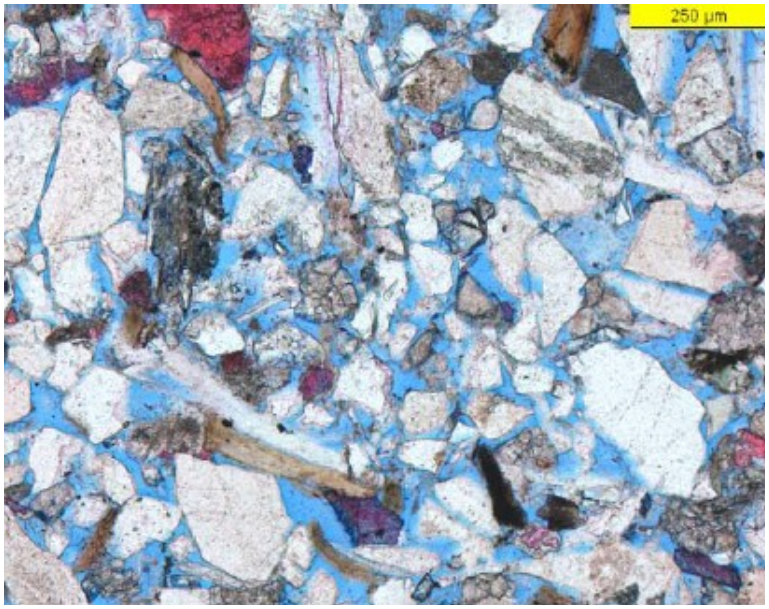

Upper Left:Overview of porous, fine grained, moderately sorted Litharenite

Lower Left: The visible scaffold grains are mainly composed of quartz, dolomite, and rock fragments. The carbonate fragments and the cement have a red color and the porosity in blue.

Upper Right: The visible scaffold grains are mainly composed of quartz and rock fragments. The calcite grains have a red color and the porosity is blue.

Lower Right: The visible scaffold grains are mainly composed of quartz and rock fragments. Additionally the mica grains can clearly be seen.

Sample 2 (1165,8 m)
Provided by RAG

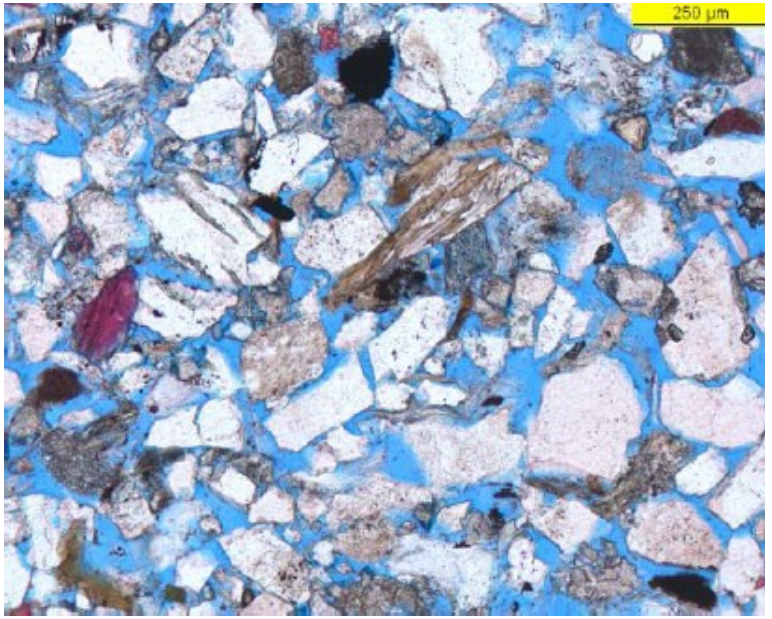

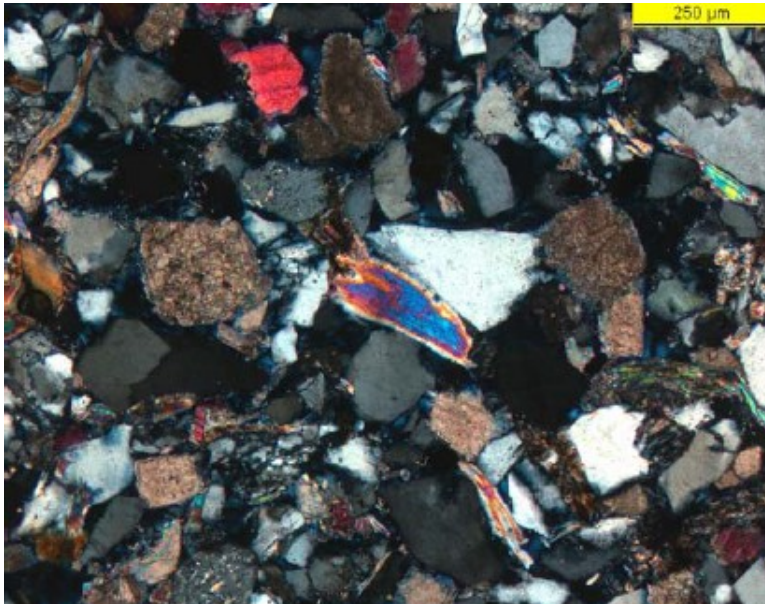

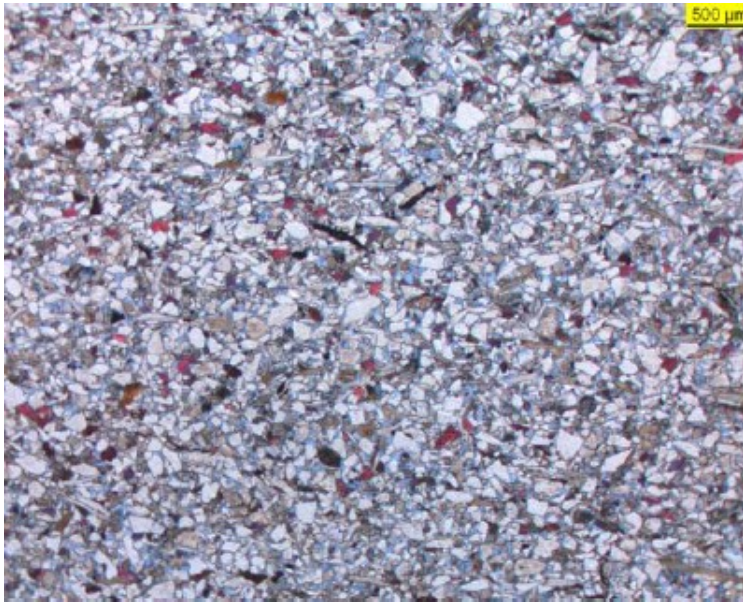

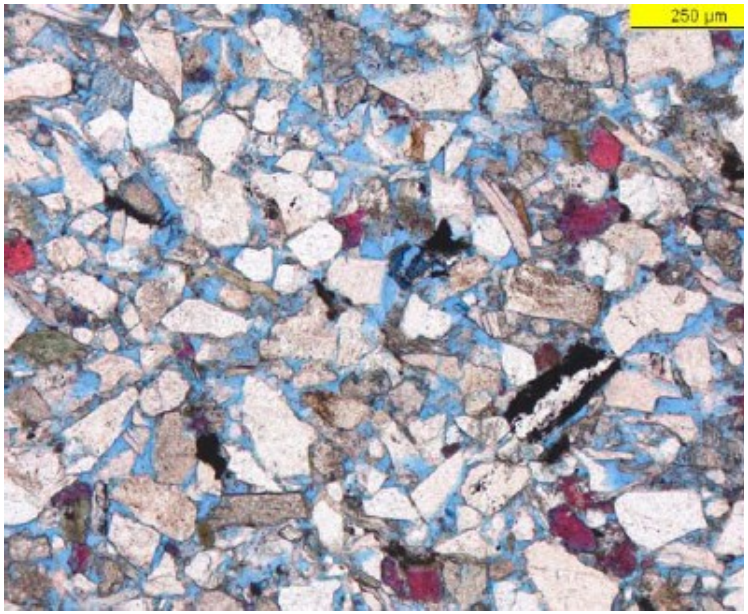

Upper Left: Overview of porous, fine grained, well sorted Litharenite

Lower Left: The scaffold grains are mainly composed of quartz and rock fragments like dolomite, calcite (red color) and muscovite. The dolomite shows traces of marginal siderite growth along its grains.

Upper Right: Same as Lower Left

Lower Right: The visible scaffold grains are mainly composed of quartz, feldspar and rock fragments. The calcite grains have a red color.

Sample 3 (1169,13 m)
Provided by RAG

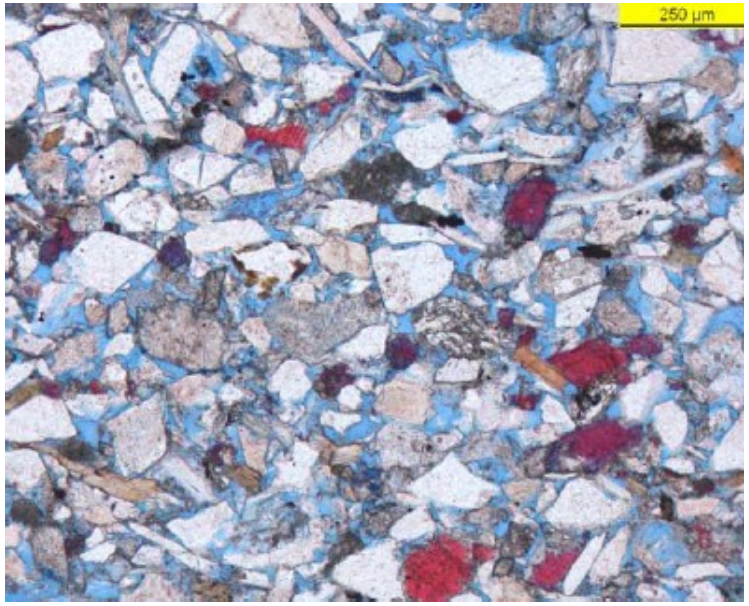

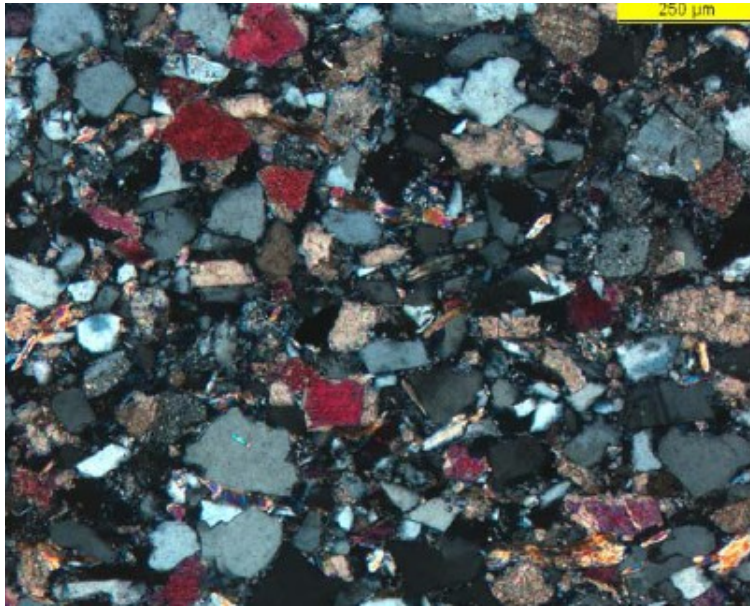

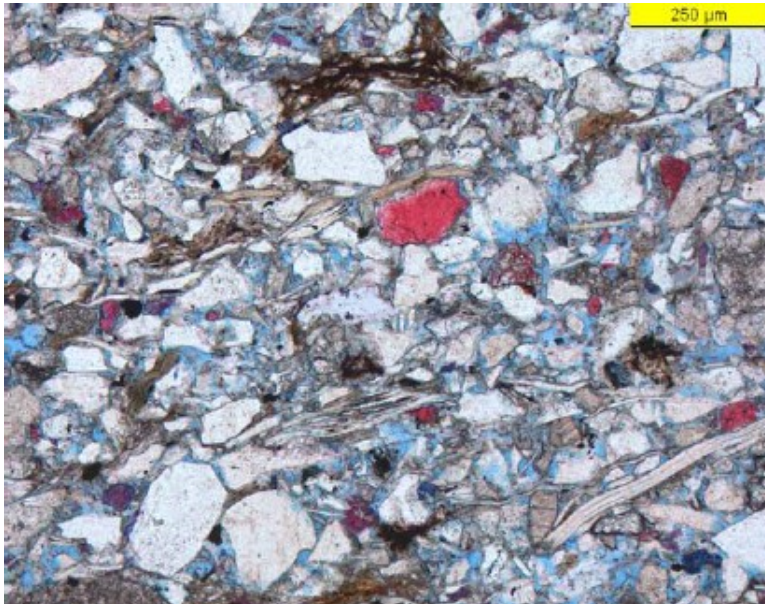

Upper Left: Overview of compacted, bad sorted Litharenite.

Lower Left: The scaffold grains are mainly composed of quartz and rock fragments like dolomite, calcite (red color) and muscovite. The dolomite shows traces of marginal siderite growth along its grains.

Upper Right: Same as Lower Left

Lower Right: The visible scaffold grains are mainly composed of quartz and rock fragments.

Sample 4 (1174,73 m)
Provided by RAG

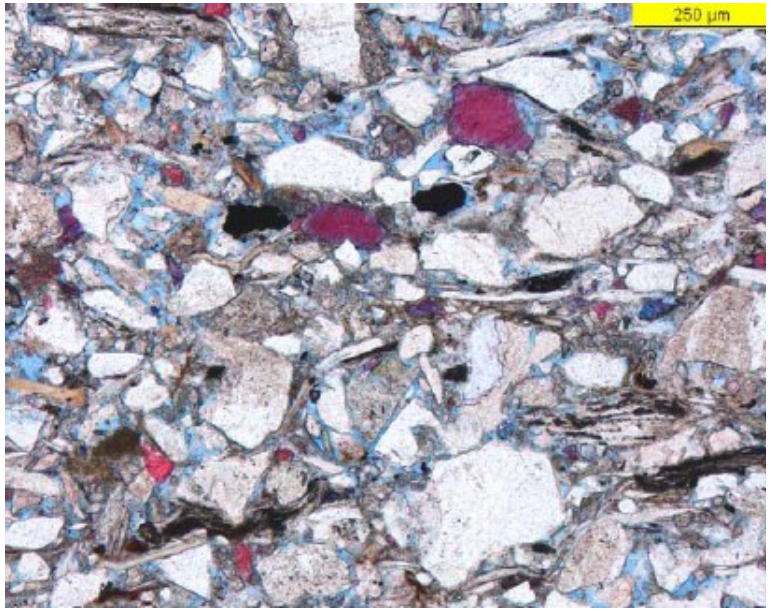

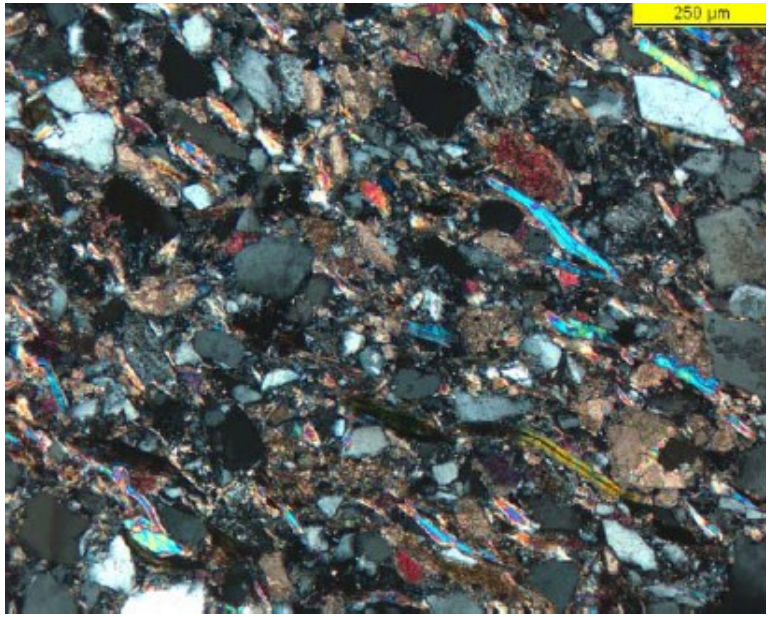

Appendix 2 Thin sections of core sample 2

	1/1 (1211 m)	1/5 (1225 m)	2/3 (1233 m)	2/4 (1240 m)
Monokristalliner Quarz	7,4	12,9	10,7	14,8
Polykristalliner Quarz	1,0	3,3	0,7	2,7
Hornstein	0,3	1,0	0,7	0,3
Feldspäte	6,1	5,3	4,6	7,7
Kristallinbruchstücke	1,7	3,0	3,6	1,7
Vulkanische Gesteinsbruchstücke	0,0	0,0	0,0	0,0
Bioklasten	0,3	2,3	2,0	0,3
Dolomit	3,0	4,6	2,3	3,4
Kalkstein	4,7	4,0	2,6	4,0
Sandstein/Siltstein	0,0	0,0	0,0	0,0
Tonklasten	0,3	0,3	0,0	0,0
Glimmer	2,4	2,6	2,0	1,0
Glaukonit	0,0	0,7	0,7	1,0
Schwermineralien	0,0	0,3	0,0	0,0
Kalzitzement	6,1	2,6	2,3	5,4
Dolomitzement	0,0	0,0	0,0	0,3
Ankeritzement	0,0	0,0	0,0	0,0
Sideritzement	0,0	0,0	0,0	0,0
Matrix (Ton+feinkörnige Karbonate)	67,3	56,3	64,5	58,1
Quarzzement	0,0	0,0	0,0	0,0
Opake Substanz	0,3	0,0	1,3	0,0
MAXIMALE KORNGRÖSSE (mm), 50 Körner	0,23	0,45	0,19	0,28
MITTLERE KORNGRÖSSE (mm), 50 Körner	0,08	0,091	0,088	0,094

Figure 35: Results of the thin section analysis core sample 1
Provided by RAG

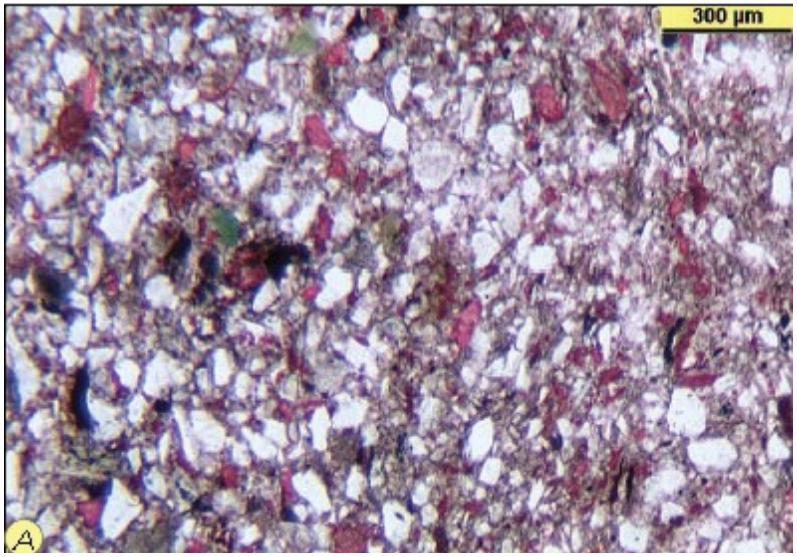

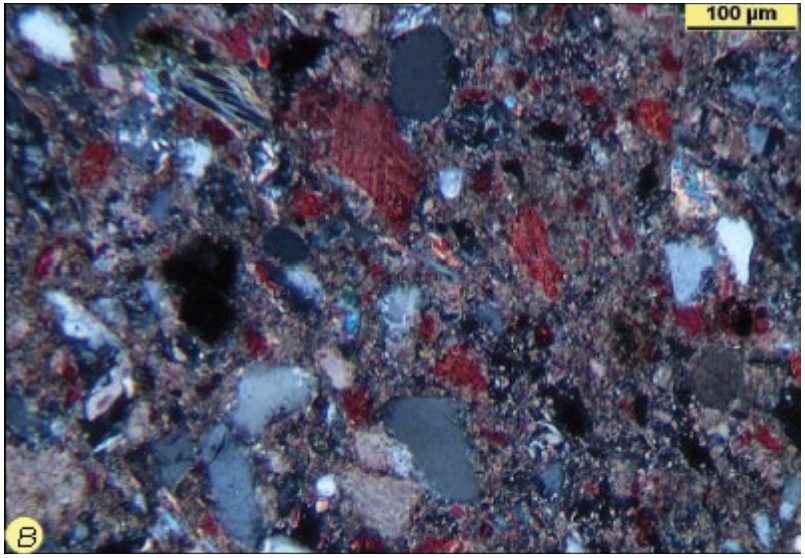

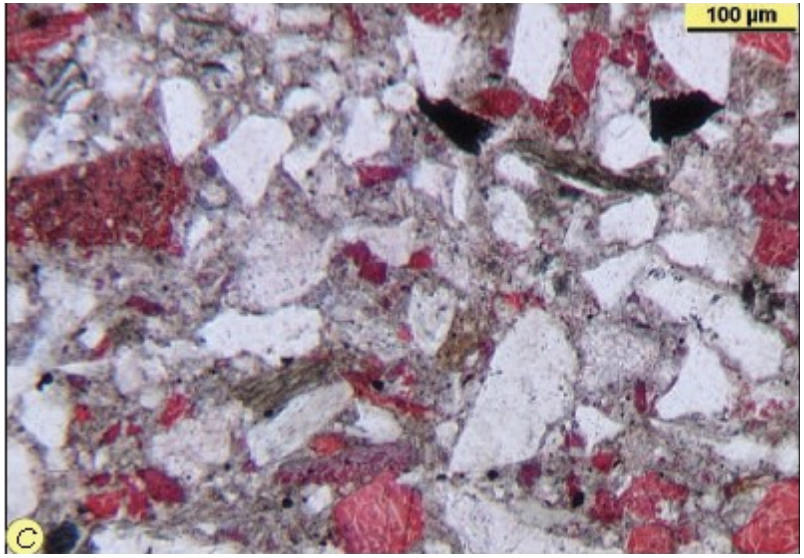

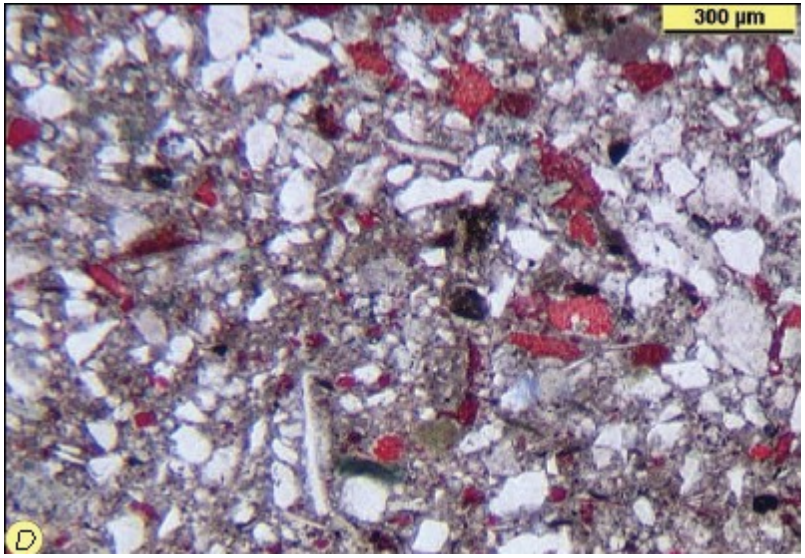

A: Sample 1 (1211 m); thin section overview; fine grained lithic wackestone

B: Detail of sample 1 (1211m); the grains are mainly composed of quartz, calcite, dolomite and mica. The matrix is composed of marly clay.

C: Sample 2 (1225 m); fine grained lithic wackestone; calcite, dolomite, siliciclastic quartz particles as well as the marly clay matrix can clearly be seen.

D: Thin section overview; sample 3 (1233 m); fine grained lithic wackestone

Provided by RAG

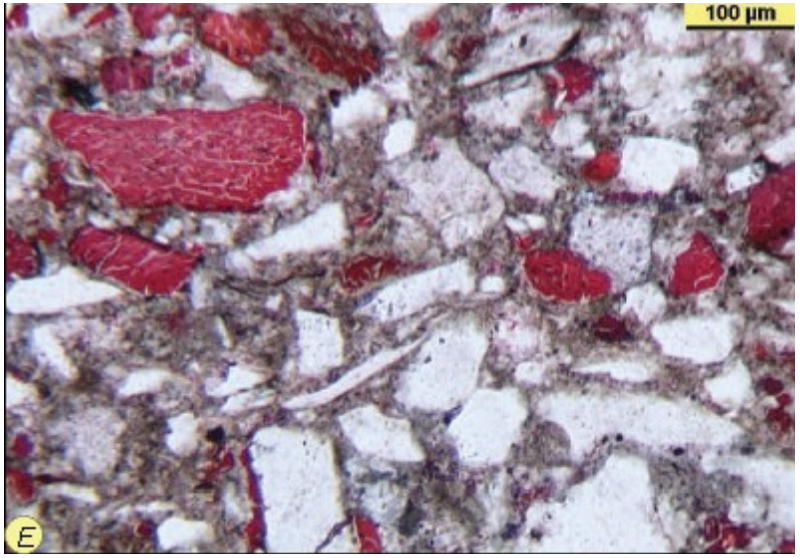

E: finegrained lithic wakestone (1233 m); calcite, quartz, mica particles and the marly clay matrix can be seen.

F: sample 4 (1240 m); lithic wakestone; the scaffold is mainly composed of calcite, dolosparite, mica, chloride and siliciclastic particles. Additionally some forminifera can be seen.

G: Like F (1240 m)

H: (1240 m); Detail picture of F which shows calcite, dolomite, siliciclastic particles and silica sponge needles

Provided by RAG